

Summer 2006

## Parameter Estimation of Spacecraft Fuel Slosh Using Pendulum Analog

Keith L. Schlee

*Embry-Riddle Aeronautical University - Daytona Beach*

Follow this and additional works at: <https://commons.erau.edu/db-theses>



Part of the [Space Vehicles Commons](#)

---

### Scholarly Commons Citation

Schlee, Keith L., "Parameter Estimation of Spacecraft Fuel Slosh Using Pendulum Analog" (2006).  
*Theses - Daytona Beach*. 181.

<https://commons.erau.edu/db-theses/181>

This thesis is brought to you for free and open access by Embry-Riddle Aeronautical University – Daytona Beach at ERAU Scholarly Commons. It has been accepted for inclusion in the Theses - Daytona Beach collection by an authorized administrator of ERAU Scholarly Commons. For more information, please contact [commons@erau.edu](mailto:commons@erau.edu).

**PARAMETER ESTIMATION OF SPACECRAFT  
FUEL SLOSH USING PENDULUM ANALOGS**

by

Keith L. Schlee

A Thesis Submitted to the  
Graduate Studies Office  
In Partial Fulfillment of the Requirements for the Degree of  
Master of Science in Aerospace Engineering

Embry-Riddle Aeronautical University  
Daytona Beach, Florida  
Summer 2006

UMI Number: EP32094

### INFORMATION TO USERS

The quality of this reproduction is dependent upon the quality of the copy submitted. Broken or indistinct print, colored or poor quality illustrations and photographs, print bleed-through, substandard margins, and improper alignment can adversely affect reproduction.

In the unlikely event that the author did not send a complete manuscript and there are missing pages, these will be noted. Also, if unauthorized copyright material had to be removed, a note will indicate the deletion.

UMI<sup>®</sup>

---

UMI Microform EP32094  
Copyright 2011 by ProQuest LLC  
All rights reserved. This microform edition is protected against  
unauthorized copying under Title 17, United States Code.

---

ProQuest LLC  
789 East Eisenhower Parkway  
P.O. Box 1346  
Ann Arbor, MI 48106-1346

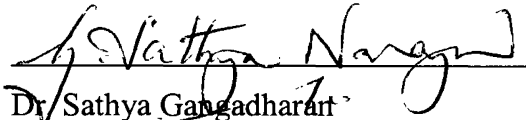
# PARAMETER ESTIMATION OF SPACECRAFT FUEL SLOSH USING PENDULUM ANALOGS

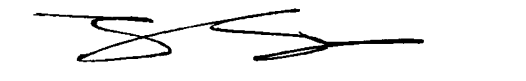
by

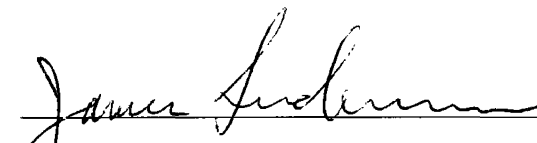
Keith L. Schlee


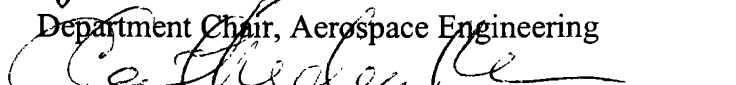
This thesis was prepared under the direction of the candidate's thesis committee chairman, Dr. Sathya Gangadharan, Department of Engineering Science, and has been approved by the members of his thesis committee. It was submitted to the Aerospace Engineering Department and was accepted in partial fulfillment of the requirements for the degree of Master of Science of Aerospace Engineering.

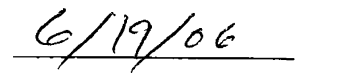
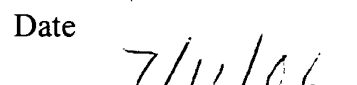
## THESIS COMMITTEE:

  
Dr. Sathya Gangadharan  
Chairman

  
Dr. Yi Zhao  
Co-Chairman

  
James Sudermann  
Member

  
Department Chair, Aerospace Engineering  
  
Christina Frederick-Recascino, Associate Provost

  
Date  
  
Date

## ACKNOWLEDGEMENTS

The author would like to thank James Sudermann, Dr. Charles Walker, and the rest of the ELV Mission Analysis Branch at NASA Kennedy Space Center for their support. Thanks are also to Dr. Sathya Gangadharan and James Ristow at Embry-Riddle Aeronautical University, to Dr. Carl Hubert at Hubert Astronautics, and to Dr. Bora Eryilmaz and Rohit Shenoy of The MathWorks, Inc. for all their guidance and help. The author would also like to thank Don Bouvier (Embry-Riddle Aeronautical University) for his help in the fabrication of the experimental setup.

The author also extends appreciation and gratitude to his friends and family for providing the assistance and encouragement needed to complete this research project.

## ABSTRACT

Author: Keith L. Schlee  
Title: Parameter Estimation of Spacecraft Fuel Slosh Using Pendulum Analogs  
Institution: Embry-Riddle Aeronautical University  
Degree: Master of Science in Aerospace Engineering  
Year: 2006

The nutation (wobble) of a spinning spacecraft in the presence of energy dissipation is a well-known problem in dynamics and is of particular concern for space missions. Its rate of growth is characterized by the Nutation Time Constant (NTC). For analytical prediction of the NTC, fuel slosh is often modeled using simple mechanical analogs such as pendulums or rigid rotors coupled to the spacecraft. Identifying model parameter values which adequately represent the sloshing dynamics is the most important step in obtaining a good NTC estimate. Currently, the identification of the model parameters is a laborious trial-and-error process in which the equations of motion for the mechanical analog are hand-derived, evaluated, and their results compared with the experimental results. This research is a pioneering effort toward automating the parameter identification process by using a MATLAB/SimMechanics based computer simulation modeling of a free-surface fuel slosh in a spherical propellant tank of a spacecraft.

## TABLE OF CONTENTS

ACKNOWLEDGMENTS.....	iii
ABSTRACT.....	iv
LIST OF TABLES.....	vii
LIST OF FIGURES.....	viii
Chapter	
1. INTRODUCTION.....	1
2. PROBLEM DEFINITION.....	4
3. METHOD OF APPROACH.....	7
4. SETUP OF DATA ACQUISITION HARDWARE AND SOFTWARE.....	15
5. PREPARATION FOR DATA COLLECTION.....	17
5.1. Mounting the Pendulum/Tank Assemblies.....	17
5.2. Measuring of the Pendulum Ballast/Tank Liquid.....	19
5.3. Calibration of the Force Transducer.....	20
5.4. Pendulum Assembly Only: Proper Pendulum Length.....	21
5.5. Pendulum Assembly Only: Pendulum's Moment of Inertia.....	22
5.6. Tank Assembly Only: Force Transducer Mounting Location.....	23
6. CALIBRATION OF EXPERIMENT AND SIMULATION.....	25
6.1. Data Processing.....	25
6.2. SLOSH Code Natural Frequency Verification.....	28
6.3. Frozen Mass Testing.....	30
7. FROZEN MASS PARAMETER ESTIMATION.....	32
8. PENDULUM FRAME AND TANK PARAMETER ESTIMATION.....	39
8.1. Test Procedure.....	39
8.2. Pendulum Frame Results.....	43
8.3. Tank Results.....	45
9. CASE STUDIES FOR 60% TANK FILL LEVEL.....	50

9.1. Test A3 Case Studies.....	51
Case 1. Test A3 30 Second Optimization with Default Limits.....	51
Case 2. Test A3 30 Second Optimization without Pendulum Length Limits.....	53
Case 3. Test A3 30 Second Optimization with SLOSH Pendulum Length.....	55
Case 4. Test A3 30 Second Optimization with Spring Constant set to Zero.....	56
9.2. A1-A3 Multiple Dataset Optimization.....	58
9.3. Frequency Sweep for Tank at an A Series Fill Level.....	61
10. DISCUSSION.....	63
11. CONCLUSION.....	63
12. FUTURE WORK.....	64
REFERENCES.....	65
APPENDICES.....	66
APPENDIX A. Pendulum/Tank Assembly Construction and Locomotive Assembly Properties.....	67
APPENDIX B. SLOSH Code Output Tables.....	75
APPENDIX C. Ballast and Liquid Measurement Tables.....	78
APPENDIX D. M-Code Incorporating the “lsqnonlin” Algorithm.....	81
APPENDIX E. “Frozen” Tank Test Results.....	89
APPENDIX F. “Frozen” Pendulum Frame Test Results.....	93
APPENDIX G. Pendulum Frame Test Results.....	103
APPENDIX H. Tank Test Results.....	110



## LIST OF TABLES

Table 3.1	Pendulum Geometry for 8" Diameter Sphere.....	9
Table 5.1	Pendulum Mass and Geometric Properties.....	21
Table 5.2	Pendulum Cylinder Properties and Moment of Inertia Values.....	22
Table 5.3	Tank Assembly Mass and Geometric Properties.....	23
Table 6.1	Summary of Test Durations.....	26
Table 6.2	Natural Frequency (NF) Comparisons.....	29
Table 7.1	Frozen Mass Test Parameter Estimation Limits.....	33
Table 7.2	Newton's Nonlinear Least Squares M-Code Parameter Identification Results for a 60% Frozen Fill Level.....	34
Table 7.3	Parameter Estimator Toolbox Parameter Identification Results for 60% Frozen Fill Level.....	39
Table 8.1	Pendulum Frame and Tank Test Parameter Estimation Limits.....	40
Table 8.2	60% Pendulum Results for Each Method.....	45
Table 8.3	60% Tank Results for Each Method.....	47
Table 8.4	Beat Frequency and Natural Frequency Calculation.....	50
Table 9.1	Test A3 30 Second Optimization Results.....	53
Table 9.2	Test A3 Unlimited Pendulum Length Results.....	54
Table 9.3	Test A3 SLOSH Pendulum Length Results.....	56
Table 9.4	Test A3 with Zero Spring Constant and Variable Pendulum Mass Results.....	58
Table 9.5	A Series (Frozen) Multiple Dataset Optimization Results.....	60
Table 9.6	A Series (Tank) Multiple Dataset Optimization Results.....	60
Table 9.7	A Series Frequency Sweep Data Comparison.....	62

## LIST OF FIGURES

Figure 2.1	Schematic Diagram of SSTR.....	4
Figure 2.2	Block Diagram of the Parameter Estimation Process.....	6
Figure 2.3	Schematic Diagram of 1-DOF Pendulum Analog.....	6
Figure 3.1	SLOSH Code Pendulum/Tank Equivalent and Data Example.....	8
Figure 3.2	Liquid Mass Distribution for 8" Diameter Sphere.....	9
Figure 3.3	Schematic Diagram of the Four Group Locations.....	10
Figure 3.4	Engineering Drawing of Group 1 Assembly.....	11
Figure 3.5	SimMechanics Model of 1-DOF Pendulum.....	12
Figure 3.6	Schematic Diagram of 1-DOF Fuel Analog.....	13
Figure 3.7	SimMechanics Response for Sphere at 60% Fill Level.....	14
Figure 3.8	SimMechanics Input for Sphere at 60% Fill Level.....	14
Figure 4.1	Data Measurement Hardware.....	15
Figure 4.2	LabVIEW Block Diagram for Force and Frequency Collection.....	16
Figure 4.3	LabVIEW User Interface Displays Readings for Force and Frequency.....	17
Figure 5.1	Balancing and Vertical Positioning of the Tank Assembly.....	18
Figure 5.2	Aligning the “Stinger” with the Force Transducer Mounted to the Pendulum Assembly.....	18
Figure 5.3.	Weighing the Ballast Container.....	19
Figure 5.4.	Force Transducer Calibration.....	20
Figure 5.5.	Center of Mass Locations of Tank Assembly at Various Fill Levels.....	24
Figure 5.6	Center of Mass Marks on Transducer Mounting Rail.....	24
Figure 6.1	“Filter Designer” for Signal Processing Toolbox.....	26
Figure 6.2	Comparison of Unfiltered and Filtered Data (70% at 1.855Hz).....	28
Figure 6.3	Natural Damping of Tank at 60% Fill Level.....	29
Figure 6.4	Natural Damping Slosh Positions for 60% Fill Level.....	29

Figure 6.5	Simulation Verification Using Measured (Not Estimated) Parameters (60% at 1.953 Hz).....	31
Figure 6.6	Frozen Tank Test Comparison (60% at 1.953 Hz) .....	32
Figure 7.1	Frozen Mass Parameter Identification Results Using M-Code (60 % at 1.855Hz) .....	35
Figure 7.2	Parameter Estimator Graphical User Interface During Frozen Mass Test (60% at 1.855Hz).....	36
Figure 7.3	Real-time Measured vs. Response Plot (60% at 1.855Hz).....	37
Figure 7.4	Real-time Parameter Trajectory Plots (60% at 1.855Hz).....	38
Figure 8.1	Generic Low Damping Simulation Output with Pendulum.....	41
Figure 8.2	Generic Low Damping Simulation Output with Pendulum.....	42
Figure 8.3	Pendulum Test A3 (60% at 1.770 Hz).....	43
Figure 8.4	Pendulum Test B3 (70% at 1.953 Hz).....	44
Figure 8.5	Tank Test C3 (80% at 2.441 Hz).....	46
Figure 8.6	Tank Test A3 (60% at 1.953 Hz).....	46
Figure 8.7	Spring Constants at Various Fill Levels using Default Limits.....	48
Figure 8.8	Damping Constants at Various Fill Levels using Default Limits.....	49
Figure 8.9	Spring Damping Ratio for Various Fill Levels using Default Limits.....	49
Figure 9.1	Test A3 Optimization Results for 30 Seconds (1.953 Hz).....	52
Figure 9.2	Zoomed in View of Test A3 Optimization Results.....	52
Figure 9.3	Test A3 Optimization with Unrestricted Pendulum Length.....	54
Figure 9.4	Test A3 Optimization with SLOSH Pendulum Length.....	55
Figure 9.5	Test A3 Predicted Spring Constants and Pendulum Lengths.....	57
Figure 9.6	Test A3 Optimization with Spring Constant Equal to Zero.....	57
Figure 9.7	Block Diagram of A1-A3 Multiple Dataset Optimization.....	59
Figure 9.8	A1-A3 Multiple Dataset (Frozen) Optimization.....	59
Figure 9.9	A1-A3 Multiple Dataset (Tank) Optimization.....	60
Figure 9.10	A Series Frequency Sweep Data Comparison.....	62

## 1. INTRODUCTION

Spinning a spacecraft or an upper stage is a well-established method for stabilizing a space vehicle with a minimum of hardware, complexity, and expense. While spinning a deployed spacecraft over its operational lifetime has generally fallen out of style in favor of the more modern three axis stabilized active systems popular today, there still is a community of users that have to deal with spin stabilized upper stage dynamics. Many NASA and DoD payloads are launched on Boeing Delta II expendable launch vehicles with spinning solid rocket third stages. This particular version of the Delta II has been very popular for NASA interplanetary missions. Consequently, NASA's Expendable Launch Vehicle program office at Kennedy Space Center has been investigating ways to improve their understanding and ability to model spinning upper stage dynamics. While this research work has important near term applications for expendable launch vehicles, it also has significant implications for NASA's future manned space program. Spinning a large manned vehicle (or perhaps segments of one connected by a long tether) is the only practical way to obtain "artificial gravity". Long duration space missions may require some form of artificial gravity to counteract the effects of extended weightlessness on the human body.

Liquid slosh in the fuel tanks of an attached spacecraft has been a long standing concern for space missions with a spinning upper stage. Loss of rotational kinetic energy through the movement of liquid propellants affects the gyroscopic stability of the combined spacecraft and upper stage. Energy loss leads to an ever increasing wobble or "nutation" which can grow and cause severe control issues (Hubert 2003). The more vigorous the slosh the greater the energy loss and hence the greater the nutation. The "nutation angle" is defined as the angular displacement between the principal axis of rotation of the spacecraft and its angular momentum vector and is a measurement of the magnitude of the nutation (Wertz 1978). The amount of time it takes for the nutation angle to increase by a factor of  $e^1$  is defined as the Nutation Time Constant (NTC), and is a key parameter in assessing the stability of the spinning spacecraft during the upper stage burn. The accurate determination of the NTC is very difficult to calculate accurately during the early stages of spacecraft design.

There is a high degree of uncertainty in predicting the effect of liquid propellant motion in spinning spacecraft. The resulting nutation growth can be excessive and can pose a threat to the mission. ATS-5 in 1969 was lost because of excessive and unanticipated nutation growth. Purely analytical methods of predicting the influence of onboard liquids have been generally unsatisfactory (Hubert 2003). The NTC values provided analytically are quite often significantly different than actual flight values. Hence, there is a need to identify conditions of resonance between nutational motion and liquid modes and to understand the general characteristics of the liquid motion that cause the problem in spinning spacecraft. The current research is a first step in trying to understand and model certain modes of induced resonance found during experimental testing and during flight. This study will focus on the modeling of fluid motion and will utilize the results obtained to develop a more accurate prediction of the fuel slosh effects on spin stabilized spacecraft.

During the initial design of spacecraft, use of purely analytical means of predicting the influence of onboard liquids was not satisfactory. Computational fluid dynamics software packages provide some insight, but it turns out that they have several shortcomings. Their complexity and inability to accurately model the coupling effects of sloshing mass on the six degree-of-freedom motion experienced by the spacecraft make their application problematic. Liquid oscillations in spinning tanks have been studied in the past. Liquid oscillations in spinning fuel tanks produce very different response characteristics compared to those of non-spinning fuel tanks (Greenspan 1969). An energy sink model was originally developed by Thomson (1961) to include the effects of small, passive sources of energy dissipation. This model does not work well for spacecraft fuel slosh energy dissipation if the liquid mass is a large fraction of the total mass of the spacecraft.

Extensive analysis has been done on the different tank shapes and locations, as well as the use of propellant management devices (PMD). A summary of this analysis, like that reported by Hubert (2001) shows the vast differences in possible behaviors of different designs. For the off-spin-axis-mounted, cylindrical tanks with hemispherical end-caps that have been popular in spacecraft programs, a number of relatively simple mechanical models have been developed. Hubert also notes that one of the most difficult

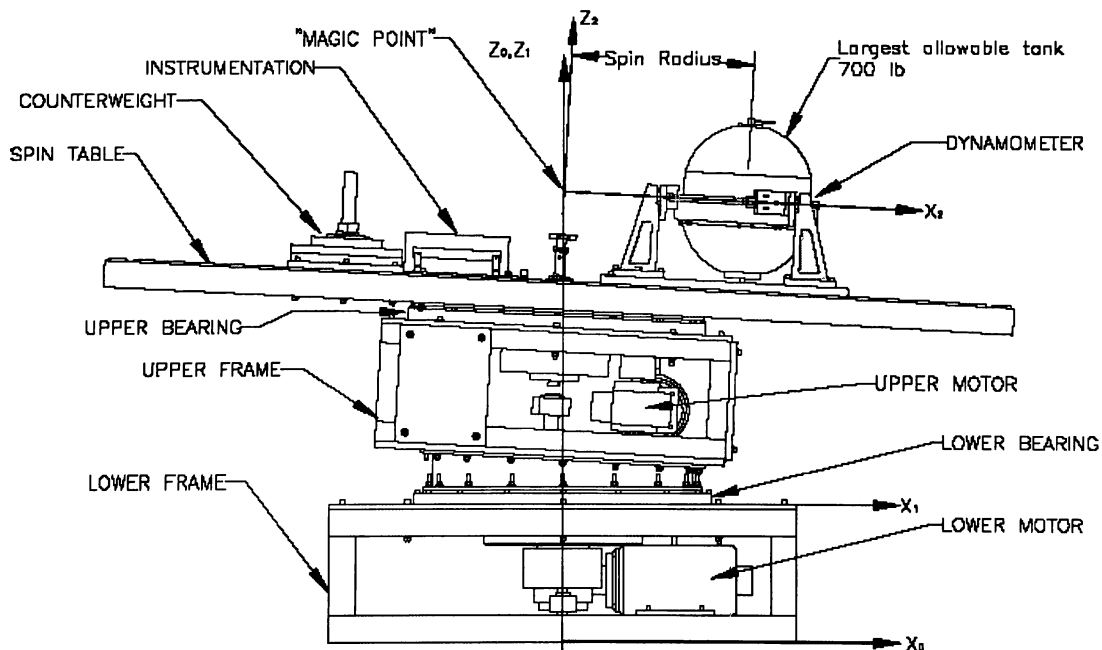
aspects of employing such mechanical models is in the selection of appropriate parameters in the model. Use of mechanical analogs such as pendulums and rotors to simulate sloshing mass is a common alternative to fluid modeling. A homogeneous vortex model of liquid motions in spinning tanks and an equivalent mechanical rotor model was developed by Dodge et al. (1994). An approximate theory of oscillations that predicts the characteristics of the dominant inertial wave oscillation and the forces and moments on the tank are described. According to Dodge et al., the pendulum model simulates a motion that does not involve an oscillation of the center of mass. Therefore, it is not a valid model of inertial wave oscillations. Weihs and Dodge (1991) illustrate that the free surface effects can be ignored when the liquid depth is small.

A 3-D pendulum model was proposed by Green et al. (2002). There was evidence of liquid resonance from the experimental data. The resonance was closely tied to the tangential torque and to a lesser degree to the radial torque, and there was little or no resonance in the force measurements. Green et al., proposed a rotary oscillator concept to simulate the torque resonance in tangential and radial directions. This rotary oscillator model was superimposed on the pendulum model to provide the overall response of liquid oscillation in the tank.

The current research effort proposed is directed toward modeling fuel slosh on spinning spacecraft using simple pendulum analogs (Schlee et al. 2005 [13-15]). The pendulum analog will model a spherical tank with no PMD's. An electric motor will induce the motion of the pendulum to simulate free surface slosh. Parameters describing the simple pendulum models will characterize the modal frequency of the free surface sloshing motion. The one degree of freedom model will help to better understand fuel slosh and will serve as a stepping stone for complex simulations to accurately predict the NTC with less time, cost, and effort in the future.

## 2. PROBLEM DEFINITION

Various simulation parameters are estimated by matching the pendulum/rotor model response to the experimental response of full sized test tanks in NASA's Spinning Slosh Test Rig (SSTR) located at the Southwest Research Institute (SwRI) in San Antonio, Texas. The experimental set-up of the SSTR is shown in Figure 2.1. The SSTR can subject a test tank to a realistic nutation motion, in which the spin rate and the nutation frequency can be varied independently, with the spin rate chosen to create a centrifugal acceleration large enough to ensure that the configuration of the bladder (PMD) and liquid in the tank is nearly identical to the zero-g configuration. A complete description of the actual tests, data acquisition and analyses of data for the Contour mission is provided by Green, et al. (2002). The propellant motion is simulated using models with various parameters (inertia, springs, dampers, etc.) and the problem reduces to a parameter estimation problem to match the experimental results obtained from the SSTR.

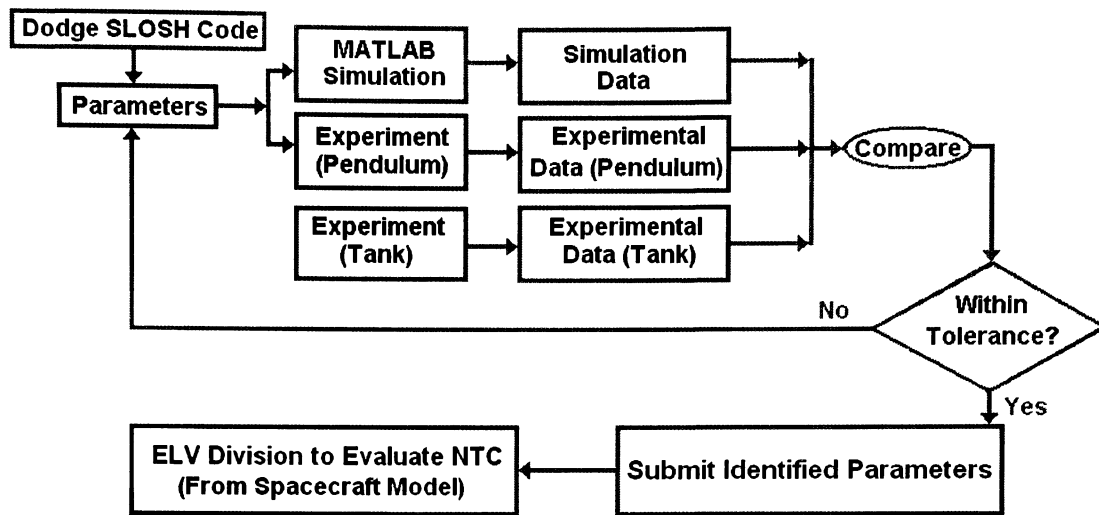


**Figure 2.1. Schematic Diagram of SSTR**

The SSTR can accommodate a full-sized fuel tank complete with any internal PMD for testing. The SSTR measures and records the force and torque response of the fuel tank to the internal slosh motion of the propellant. It has the capability to identify and characterize slosh resonances. The data from the tests are used to derive model parameters that are then used in the slosh blocks of a MATLAB/SimMechanics-based spacecraft and upper stage simulation. Currently the identification of the model parameters is a laborious trial-and-error process in which the equations of motion for the mechanical analog are hand-derived, evaluated, and compared with the experimental results.

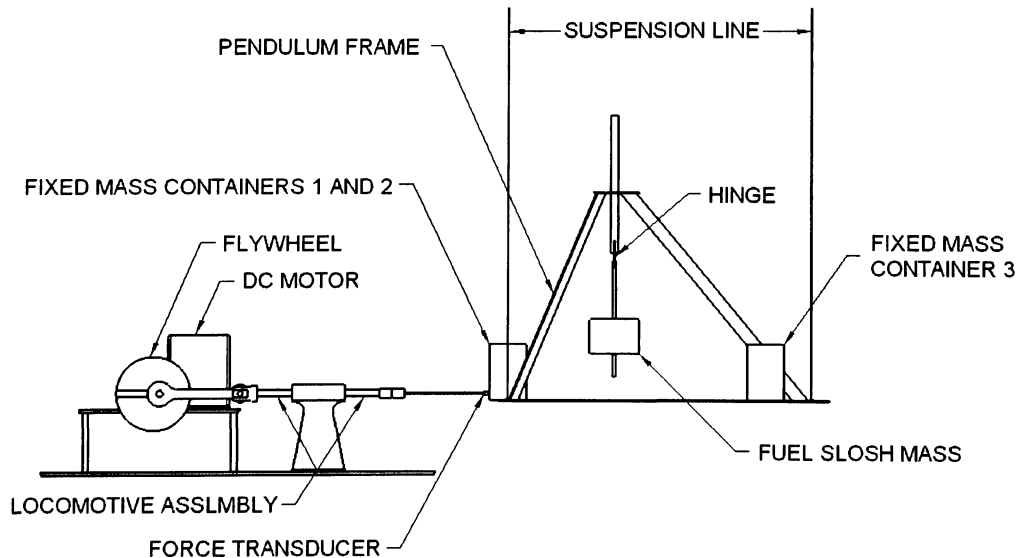
The current research is an effort to automate the process of slosh model parameter identification using a MATLAB/SimMechanics-based computer simulation of the experimental SSTR setup. Two different parameter estimation and optimization approaches are being evaluated and compared in order to arrive at a reliable and effective parameter identification process. The first approach will be conducted using Newton's nonlinear least squares method, or the MATLAB "lsqnonlin" algorithm. The second estimation method is a "black box" approach using MATLAB's Parameter Estimation Toolbox. To evaluate each parameter identification approach, a simple one-degree-of-freedom pendulum experiment is being constructed and motion will be induced by an electric motor through a "locomotive-arm" assembly. By applying the estimation approach to a simple system with known characteristics, its effectiveness and accuracy can be evaluated. The same experimental setup can then be used with fluid-filled tanks to further evaluate the effectiveness of the process. Ultimately, the proven process can be applied to the full sized SSTR simulation for fast, accurate, and reliable determination of the slosh model parameters for a particular spacecraft mission. A global view of this parameter estimation procedure is illustrated in Figure 2.2.





**Figure 2.2. Block Diagram of the Parameter Estimation Process**

The problem with modeling the complete SSTR as a starting point is that there is considerable complexity in the SSTR experimental setup. By reducing the problem to that seen in Figure 2.3, a better understanding can be made of the effectiveness of the optimization and estimation approaches and to the fundamental slosh behaviors of the liquid without having to model all of the complexity of the SSTR<sup>1</sup> (Gangadharan et al. 1991).



**Figure 2.3. Schematic Diagram of 1-DOF Pendulum Analog**

<sup>1</sup> A description of the construction of the 1-DOF pendulum analog can be seen in Appendix A.

The fixed mass represents the amount of propellant that is not undergoing free surface slosh while the free surface fuel slosh mass is represented by the mass attached to the pendulum. This is discussed further in the following section. Motion of the pendulum analog is induced by an electric motor through a “locomotive-arm” assembly. This robust setup can yield very accurate sustained frequencies. Forces are measured using a Sensotek Model 31 force transducer rated at  $\pm 2.268$  Volts per kilogram.

### **3. METHOD OF APPROACH**

A spherical tank with no PMD’s undergoing free surface slosh is the simplified model for the pendulum parameters. Free surface slosh has a well defined resonant frequency (Hubert 2003). The only sloshing motion assumed to be taking place in this simplified model is a surface wave. The rest of the liquid is essentially at rest and can be treated like a fixed mass. Initial pendulum properties are found by the use of a program developed by Dodge at SwRI. This “Dodge” (SLOSH) code predicts the modes of the fuel tank with that of a pendulum. The tank/fuel parameters such as shape, kinematic viscosity, and liquid fill level are provided as input to the program<sup>2</sup>. An illustration of the tank/pendulum definition along with values for various pendulum parameters for an 8 inch diameter spherical tank is shown in Figure 3.1.

Using the tank/fuel parameters as input to the SLOSH code, a pendulum “equivalent” can be determined from the code. The physical parameters provided by the code include the liquid’s fixed and pendulum masses as well as the pendulum length. First and second mode slosh data are also output by the code. The first mode parameters (sloshing mass) represent the majority of the propellant undergoing free surface slosh while the second mode represents a small correction factor for the first mode. This correction factor is an order of magnitude smaller than the first mode. Therefore, it can be added to the first mode mass with minimal error.

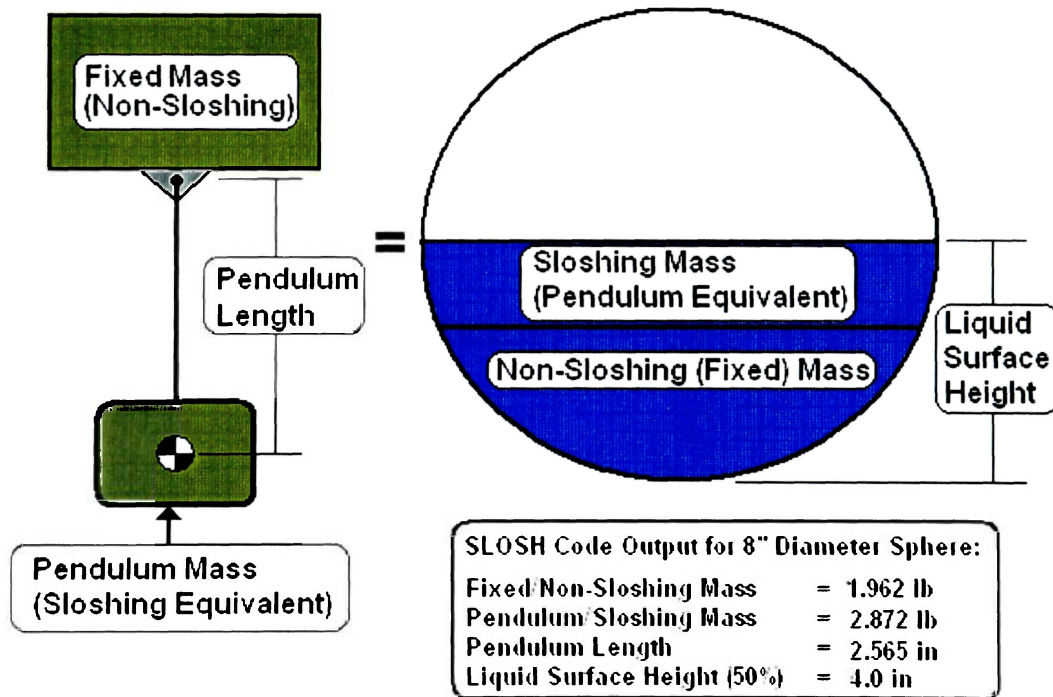
After running the code for several fill levels, several plots can be created from the data. Figure 3.2 shows the mass distribution for various fill levels for an 8 inch diameter sphere using water as the liquid. For laboratory testing, water is a widely used

---

<sup>2</sup> SLOSH code values for 8" diameter sphere at various fill levels are provided in Appendix B.

substitute for modeling hazardous propellants. The properties of liquid water (density, viscosity, etc.) are in very close proximity to those of hydrazine, the most commonly used propellant. The code predicts that the maximum sloshing mass will occur at approximately 60% fill level. Table 3.1 indicates the various pendulum lengths that are required for different fill levels.

While the simulation will test this entire range of fill levels, the 1-DOF pendulum experiment will be limited to 60-80% fill levels. This is due to the fixed mass constraint of the pendulum frame for the lower end and a tank fill restriction for the upper end. For the “tank” experiment, fill levels below 60% can be tested due to light weight of the tank.



**Figure 3.1. SLOSH Code Pendulum/Tank Equivalent and Data Example**

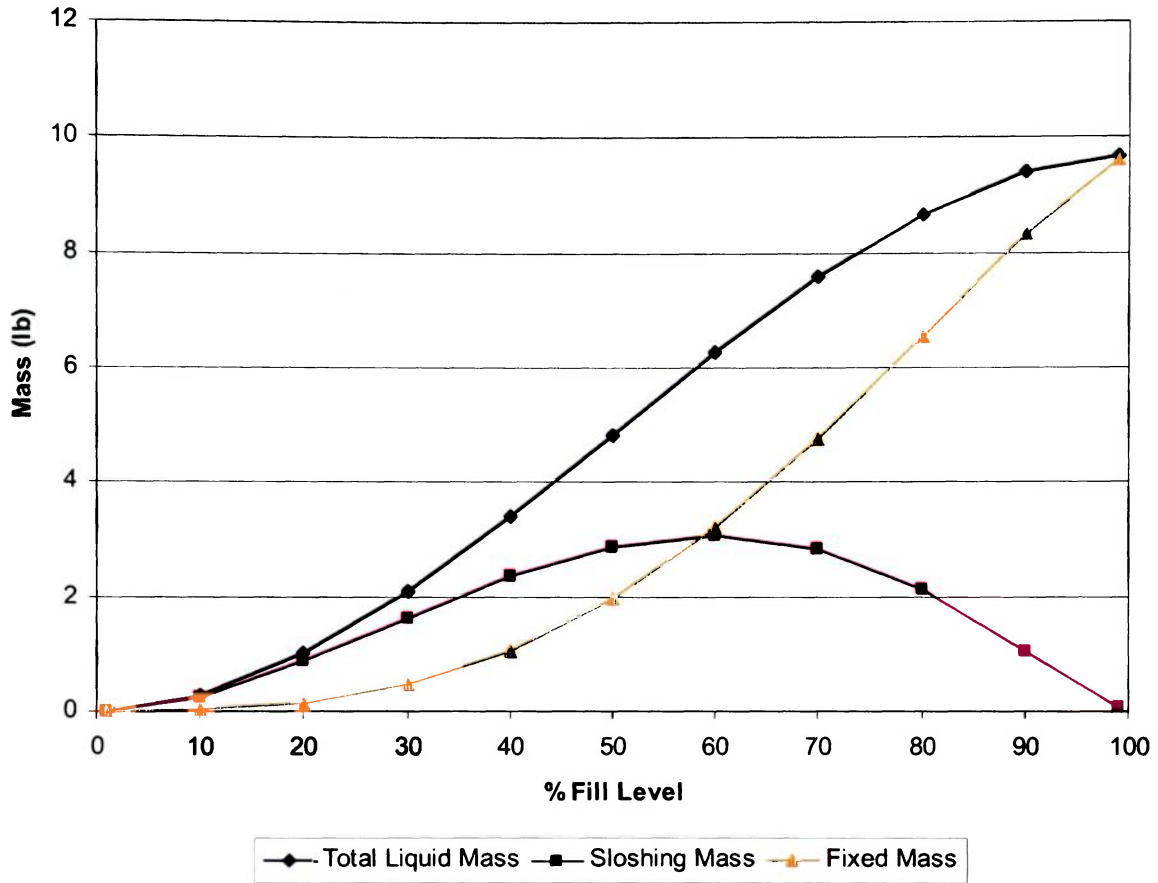
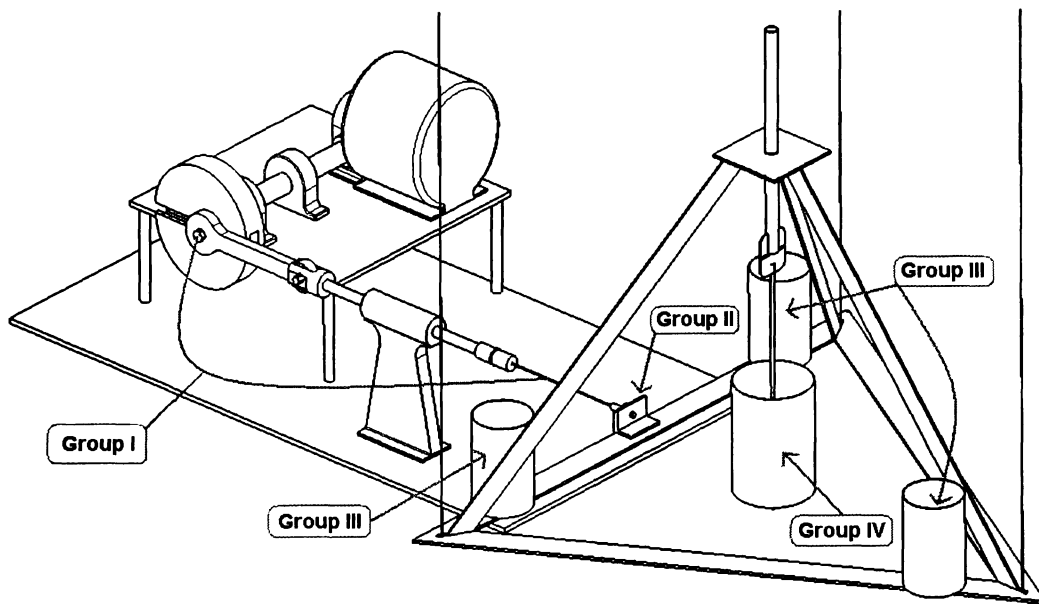


Figure 3.2. Liquid Mass Distribution for 8" Diameter Sphere

Table 3.1  
Pendulum Geometry for 8" Diameter Sphere

Fill Level	1%	10%	20%	30%	40%	50%	60%	70%	80%	90%	99%
Pendulum Length (in)	3.872	3.735	3.737	3.779	3.835	3.891	3.945	3.918	3.725	2.947	0.080

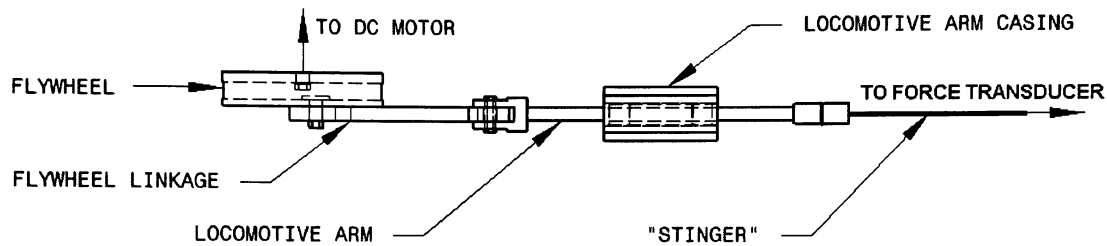
Using the code's data distributions along with the geometric/material characteristics obtained from the experimental setup (Figure 2.3), a computer simulation of the one DOF pendulum analog can be developed using SimMechanics software (Wood and Kennedy, 2003) as illustrated in Figures 3.3 and 3.5. Each of the different parts of the simulation model is located in one of the following four groups:



**Figure 3.3. Schematic Diagram of the Four Group Locations**

Group 1: This group simulates the electric motor and locomotive arm assembly. The locomotive arm consists of five different parts starting with the DC motor. These are the flywheel, flywheel linkage, locomotive arm (piston), and the “stinger” as illustrated in Figure 3.3. The “stinger” is a flexible metal rod designed to absorb forces that are not coincident with the axis of the locomotive arm. The rest of the locomotive arm assembly is assumed to be rigid. Geometric parameters such as component mass and moments of inertia are fixed in this group. Various locomotive arm assembly parameters are listed in Appendix A. Angular velocity correction (rad/s) for the flywheel and the initial flywheel angle (rad) are input parameters for this group. These parameters are represented as the SimMechanics

blocks labeled “Initial Flywheel Angle” and “Angular Velocity Correction” in group one in Figure 3.5.



**Figure 3.4. Engineering Drawing of Group 1 Assembly**

Group 2: The location of the force transducer in Figure 3.3 is represented by this group. The force transducer connects the pendulum frame to the locomotive arm assembly. The forces due to the frozen and the sloshing masses are recorded in this group as a two-column spreadsheet. The first column represents time (sec) while the second column represents force (lb). The time-step for each measurement is 10 ms. Typical testing times range from 15-30 seconds. In Figure 3.5, the force transducer is represented by the “Weld3” block.

Group 3: Parameters in this group include the non-sloshing fuel mass (lb). This mass has rigid geometric properties defined by the frame assembly illustrated in Figure 3.3. The frame is constructed using 1/8" aluminum beam (with a mass of 3.213 lb) and is represented as the “Tank Mass” block in Figure 3.5.

Group 4: Group four simulates the sloshing fuel and is considered to be critical in the parameter estimation process. Fuel mass (lb), hinge spring (ft-lb/rad), hinge damping (ft-lb/rad/sec), and pendulum length (in) are all possible parameters in this group. The pendulum container weighs 0.345 lb. These parameters are represented as the “Pendulum Mass” and the “Joint Spring & Damper” in Figure 3.5.

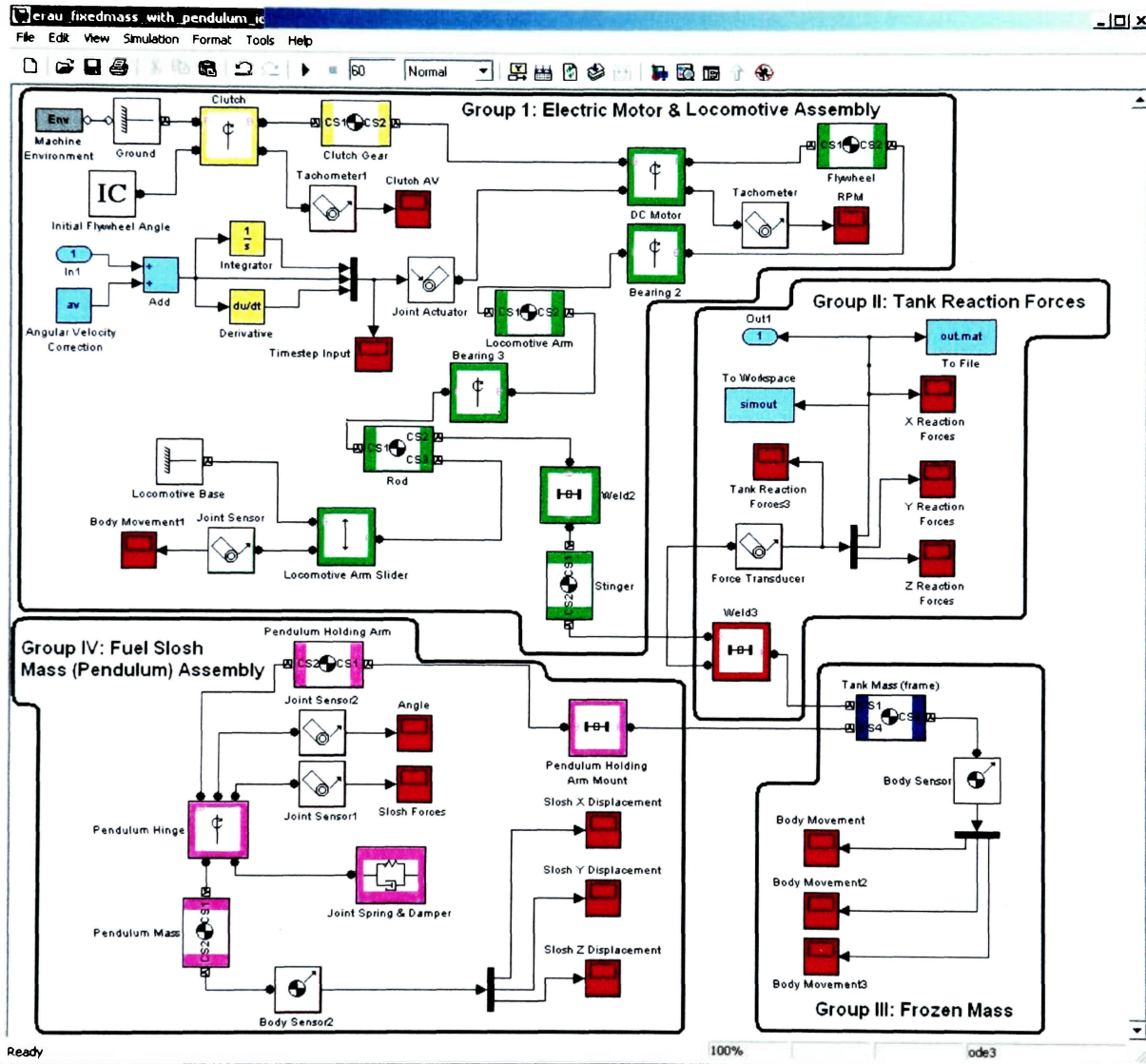
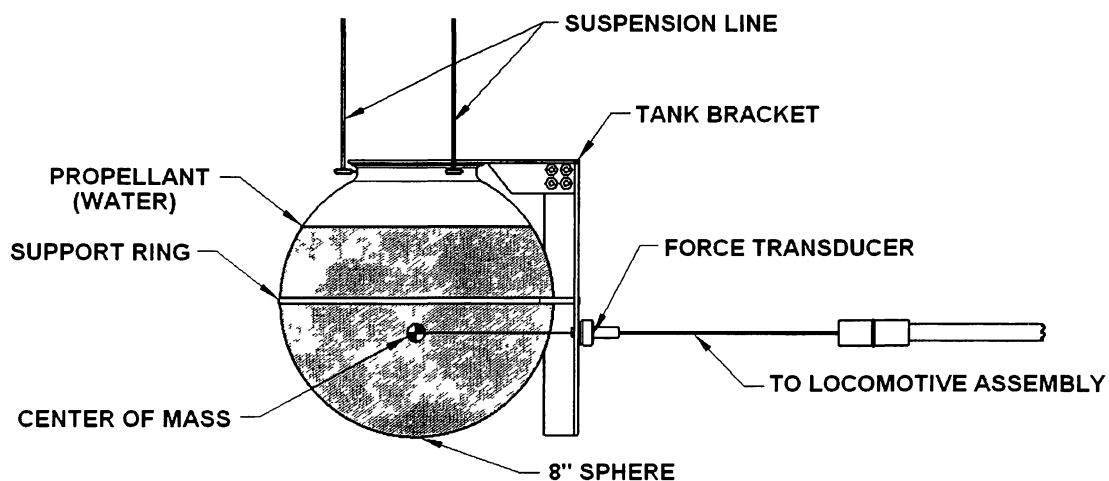


Figure 3.5. SimMechanics Model of 1-DOF Pendulum

For the “tank” experiment, groups III and IV are replaced with an 8 inch diameter sphere as illustrated in Figure 3.6. The sphere is a transparent acrylic globe designed to accommodate fill levels of approximately 80%. The propellant (water in this case) will be tested experimentally to verify the pendulum analog. That is, the simulation is not modified in any way whether or not the measured data given to it originates from the pendulum frame or the tank assembly. The mass of the sphere with mounting brackets is 0.818 lb.

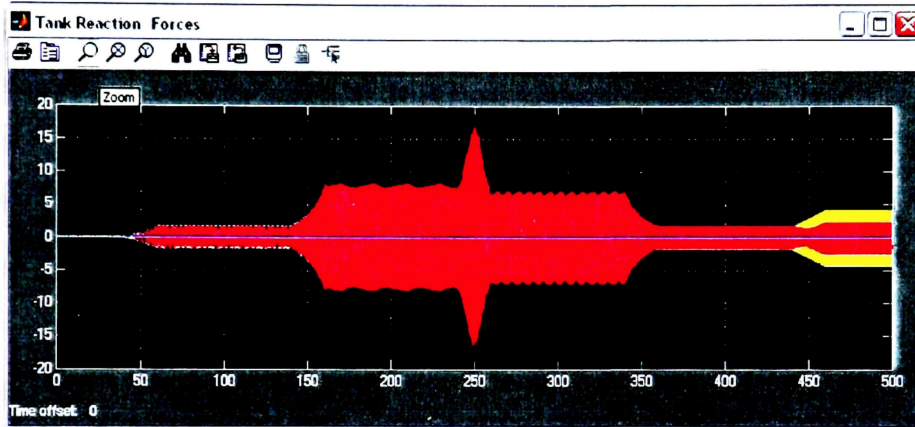


**Figure 3.6. Schematic Diagram of 1-DOF Fuel Analog**

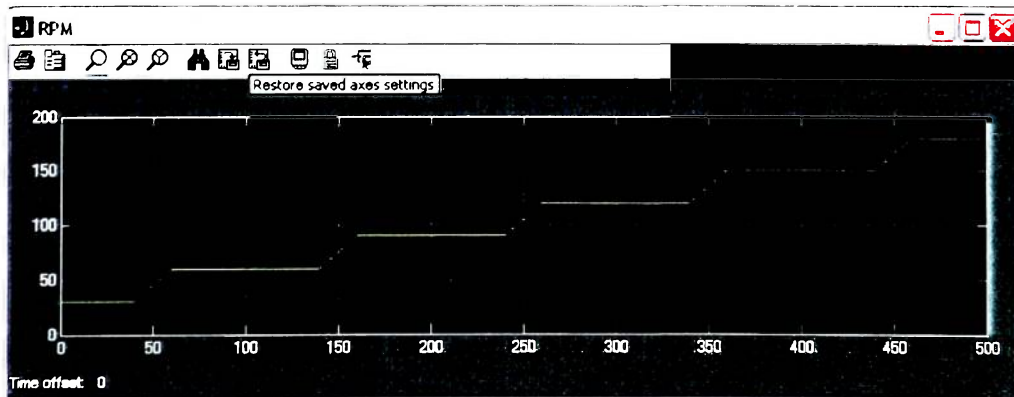
As a proof-of-concept, results from this SimMechanics simulation incorporating the one DOF pendulum analog matches those predicted by the SLOSH code for a sphere at a 60% fill level with an arbitrarily chosen diameter of 12 inches. The simulated locomotive assembly, Group I, is driven by parameters determined by the user as illustrated in Figure 3.7. At the start of the simulation ( $t = 0$  s), the frequency is 0.5 Hertz (30 revolutions per minute (RPM)) and at time equal to 500 seconds, the frequency is equal to 3.0 hertz (180 RPM). Figure 3.8 is the force response that would be experienced by the force transducer in the experiment. By comparing the RPM data in Figure 3.7 to the force data in Figure 3.8, the natural frequency of the pendulum can be found. At approximately 250 seconds, the pendulum reaches its first mode at a frequency of approximately 1.71 hertz. This frequency matches the natural frequency prediction of



the SLOSH code. The natural frequency is inversely proportional to the square root of the length of the pendulum. For the case of a 60% fill level, the length was found to be 3.348 in.



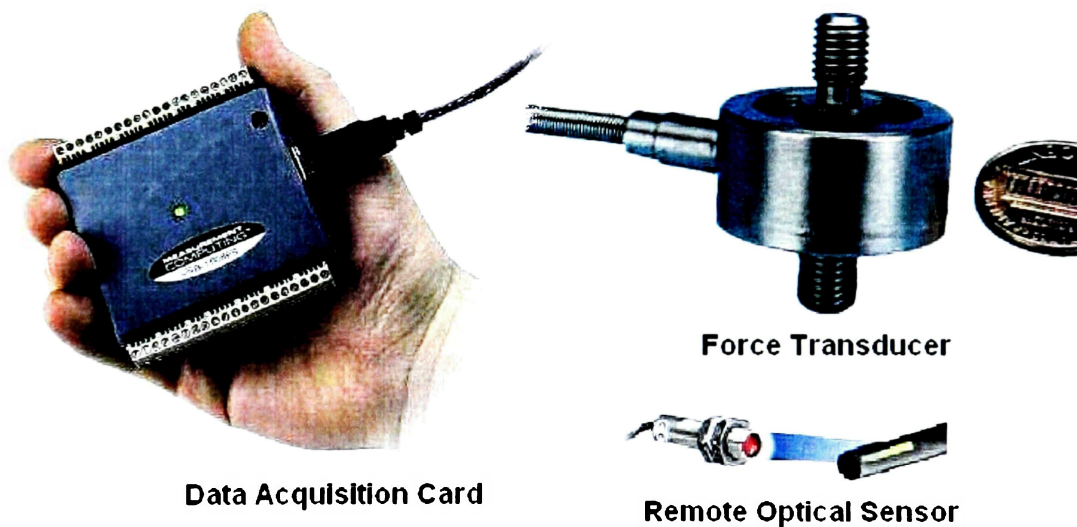
**Figure 3.7. SimMechanics Response for Sphere at 60% Fill Level  
(Force (lb) vs. Time (s))**



**Figure 3.8. SimMechanics Input for Sphere at 60% Fill Level  
(Rotational Speed (rev/min) vs. Time (s))**

#### **4. SETUP OF DATA ACQUISITION HARDWARE AND SOFTWARE**

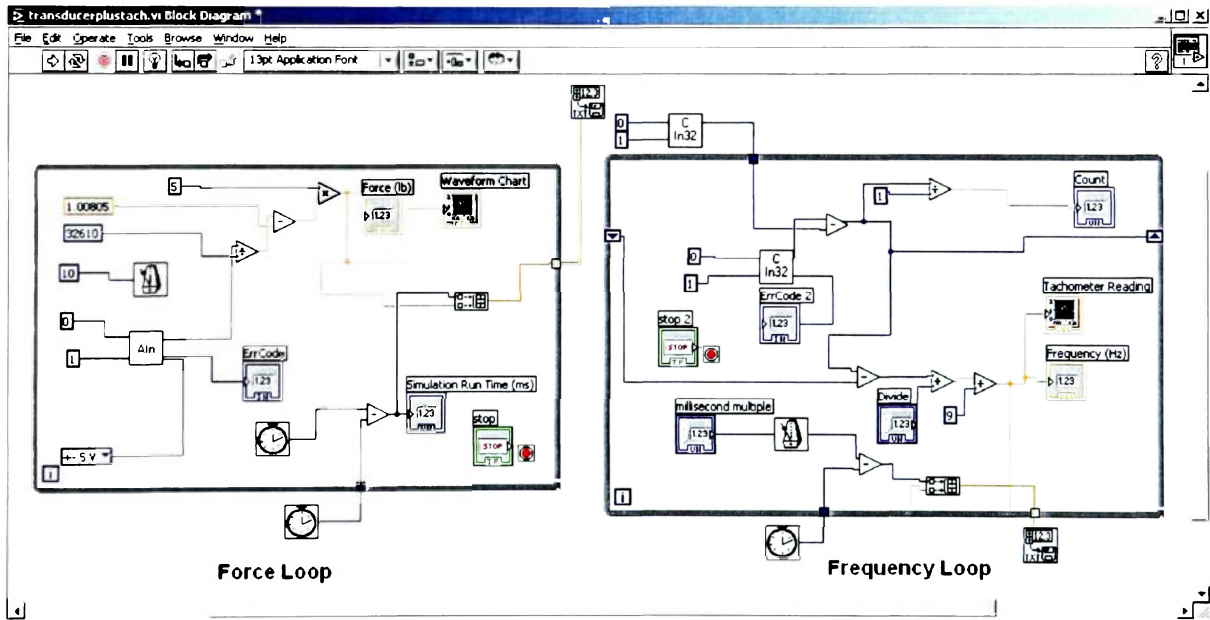
Before any data can be collected, the data acquisition hardware and software needs to be configured. The computer used for collecting the data is a Dell GX 280 with 2 GB of memory running Windows XP. Two datasets were collected in the experiment. These datasets include force (lb) vs. time (s) and frequency (Hz) vs. time (s). The frequency is measured using a Monarch Instrument Remote Optical Sensor (ROS) and force is measured using a Honeywell Sensotec Model 31  $\pm$  5 lb force transducer (or load cell). This measured data is then recorded using a Measurement Computing PMD-1680FS external USB data acquisition card (DAQ). The hardware used in the experiment is shown in Figure 4.1.



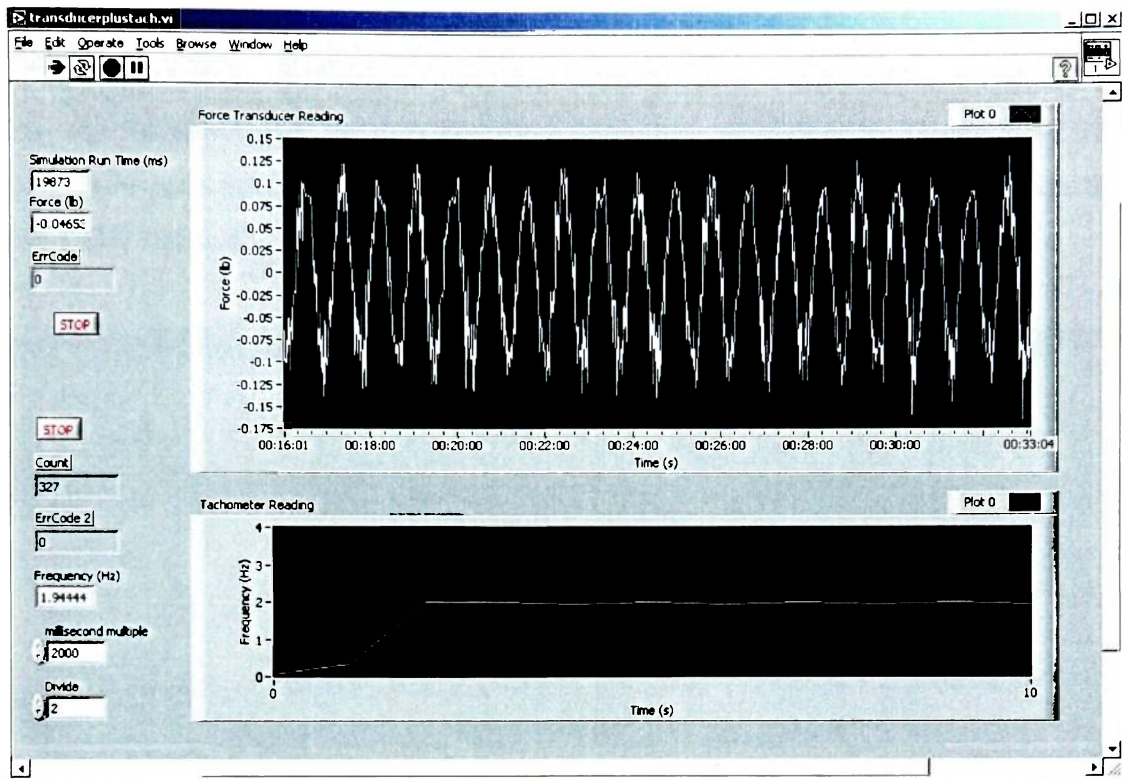
**Figure 4.1. Data Measurement Hardware**

LabVIEW is used as the data acquisition software to collect the data. Figure 4.2 shows the block diagram for collecting the force and frequency data. The numbers on the force loop are correction factors to calibrate the force transducer. The transducer is rated at one Volt per pound so the numbers are adjusted so that, when one pound is applied to the transducer, LabVIEW indicates “1”. With no load applied to the transducer, LabVIEW indicates “0”. The frequency loop uses a built in counter in the data acquisition card to accept count information from the optical tachometer. Figure 4.3

shows the LabVIEW user interface that displays the readings for force and frequency. When the software is operating correctly, this is the only interface used. The force transducer reading is shown on the upper window while the frequency is shown on the lower window. The simulation running time is displayed on the left for the force transducer reading along with the current force reading. The “stop” buttons on the left side of each display stop the simulation and export the collected data as a two column “Excel” file. The frequency count is also displayed on the left of the tachometer reading along with the frequency. The “millisecond multiple” is a timer that controls how many counts are taken in for calculating each frequency point. Increasing the time between samples can increase the frequency accuracy because calculating the frequency is a reactive step. After several trial-and-error tests, it was found that a 2 second sample interval proved to be sufficient.



**Figure 4.2. LabVIEW Block Diagram for Force and Frequency Collection**



**Figure 4.3. LabVIEW User Interface Displays Readings for Force and Frequency**

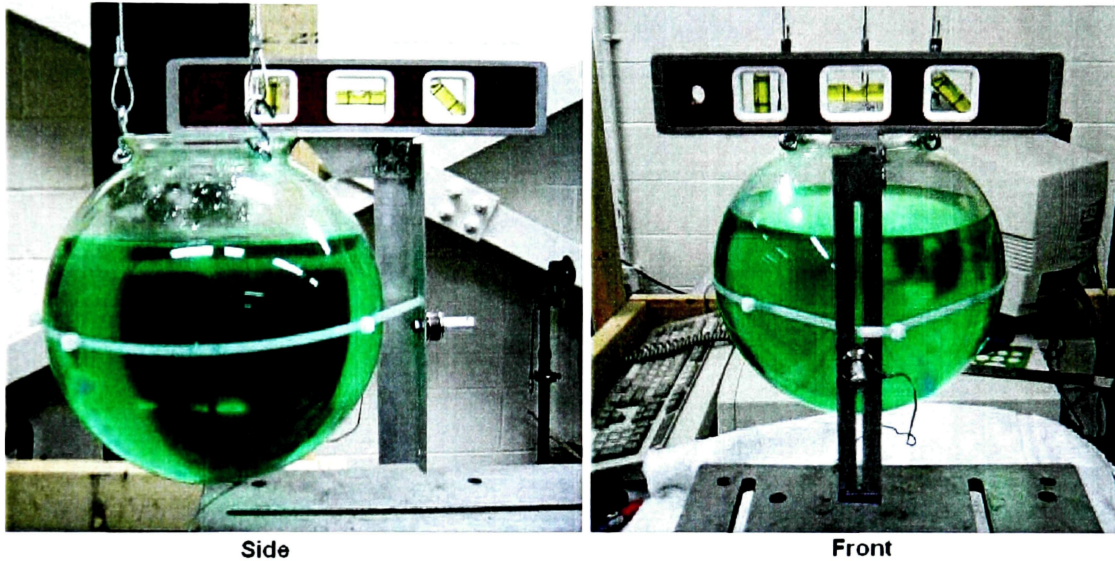
## **5. PREPARATION FOR DATA COLLECTION**

Before the data can be collected, several steps must be followed to ensure the accuracy of the data. Steps common for both the pendulum frame experiment and the tank experiment include hanging the pendulum/tank assemblies, measuring the pendulum ballast/tank liquid, and calibration of the force transducer. For the pendulum frame, the proper pendulum length as well as the pendulum's moment of inertia must be calculated. For the tank, the proper mounting positions for the force transducer must be determined.

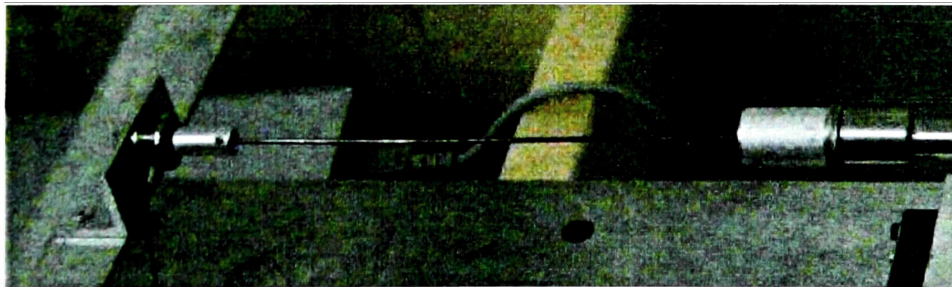
### **5.1. Mounting the Pendulum/Tank Assemblies**

Both the pendulum frame and the tank need to be balanced so that the motion of the pendulum and the fluid slosh simulates a one degree-of-freedom system. Figure 5.1 illustrates this balancing procedure for hanging the propellant tank. Turnbuckles on the

mounting frame (Appendix A) are used for vertical position and fine balance adjustments of both assemblies. For coaxial adjustment, the locomotive assembly is positioned so that the “stinger” lines up with the force transducer as shown in Figure 5.2. The transducer set screw is then used to adjust the output voltage to zero based on the LabVIEW readout<sup>3</sup>.



**Figure 5.1. Balancing and Vertical Positioning of the Tank Assembly**



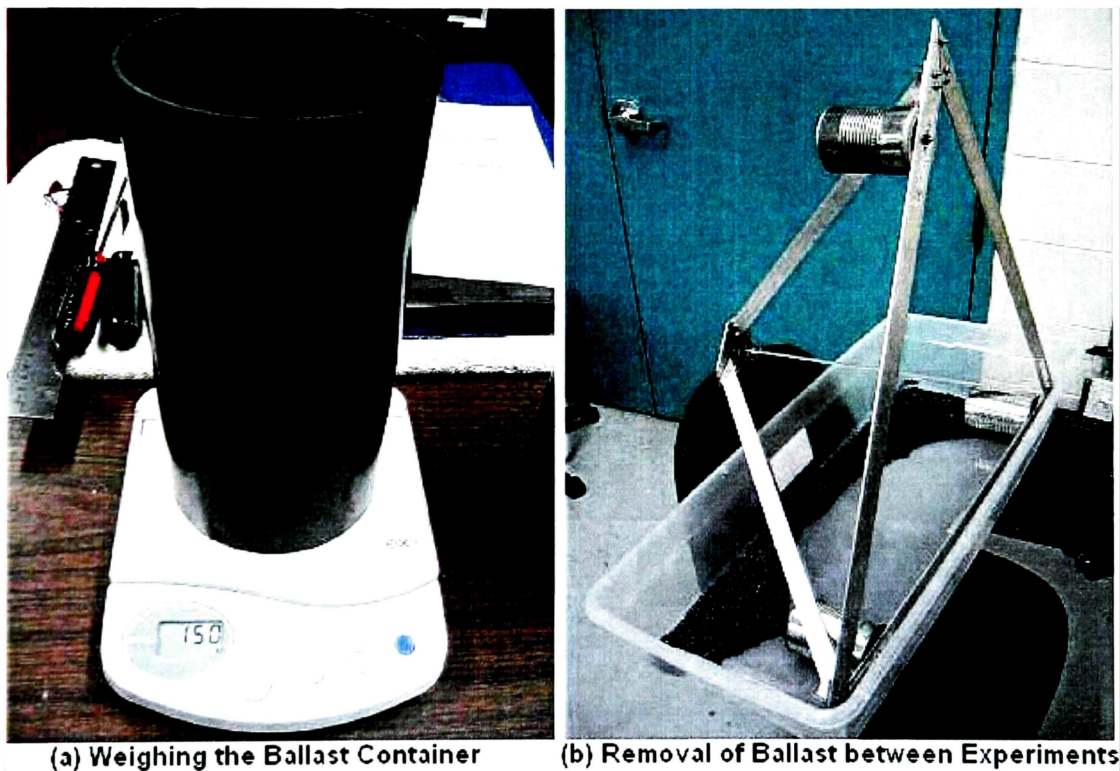
**Figure 5.2. Aligning the “Stinger” with the Force Transducer Mounted to the Pendulum Assembly**

---

<sup>3</sup> The flywheel must also be set to  $\pm 90$  degrees, or the “neutral” position.

## 5.2. Measuring of the Pendulum Ballast/Tank Liquid

Both the pendulum ballast and the water were measured using a Royal eX5 five pound postal scale accurate to  $\pm 0.0022$  lb (1 gram). The ballast for the pendulum is lead pellets weighing about one fourth of a gram each. With the ballast and liquid, obtaining the masses required by the SLOSH code was obtained without any difficulty<sup>4</sup>. Figure 5.3(a) illustrates the measurement of the ballast. The liquid is measured in a similar way. Figure 5.3(b) illustrates the removal of the ballast from the pendulum assembly between tests. It was found that it is faster to disconnect the force transducer and the pendulum frame and dump out the ballast than to remove it manually.

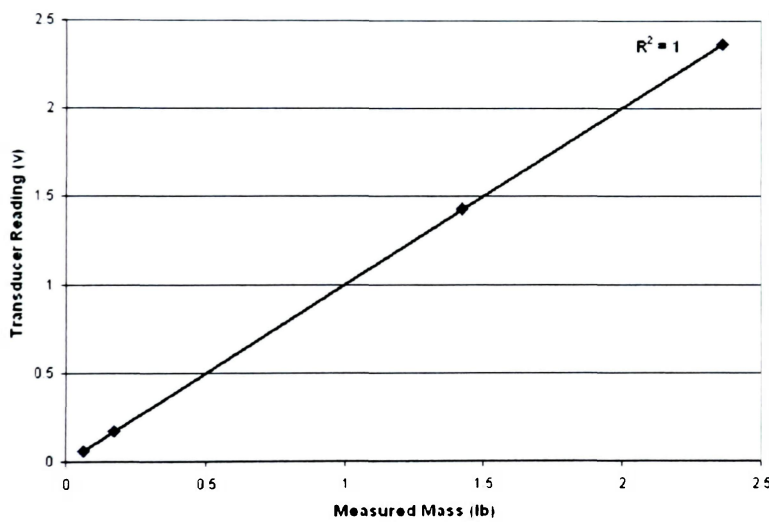


**Figure 5.3. Weighing the Ballast Container**

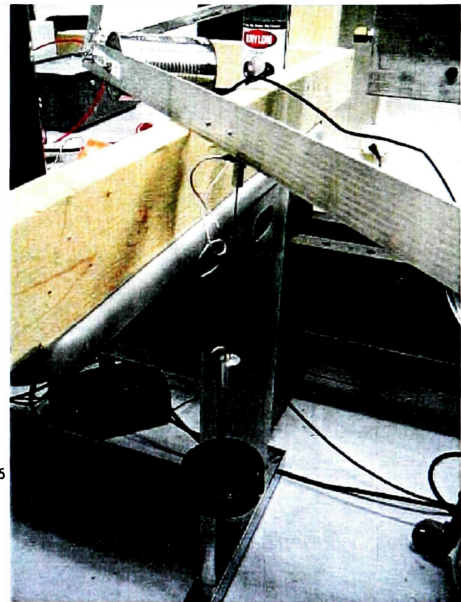
<sup>4</sup> Ballast and liquid measurement tables are provided in Appendix C.

### 5.3. Calibration of the Force Transducer

Even though the force transducer was calibrated by the vendor, it was still tested to verify its accuracy. Figure 5.4(a) illustrates the addition of weight to induce a tension force in the transducer. Figure 5.4(b) shows the linear calibration curve for the force transducer. The equipment to test for compression loads was not available. However, due to the  $R^2$  value being one (perfectly linear voltage reading vs. measured mass), the transducer was deemed accurate.



Above (a) Force Transducer Calibration  
Right (b) Force Transducer Calibration Testing



**Figure 5.4. Force Transducer Calibration**

#### 5.4. Pendulum Assembly Only: Proper Pendulum Length

The pendulum's center of mass was calculated by the centroid equation:

$$y_{CG} = \frac{\sum \bar{y}M}{\sum M} \quad (1)$$

Where:

$y_{CG}$  = System center of mass (CG)

$\bar{y}$  = Local center of mass

$M$  = Mass of part

Data provided by Table 5.1 was used to determine the pendulum's center of mass of the pendulum assembly.

**Table 5.1**  
**Pendulum Mass and Geometric Properties**

Fill Level	60%	70%	80%
Pendulum Height (in)	0.9173	0.8346	0.6024
Pendulum Mass (lb)	2.7050	2.4647	1.7747
Pendulum Rod Mass (lb)	0.0882	0.0882	0.0882
Pendulum Rod Length (in)	4.2008	4.2008	4.2008
SLOSH Predicted Pendulum Length (in)	2.2327	1.8669	1.4457
Pendulum Mounting Bolt Height (in)	0.3429	0.3429	0.3429
CG Location Reference Point* (in)	3.0386	2.6188	2.0572
*This point marks the bolt location reference point on the pendulum rod to match the predicted SLOSH center of mass location			

The final center of mass location reference points are marked on the pendulum rod for each simulated fill level.



### 5.5. Pendulum Assembly Only: Pendulum’s Moment of Inertia

Ensuring that the simulation has the proper moment of inertia is a very important step. Unlike the locomotive assembly, which has fixed motion determined by the flywheel’s angular velocity, the pendulum is able to move independently. The pendulum container was assumed to be an ideal cylinder where:

$$I_{xx} = I_{yy} = \frac{1}{12} Mh^2 + \frac{1}{4} MR^2$$

$$I_{zz} = \frac{1}{2} MR^2$$
(2)

Where:

- $M$  = Cylinder mass
- $h$  = Cylinder height
- $R$  = Cylinder radius

Table 5.2 provides information on the pendulum cylinder properties as well as the moment of inertia values for the pendulum container<sup>5</sup>.

**Table 5.2**  
**Pendulum Cylinder Properties and Moment of Inertia Values**

Fill Level	60%	70%	80%
Pendulum Radius (in)	1.9528	1.9528	1.9528
Pendulum Height (in)	0.9173	0.8346	0.6024
Pendulum Mass (lb)	2.7050	2.4647	1.7747
Ixx (lb/in <sup>2</sup> )	2.7684	2.4927	1.7455
Iyy (lb/in <sup>2</sup> )	2.7684	2.4927	1.7455
Izz (lb/in <sup>2</sup> )	5.1575	4.6993	3.3837

<sup>5</sup> These moment of inertia values were also used for the “tank” tests.

## F. Tank Assembly Only: Force Transducer Mounting Location

In order to ensure that the center of mass of the tank assembly lines up with the force transducer, the vertical center of mass at all fill levels was calculated using the information in Table 5.3.

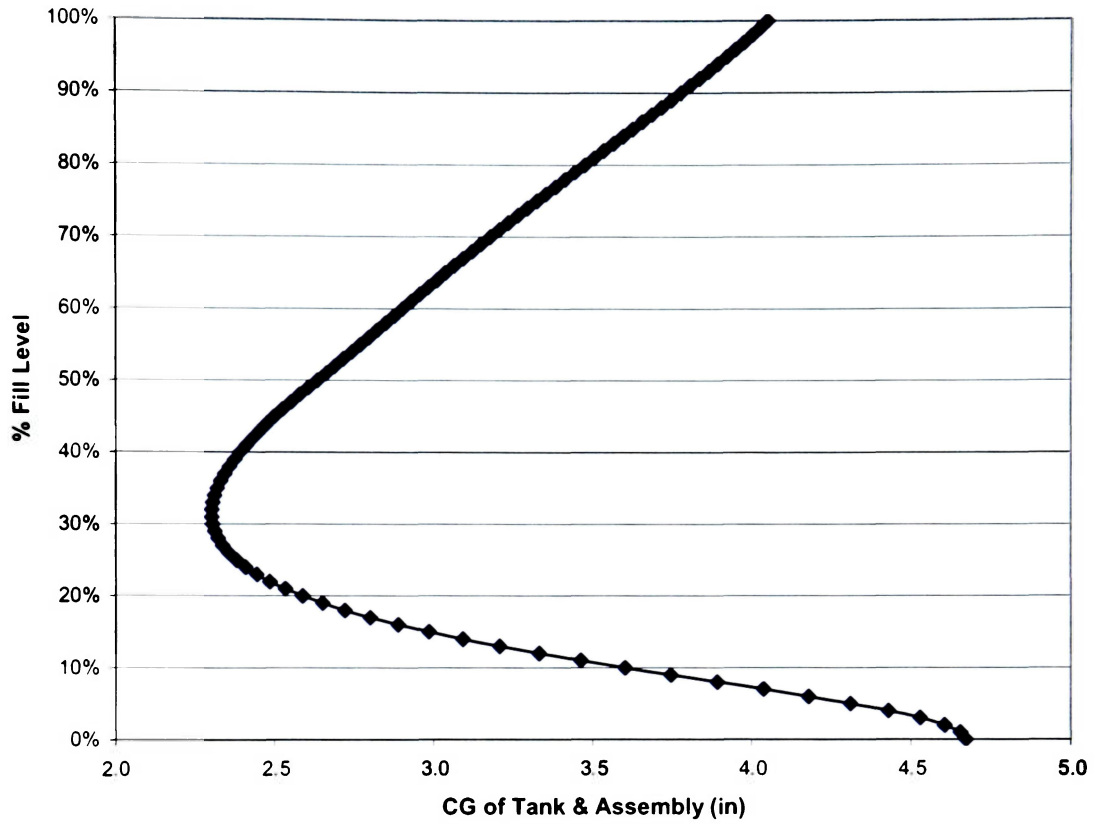
**Table 5.3**  
**Tank Assembly and Geometric Properties**

Water Density (lb/in <sup>3</sup> )	0.03604
Dry Tank Mass (lb)	0.55560
Top Mount Mass (lb)	0.10465
Side Mount Mass (lb)	0.13123
Dry Tank Center of Mass Location (in)	4.00000
Top Mount Center of Mass Location (in)	3.71800
Side Mount Center of Mass Location (in)	8.28125
Water Center of Mass Location (in)	Variable <sup>6</sup>

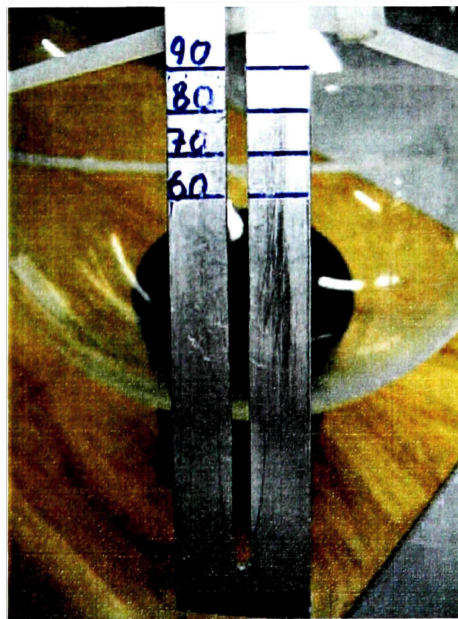
Figure 5.5 illustrates the non-linear variation of center of mass location with various fill levels. Figure 5.6 shows the “fill-level” marks on the tank assembly’s transducer mounting rail.

---

<sup>6</sup> A detailed explanation of calculating the center of mass of a liquid at variable fill levels in a sphere can be obtained from: <http://mathworld.wolfram.com/CircularSegment.html>



**Figure 5.5. Center of Mass Locations of Tank Assembly at Various Fill Levels**



**Figure 5.6. Center of Mass Marks on Transducer Mounting Rail**

## **6. CALIBRATION OF EXPERIMENT AND SIMULATION**

Before parameter estimation, three important steps must be carried out in order to calibrate the experiment and the simulation. The first step is to create a filter to process the raw data from the force transducer. The noise signals generated by the DC motor and vibrations from the mechanical components of the locomotive arm needs to be filtered. The second step is to test the validity of the SLOSH code by comparing the natural frequency of the fuel to that predicted by the code. Finally, a “frozen” mass test must be conducted to verify the proper operation of the experiment and the simulation.

### **6.1. Data Processing**

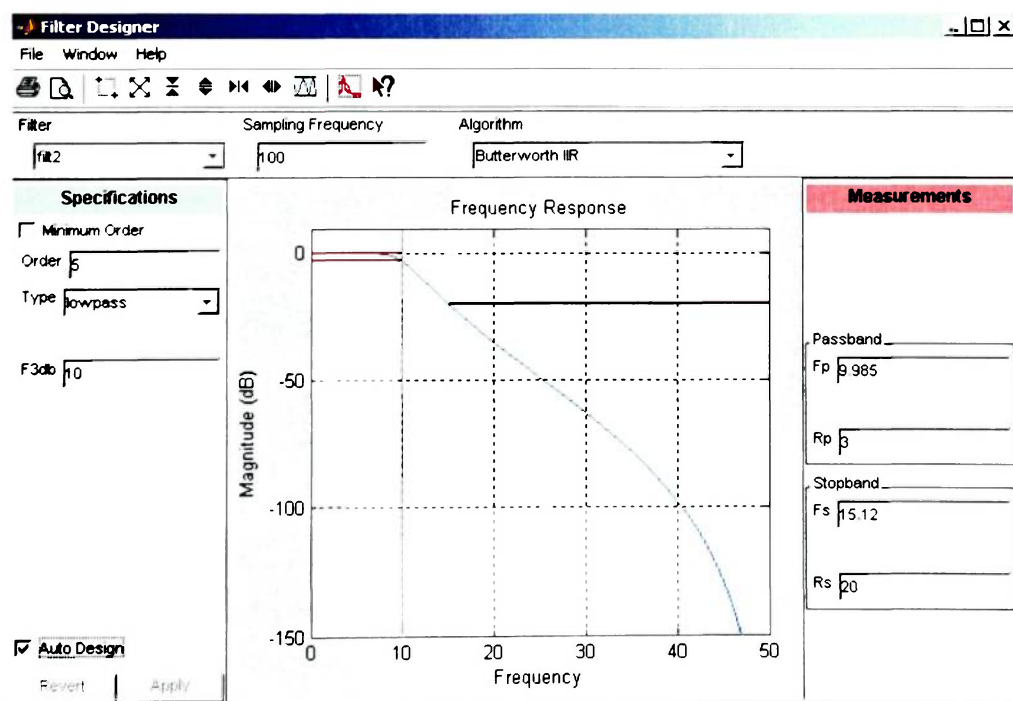
There are several components of the experimental setup that generate high-frequency noise in the data. Sources of noise for both the pendulum testing and the tank testing include vibrations from the DC motor, drive-shaft, locomotive arm bearings, and mounting hardware. This mounting hardware includes hooks, turn-buckles, and cables. The cables and turn-buckles are needed to adjust the tank/frame position to line up to the locomotive assembly. Both are located just over four feet from the force transducer in order to minimize this noise. Other sources of noise in the data come from small vibrations in the joints and from the elastic deformation of the aluminum frame. The tank, due its high rigidity and lack of moving parts, contributes little to the overall noise of the system. However, data from tank testing must still be filtered due to other noise sources mentioned above.

MATLAB’s Signal Processing (SP) Toolbox is used to filter the data. Before a filter can be applied to the data, it must be imported into MATLAB. The data collection time step size is 10 ms. The test length is determined by the type of testing used in the experiment. Table 6.1 provides the different test types and the data collection times for the experiment.

**Table 6.1**  
**Summary of Test Durations**

	Collection Time (s)	Number of Data Points
Natural Frequency (pendulum)	2-4	201-401
Natural Frequency (sphere)	2-14	201-1401
Frozen Test (pendulum)	20	2001
Frozen Test (sphere)	20	2001
Pendulum Test (actual)	30	3001
Sphere Test (actual)	30 <sup>7</sup>	3001

Once imported into MATLAB, this data can then be analyzed using the SP Toolbox. The functions of this toolbox can be categorized into three groups: signals, filters, and spectra. First, the signal must be imported into the SP toolbox. Only the raw force data needs to be imported as the frequency (step size) is given by the user. Next, a filter needs to be created using the “filter designer” feature located in the filters group as shown in Figure 6.1.



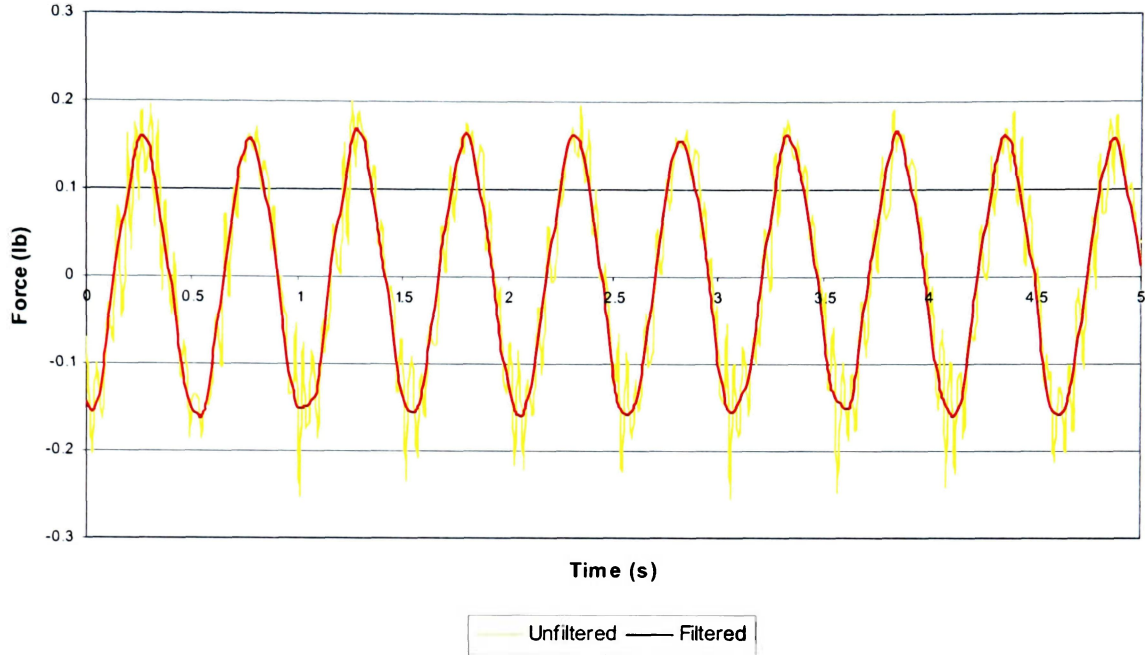
**Figure 6.1. “Filter Designer” for Signal Processing Toolbox**

<sup>7</sup> 60% fill level test length is 60 seconds.

The type of filter algorithm used is the low-pass filter using the Butterworth infinite impulse response (IIR) algorithm. This is set to filter out frequencies above 10 Hz. The “auto design” box is used to automatically set the optimal pass band and stop band settings. The sampling frequency of 100 samples per second corresponds to the data collection rate of one sample every 10 ms. After this is set, the filter can then be applied using a zero phase IIR (MATLAB function: `filtfilt`) algorithm. This algorithm is designed to maintain the proper phase relationship between the unfiltered and filtered data. Once the filter is applied to the raw signal, this new filtered signal can be exported from the SP toolbox to the Matlab workspace. The difference in the raw and filtered data is very apparent as illustrated in Figure 6.2<sup>8</sup>. The last feature of the SP toolbox is the spectrum analyzer which identifies regular periods within the data and displays peaks of common frequencies. This is a useful verification tool for comparing the frequency measured by the data acquisition software and the frequency observed by the SP toolbox. The SP tool box was used to determine the proper filter settings. It was verified that the frequency predicted by the spectra tool and that measured experimentally is within a tolerance of about 1.5%.

---

<sup>8</sup> Post-filtered data (for ALL tests) is manually set to start at a flywheel angle of approximately zero radians, or the first minimum peak amplitude of the dataset.

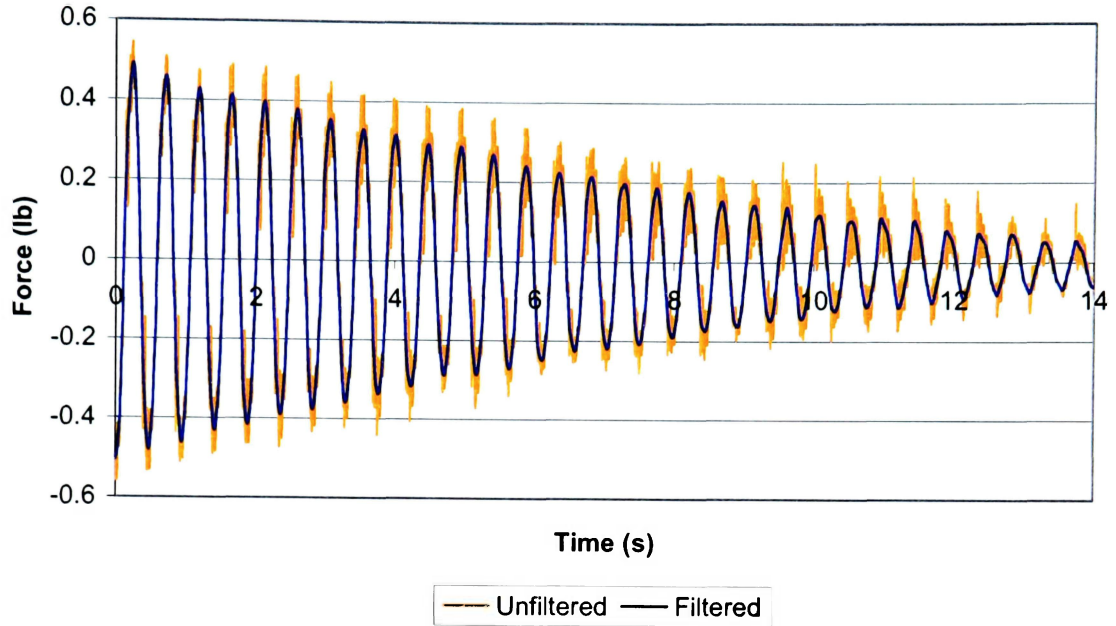


**Figure 6.2. Comparison of Unfiltered and Filtered Data (60% at 1.953Hz)**

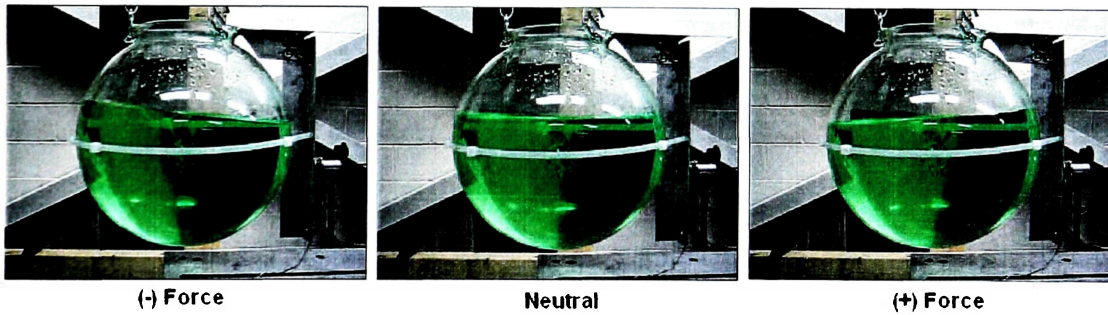
## 6.2. SLOSH Code Natural Frequency Verification

Calculating the natural frequency of the tank at various fill levels is an effective way to verify the predictions of the SLOSH code. In order to determine the natural frequency, the tank must be excited close to its predicted natural frequency. This can be determined visually as the fluid in the tank starts to slosh with a high degree of turbulence near its natural frequency. The excitation can be stopped and the fluid allowed to come to rest naturally once the vicinity of natural frequency is reached. As with a pendulum, this damped natural motion provides a very close approximation of the natural frequency<sup>9</sup>. Figures 6.3 and 6.4 illustrate the natural damping of the fluid and the three states of the fluid during this test respectively. Table 6.2 compares the natural frequency predicted by the SLOSH code to that measured experimentally.

<sup>9</sup> A pendulum coming to rest provides a frequency slightly larger than the natural frequency. In an ideal system, the pendulum motion would match the natural frequency.



**Figure 6.3. Natural Damping of Tank at 60% Fill Level**



**Figure 6.4. Natural Damping Slosh Positions for 60% Fill Level**

**Table 6.2  
Natural Frequency (NF) Comparisons**

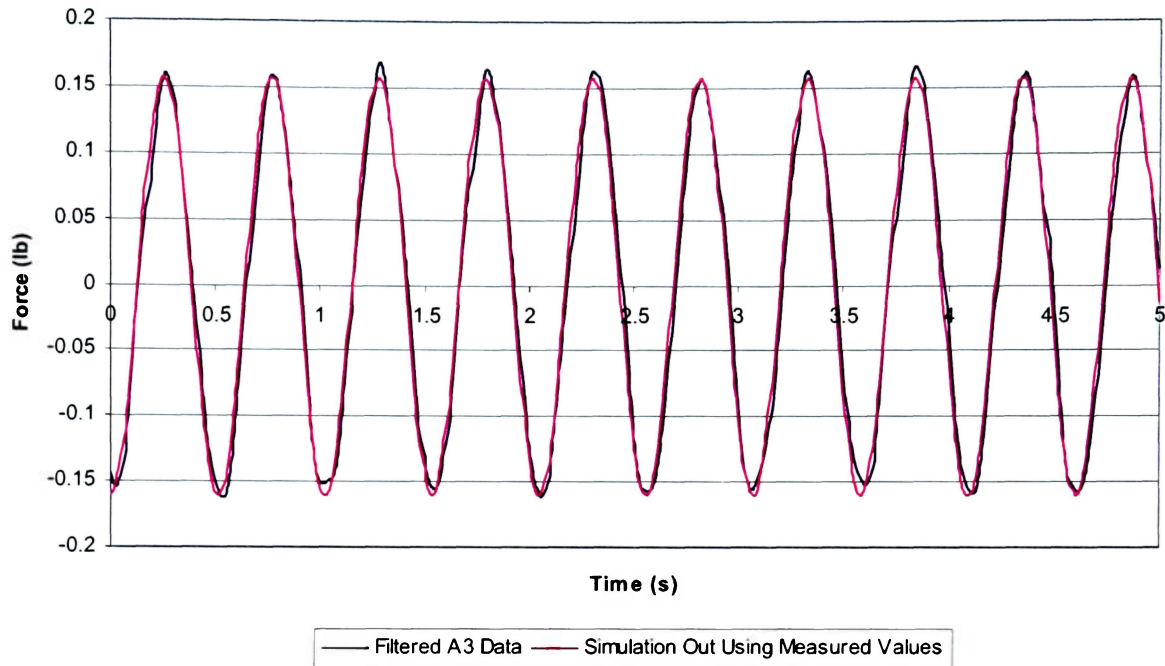
Fill Level	SLOSH Code Predicted NF	Experimentally Calculated NF	Percent Difference
60%	2.092Hz	2.148Hz	2.61%
70%	2.288Hz	2.343Hz	2.35%
80%	2.600Hz	2.734Hz	4.90%



The SLOSH code predicts the natural frequency of the tank accurately. Error for all three tests averages about 3%. The experimentally calculated natural frequencies are also slightly higher than those predicted by the SLOSH code. Possible reasons for this are that the damping in the tank is slightly higher than predicted and/or the tank is not exactly eight inches in diameter. It must be noted that the tank will be tested with fill levels ranging from 60-80%. The lower limit of 60% is close to the minimum weight of the pendulum assembly while the upper limit of 80% is due to the maximum practical fill level in the tank assembly when excited.

### **6.3. Frozen Mass Testing**

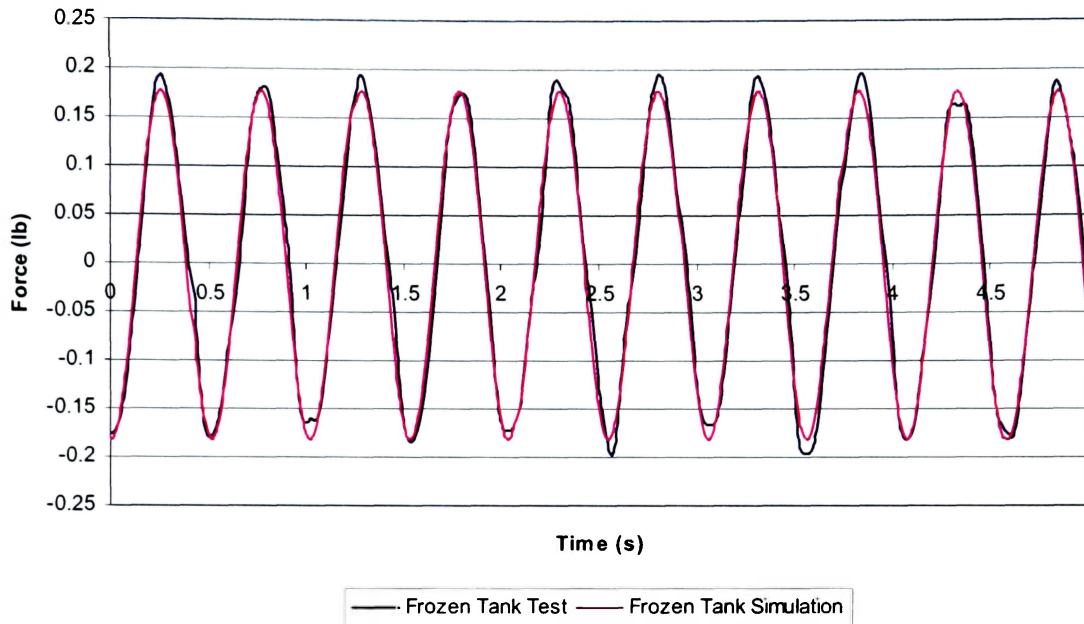
The final step before the conducting the automated parameter identification process involves frozen mass testing (Schlee et al. 2006 [16-18]). That is, the experiment and the simulation are tested with no pendulum attached in order to simulate the force response that would be expected if the water was physically frozen in the tank. With many potential sources of error in both the experiment and the simulation, the frozen mass testing is critical for a successful parameter identification method. Raw data acquisition, data filtering, simulation timing, experiment/simulation sampling rates, experiment/simulation geometry, and experiment/simulation mechanics must be synchronized for effective test results. After the trial and error process, the results of the frozen mass test are shown in Figure 6.5. The overall error in maximum force, minimum force, and overall amplitude of the forces is about 3.4%, 2.4%, and 3.0% respectively.



**Figure 6.5. Simulation Verification Using Measured (Not Estimated) Parameters  
(60% at 1.953 Hz)**

As a final verification of the frozen mass test, the water in the tank was physically frozen and tested at a 60% fill level to verify the results found in Figure 6.5. A comparison between the simulation and the frozen tank is illustrated in Figure 6.6<sup>10</sup>. Error for the overall amplitude in this test is about 3%. It must be noted that for this test, as well as all future tank tests, the mass of the tank assembly is incorporated into the simulation as a fixed mass. As a result, there is a slight increase in peak amplitude in the force response shown in Figure 6.6 from that shown in Figure 6.5. Now that the simulation and the experiment are synchronized, the automated parameter identification process can be initiated.

<sup>10</sup> Frozen tank test results are provided in Appendix D.



**Figure 6.6. Frozen Tank Test Comparison (60% at 1.953 Hz)**

## **7. FROZEN MASS PARAMETER ESTIMATION**

Now that the simulation is calibrated, the parameter estimation process is carried out. The first step in identifying the parameters is, in effect, a continuation of the frozen mass testing in the previous section. Primary parameters such as locomotive arm travel length or frozen mass can be treated as parameters for estimation. In this case, frozen mass is treated as the only parameter. The parameter is well-known and the parameter estimation process can be checked with these known values. Two parameter identification approaches each using Newton's nonlinear least squares are used to determine the parameters. The first approach is conducted traditionally using standard M-Code<sup>11</sup>. The second estimation method is a "black box" approach using MATLAB's Parameter Estimation Toolbox. Fifteen estimations were performed with each method (5 frequencies at each fill level).

Standard MATLAB M-code is used for the first approach to run Newton's method for non-linear least squares (MATLAB function: `lsqnonlin`). The first step in

<sup>11</sup> M-Code is provided in Appendix E.

this method is to define the parameters. For the frozen mass test case, one primary and two secondary parameters are considered. These are frozen tank mass, angular velocity correction constant, and initial flywheel angle. While it is obvious that the frozen tank mass is the primary parameter, the reason for the other two secondary parameters is less apparent. These parameters deal with a small phase-shift between the experimental and simulated data. Simulation operating parameters must be very accurate in order to obtain proper values for frozen mass and subsequently the pendulum properties. The angular correction factor constant is a minor correction applied to the operating frequency of the simulation to minimize the phase shift between the simulation and experimental data. This value is approximately  $\pm 0.04$  rad/s. The initial flywheel angle sets the starting angle of the flywheel. If not for this secondary parameter, the simulation would always start at a flywheel angle of zero radians. In reality, the flywheel rarely starts at this angle. Typical initial flywheel angle values, based on the standard data selection method, range from  $\pm 1$  radian. The SimMechanics blocks for both the angular velocity correction constant and the initial flywheel angle can be seen in Group I in Figure 3.4. A lower and upper bound for each parameter must be given to the algorithm as well as conditions such as initial conditions, maximum iterations, maximum function evaluations, and parameter tolerances. The experimental data such as the data illustrated in Figure 6.5 is input to provide a tolerance for convergence of the parameters being estimated. The limits used in the frozen mass parameter estimation tests can be seen in Table 7.1

**Table 7.1**  
**Frozen Mass Test Parameter Estimation Limits**

Key:	Default Limits for all Frozen Testing					
A Series: 60% Fill Level Tests	A Series (All)		B Series (All)		C Series (All)	
B Series: 70% Fill Level Tests	Lower	Upper	Lower	Upper	Lower	Upper
C Series: 80% Fill Level Tests	-2.0	2.0	-2.0	2.0	-2.0	2.0
Flywheel Initial Angle (rad)	-2.0	2.0	-2.0	2.0	-2.0	2.0
Angular Velocity Correction (rad/s)	-0.5	0.5	-0.5	0.5	-0.5	0.5
Predicted Mass (lb)	4.0	+Inf	4.0	+Inf	4.0	+Inf

The convergence criterion is defined by:

$$R = \sum [abs(E) - abs(S)]^2 \quad (1)$$

Where,

$R$  = Residual

$E$  = Reaction forces obtained from the experiment

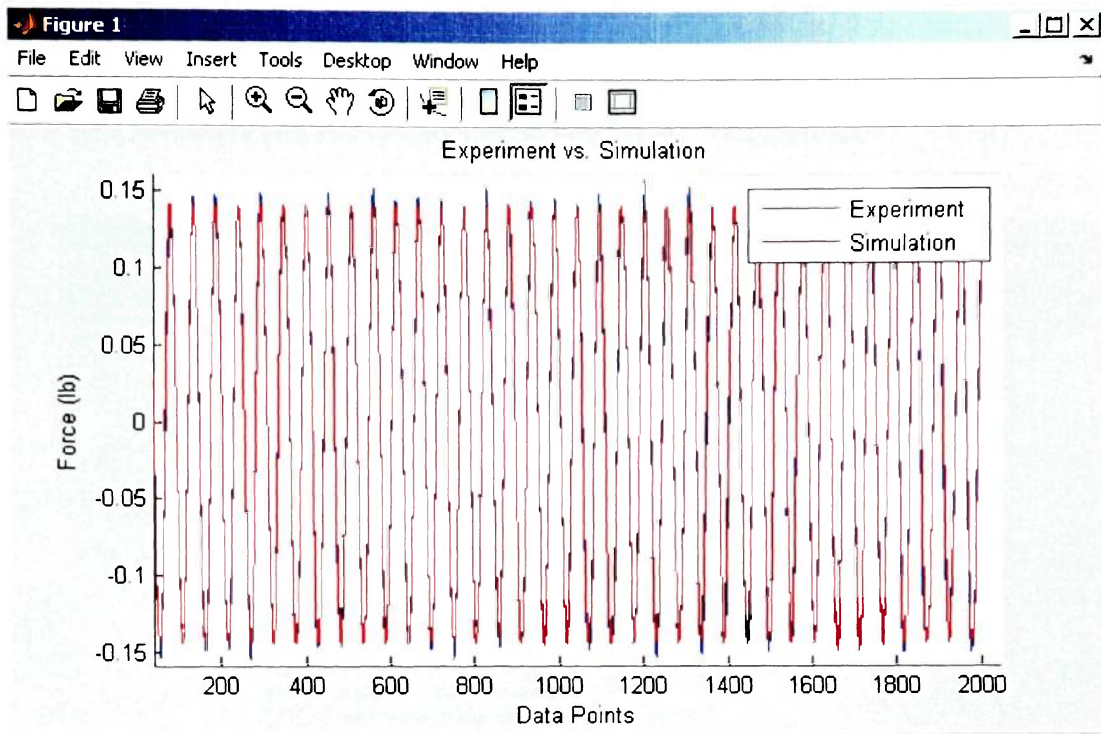
$S$  = Reaction forces obtained from the MATLAB simulation

The Parameter Estimator Toolbox refers to this residual as the “cost function”. For the frozen mass testing, the tolerance criterion for convergence of the cost function was set to 10e-6. The M-code parameter estimation results for a simulated frozen mass at 60% fill level at several different frequencies are shown in Table 7.2. Figure 7.1 provides a comparison of the results between the experiment and simulation.

**Table 7.2**  
**Newton’s Nonlinear Least Squares M-Code Parameter**  
**Identification Results for a 60% Frozen Fill Level<sup>12</sup>**

Measured 60% Mass (lb)	6.2655				
Measured Test Frequency (Hz)	1.66	1.855	1.953	2.343	2.637
Predicted Mass (lb)	6.0302	6.1236	6.1937	6.0173	5.9599
Flywheel Initial Angle (rad)	-0.2373	-0.0775	-0.1191	-0.2034	-0.5209
Angular Velocity Correction (rad/s)	0.0752	0.1159	-0.0004	0.4369	-0.0794
Mass % Difference from Measured	3.76%	2.26%	1.15%	3.96%	4.88%

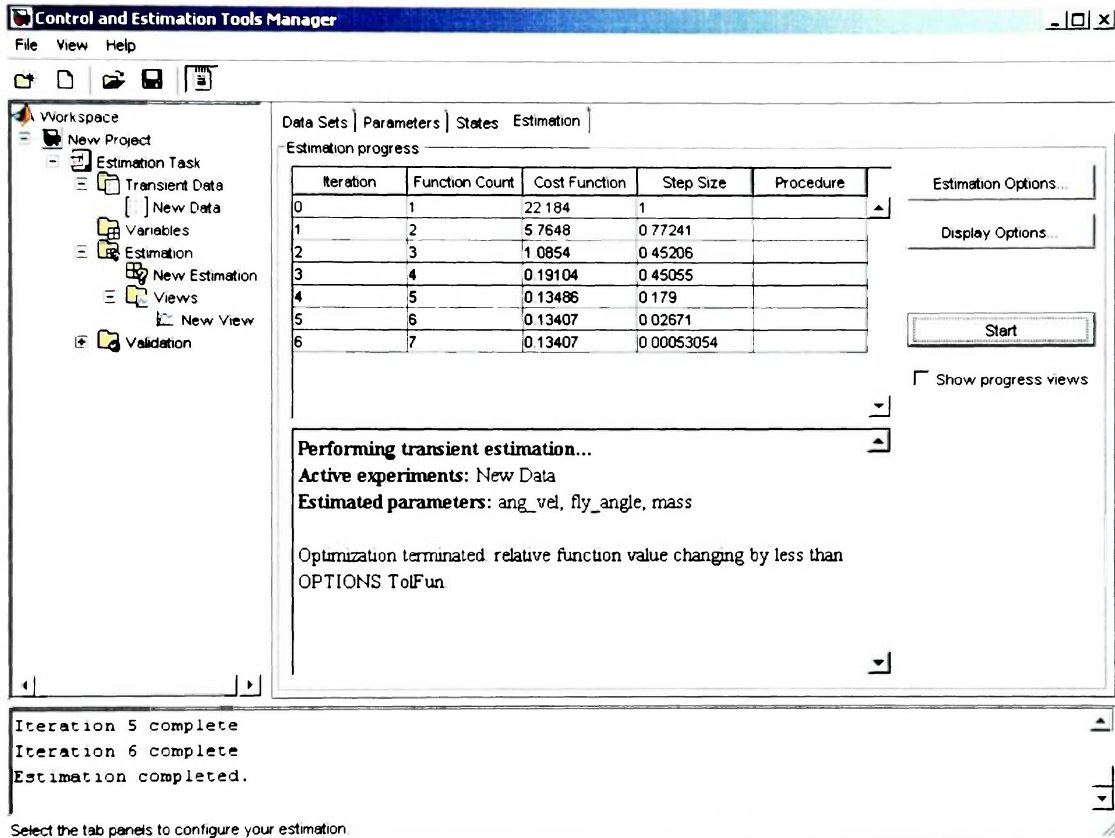
<sup>12</sup> M-Code parameter identification results for 70% and 80% fill levels are provided in Appendix F.



**Figure 7.1. Frozen Mass Parameter Identification Results Using M-Code  
(60 % at 1.855Hz)**

The second parameter identification approach uses MATLAB's Parameter Estimator Toolbox. This toolbox provides a graphical interface enabling the user to use a powerful suite of optimization tools. The Parameter Estimation toolbox user interface is illustrated in Figure 7.2. The first step in using the parameter estimator is to prepare the SimMechanics model. The estimator requires that the simulation has an output block so that it can extract output data (tank reaction force) from the model and compare it with the transient, or measured data. An optional input block can also be incorporated into the simulation. This enables the user to specify a specific frequency scheme if desired. Since these tests are performed at a constant frequency, an input table was not used. Each parameter (frozen mass, angular velocity correction, and initial flywheel angle) must also be supplied to the MATLAB workspace before starting the Parameter Estimator Toolbox. The angular velocity input (for reference) and tank reaction output blocks can be seen in Groups I and II in Figure 3.4. The measured data is imported from a spreadsheet as an input (if desired)/output data vs. time dataset. Each dataset must start

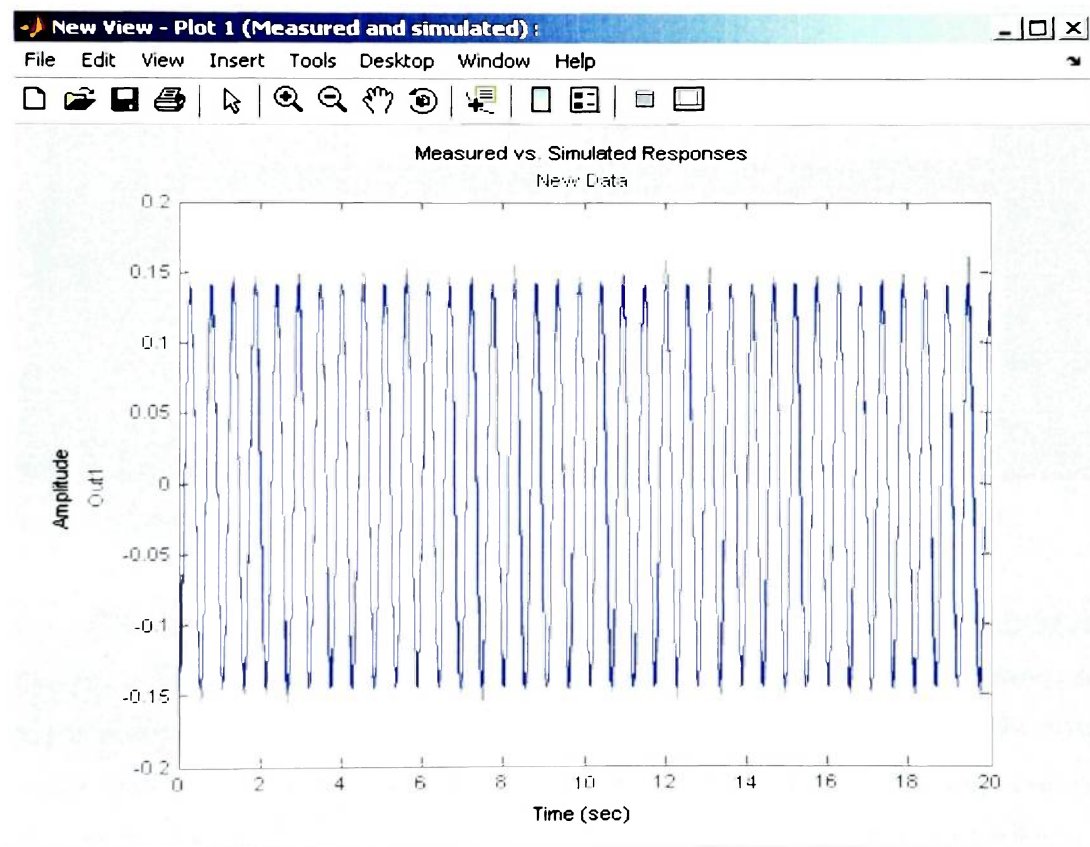
and end at the same time and have the same number of data points. For example, if a test is run for 20.00 seconds with a data collection rate of 10 ms, each column would have 2001 data points starting at 0.00 seconds and ending at 20.00 seconds.



**Figure 7.2. Parameter Estimator Graphical User Interface During Frozen Mass Test (60% at 1.855Hz)**

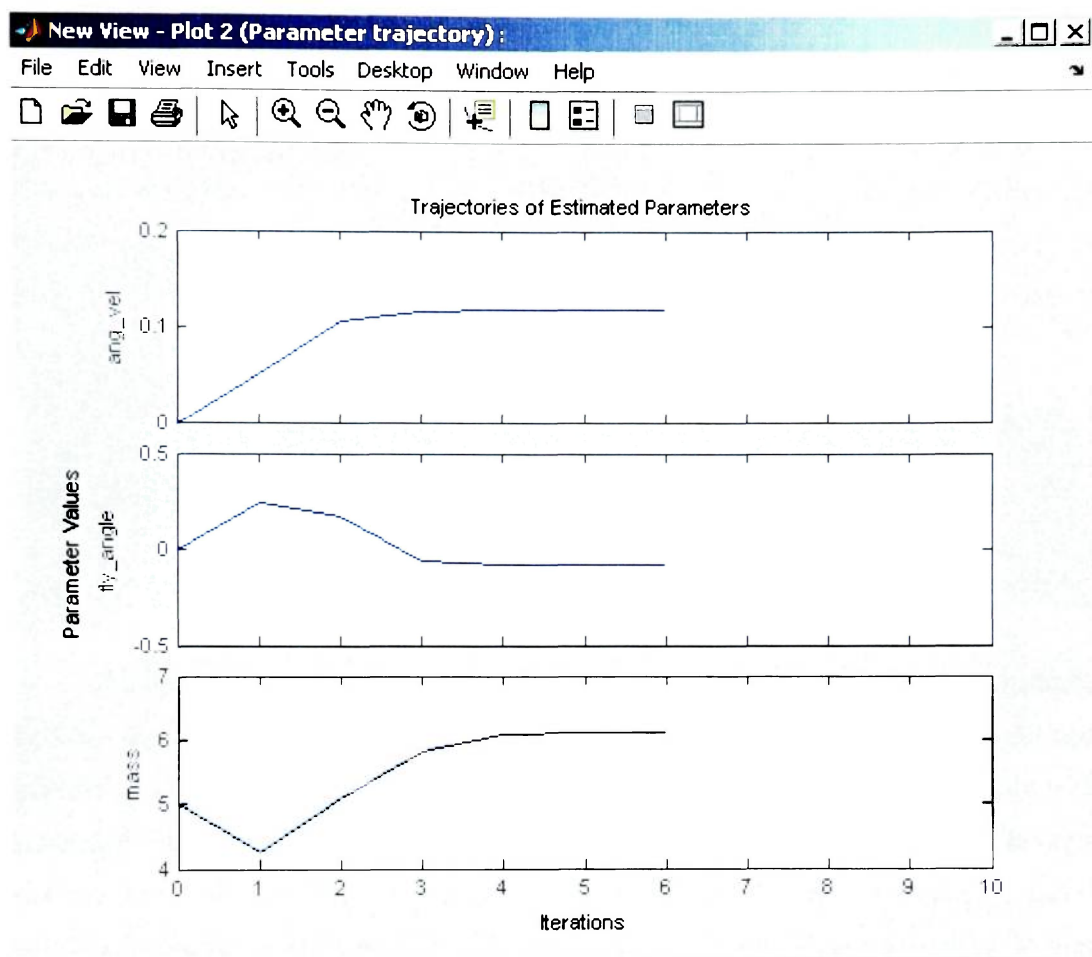
Once the measured data is entered, the variable limits can then be defined. In this case the variables for frozen tank mass, angular velocity correction constant, and initial flywheel angle are `ang_vel`, `mass`, and `fly_angle` respectively. The cost function is defined by equation (1). Once these limits are established, a new estimation can be developed. Parameter Estimator has many different optimization algorithms available. For comparison to the M-Code method, Newton's nonlinear least squares will be selected.

One of the benefits of the Parameter Estimation Toolbox is that the parameter estimation can be viewed in real-time. That is, the user can observe the parameters changing values as the optimization progresses and see how the parameters affect the simulation response. This information is referred to by MATLAB as the measured vs. simulated response and the parameter trajectory. Figure 7.3 shows the comparison of the optimized solution with the measured data while Figure 7.4 illustrates the change in parameters with each iteration during the parameter identification process.



**Figure 7.3. Real-time Measured (Grey) vs. Response (Blue) Plot (60% at 1.855Hz)**





**Figure 7.4. Real-time Parameter Trajectory Plots (60% at 1.855Hz)**

Once the parameter trajectories become constant, the parameter estimation can be manually terminated by the user for fast estimations. For more accurate estimations, the optimizer can iterate until a pre-defined stopping criterion is met as indicated in the status window of the Parameter Estimator interface shown in Figure 7.2. In this case, the stopping criterion is defined as the cost function changing by no more than  $10e-6$  for each iteration.

The Parameter Estimator results for a simulated frozen mass at 60% fill level at several different frequencies are shown in Table 7.3.

**Table 7.3**  
**Parameter Estimator Toolbox Parameter Identification**  
**Results for 60% Frozen Fill level<sup>13</sup>**

Measured 60% Mass (lb)	6.2655				
Measured Test Frequency (Hz)	1.66	1.855	1.953	2.343	2.637
Predicted Mass (lb)	6.0307	6.1241	6.1939	6.0176	5.9605
Flywheel Initial Angle (rad)	-0.2855	-0.0759	-0.1177	-0.2082	-0.5205
Angular Velocity Correction (rad/s)	0.0817	0.1192	0.0038	0.4392	-0.0714
Mass % Difference from Measured	3.75%	2.26%	1.14%	3.96%	4.87%
<b>Mass % Difference from M-Code</b>	<b>0.008%</b>	<b>0.008%</b>	<b>0.003%</b>	<b>0.005%</b>	<b>0.010%</b>

The results from Tables 7.2 and 7.3 illustrate the effectiveness of each estimation method. Both the M-Code and the Parameter Estimator Toolbox converge to the same solution value for frozen mass test case. This is an important finding because the Parameter Estimator Toolbox is a “black box” program. By knowing that its output matches Newton’s method as indicated by the graphical user interface, it can be concluded that the process of setting up the Toolbox for parameter estimation is being done correctly. Pendulum and tank parameter identification is then initiated.

## **8. PENDULUM FRAME AND TANK PARAMETER ESTIMATION**

### **8.1. Test Procedure**

Two of the parameters used in the frozen mass tests are retained for the pendulum frame and tank tests while three new parameters are added. The two parameters retained from the frozen test are the initial flywheel angle (rad) and angular velocity correction (rad/s) while the new parameters are pendulum length (in), pendulum hinge spring

---

<sup>13</sup> Parameter Estimator Toolbox parameter identification results for 70% and 80% fill levels are provided in Appendix G.

constant (ft-lb/rad), and pendulum damping constant (ft-lb/rad/sec<sup>14</sup>). Recall that the MATLAB simulation is the same for each case. This means that the simulation will be provided datasets from both the pendulum frame and tank without an indication of the type of the dataset. Three tests were conducted at each fill level for the pendulum frame and tank making it a total of 3 x 3 x 2 (18 tests). Parameters for each test were then determined using each estimation method bringing the total number of tests to 36. The upper and lower bounds of each method (M-Code and Parameter Estimator) were fixed as indicated in Table 8.1.

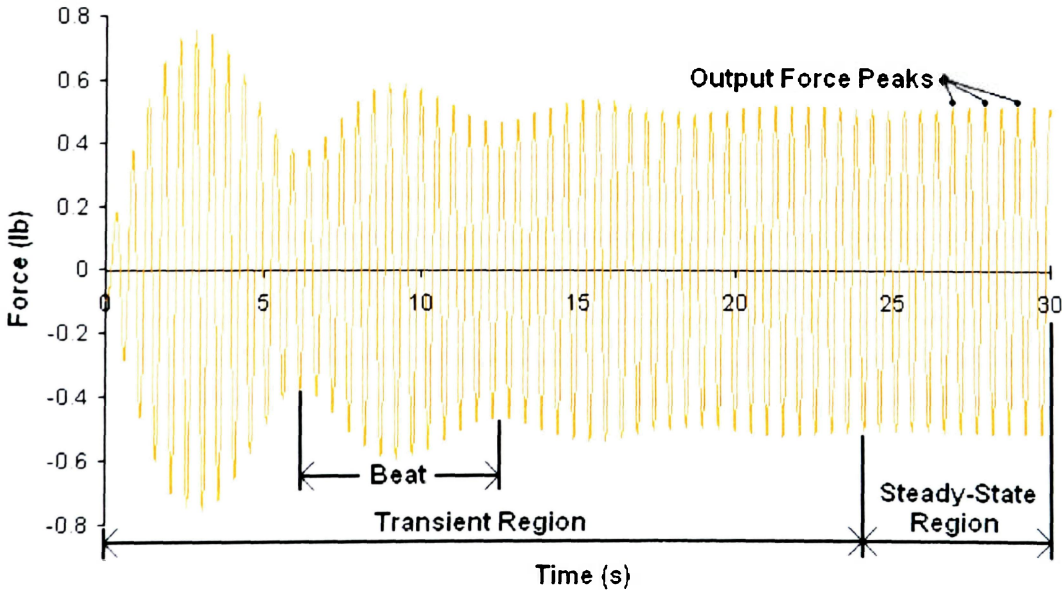
**Table 8.1**  
**Pendulum Frame and Tank Test Parameter Estimation Limits**

Key:	Default Limits for all Pendulum and Tank Testing					
A Series: 60% Fill Level Tests	A Series (All)		B Series (All)		C Series (All)	
B Series: 70% Fill Level Tests	Lower	Upper	Lower	Upper	Lower	Upper
C Series: 80% Fill Level Tests	Lower	Upper	Lower	Upper	Lower	Upper
Angular Velocity Correction (rad/s)	-0.5	0.5	-0.5	0.5	-0.5	0.5
Flywheel Initial Angle (rad)	-2.0	2.0	-2.0	2.0	-2.0	2.0
Pendulum Spring Constant (ft-lb/rad)	0.0	1.0	0.0	1.0	0.0	1.0
Pendulum Damping Constant (ft-lb/rad/sec)	0.0	1.0	0.0	1.0	0.0	1.0
Pendulum Length* (in)	1.7778	2.6667	1.4936	2.2404	1.1568	1.7352
<b>* Pendulum Length is set to +/- 20% of the Length Predicted by the SLOSH Code</b>						

Now that variables and limits are defined, the test length must be determined. When the pendulum is added to the simulation, a transient region is added to the dataset before returning to steady-state as in the frozen mass tests. These regions are illustrated in the generic pendulum low damping and high damping waveforms in Figures 8.1 and 8.2. This transient region contains the natural frequency as well as the DC motor frequency. These overlapping frequencies create a beat between the two waves. Beats take place when two waves have lightly different frequencies and the waves are superimposed over each other (Cutnell and Johnson, 1998). These beats decay over time and can vary a few seconds to more than a minute. For the high damping case, the beats decay very quickly making them unable to be determined. Taken as a whole, the dataset

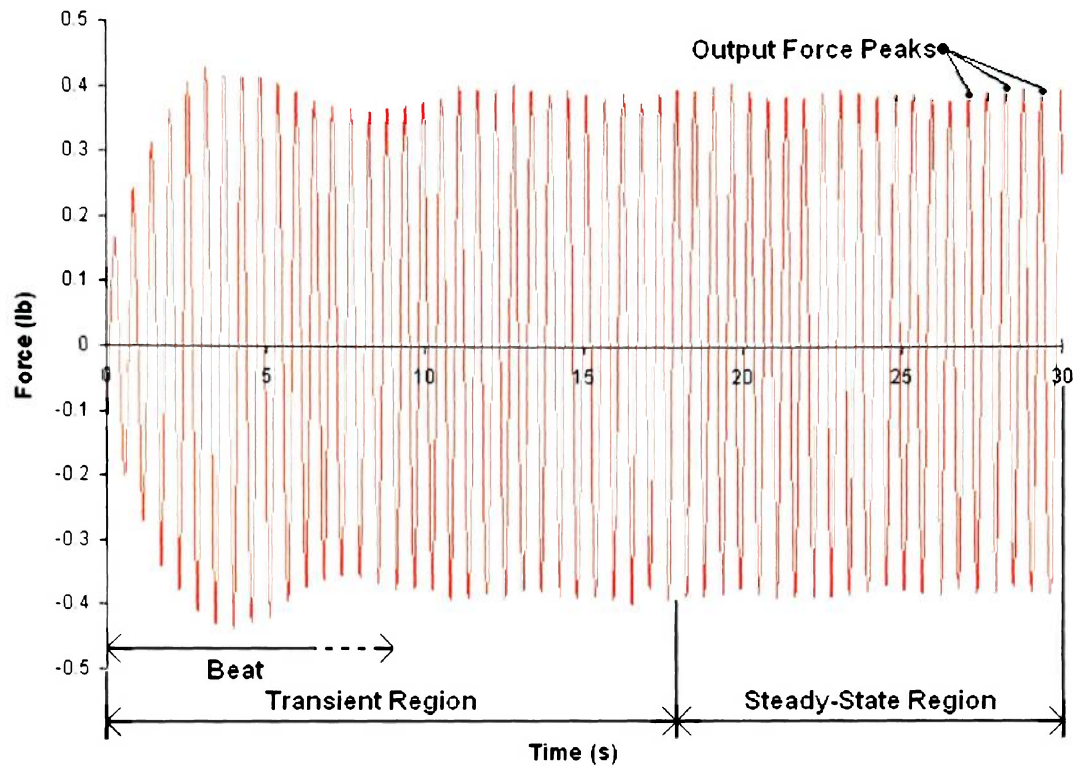
<sup>14</sup> In versions of MATLAB newer than 7.0 SP2, the model will sometimes not accept these units for spring and damping constants. For MATLAB version R2006a, the preferred units for spring and damping constant are N-m/deg and N-m/deg/sec respectively.

can generally be divided into two parts. The first part is the transient region starting at time equal to zero to time equal to wherever the end of the transient region is located. For these tests, the end of the transient region is determined by observing the peaks of the output force. If several consecutive peaks vary by less than 0.5%, the region is considered to be steady. The second part of the dataset is the steady-state region. This region starts at the end of the transient region and continues until test termination. A decision needed to be made on the type of data to be provided to the simulation. The data that can be supplied to the estimator falls into three categories. These are transient only, steady-state only, and the entire dataset. Ultimately, it was decided to optimize to the entire dataset due to its information content for estimating the pendulum parameters. In order to capture the entire dataset, the test length was decided to be 30 seconds, or 3001 data points. The only exception to this is that the A series tank tests are 60 seconds, or 6001 data points<sup>15</sup>.



**Figure 8.1 Generic Low Damping Simulation Output with Pendulum**

<sup>15</sup> Simulation first optimized using only 10 seconds of data to get a fast “ballpark” estimate of the parameters.

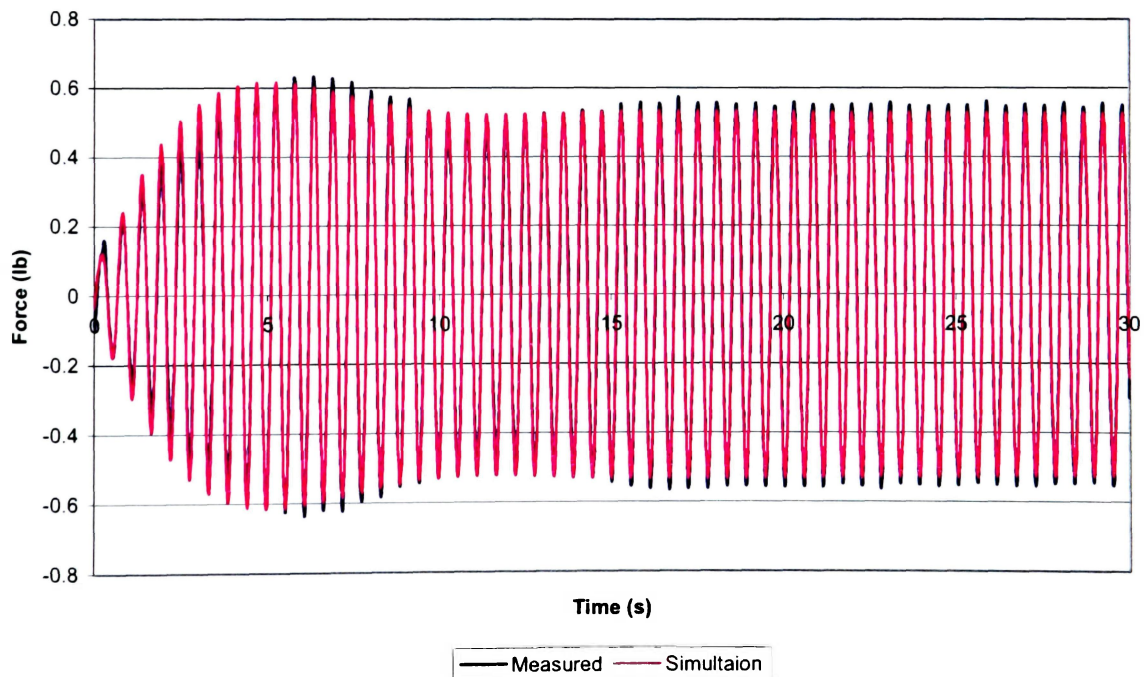


**Figure 8.2 Generic Low Damping Simulation Output with Pendulum**

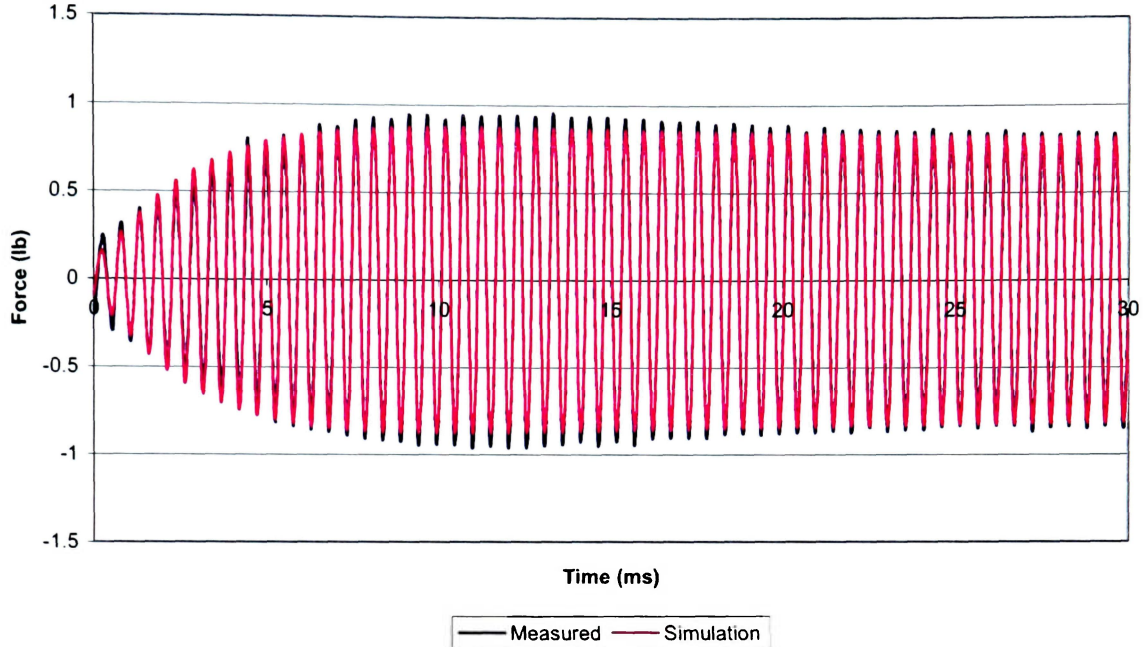
The final part needed in the procedure is determining the stopping criterion for each parameter estimation method. It was decided to use a different stopping criterion for each method. The M-Code was set to terminate after approximately 25 iterations while the Parameter Estimator was set to terminate when the cost function reached a tolerance of  $10e-6$ , or approximately 30-50 iterations. The final cost function is displayed along with the parameters in following sections as well as in the final data tables provided in Appendix G.

## 8.2. Pendulum Frame Results

There were a total of 18 pendulum frame tests with each converging successfully. Figure 8.3 illustrates a typical pendulum frame A series (60% fill level) result. Most of the B and C series (70% and 80% fill level) tests look similar to this result. Since the pendulum hinge is highly damped, the transient region is very small compared to the steady state region. It was observed that no measurable beats form in any of the datasets from the pendulum frame. Steady-state peak force errors typically are less than 5%. Figure 8.4 shows a case where the pendulum is very close to the natural frequency. The transient region lasts for almost the entire test. Transient errors are typically less than 10%. The lengths of both the transient and steady-state region were also accurately simulated with each method as shown in Figures 8.3 and 8.4. The rest of the datasets are provided in Appendix G.



**Figure 8.3. Pendulum Test A3 (60% at 1.770 Hz)**



**Figure 8.4. Pendulum Test B3 (70% at 1.953 Hz)**

Table 8.2 shows the A series test results for each estimation method. Several observations can be made from the data table. Different stopping criterions were used for each method. If one were to choose the most “accurate” parameters, it would be from the Parameter Estimator due to its higher stopping criterion tolerance as observed by the lower cost functions. Several inferences can be made from this data. The cost function rises as the frequency increases. While there are many possible reasons for this, the most likely reason is due to the fact that there is more data variability as the frequencies increase and the transient region becomes longer as the DC motor frequency approaches the natural frequency of the pendulum. Angular velocity correction, initial flywheel angle, and pendulum damping constant all remain approximately the same with each method. However, if the pendulum length and the spring constant differ, then the optimization algorithm is allowed to fully converge. More discussion on the relationship between the spring constant and pendulum length is included in the following sections.

**Table 8.2**  
**60% Pendulum Results for Each Method**

<b>Method 1 (M-Code)</b>			
Five Parameters	Fixed Mass (lb)	Pendulum Mass (lb)	
60% Fill Level Properties	3.2099	3.055	
Test ID	A1	A2	A3
Measured Test Frequency (Hz)	1.660	1.757	1.770
Angular Velocity Correction (rad/s)	-0.1124420	-0.0274759	0.1357546
Initial Flywheel Angle (rad)	-0.2676705	-0.8283001	-1.1392384
Pendulum Spring Constant (ft-lb/rad)	0.0443370	0.0454400	0.0302538
Pendulum Damping Constant (ft-lb/rad/sec)	0.0213000	0.0053249	0.0024797
Predicted Pendulum Length (in)	2.6167000	2.2831900	2.1315700
<b>Cost Function</b>	<b>0.41629</b>	<b>0.89570</b>	<b>2.52411</b>
<b>Method 2 (Parameter Estimator)</b>			
Test ID	A1	A2	A3
Measured Test Frequency (Hz)	1.660	1.757	1.770
Angular Velocity Correction (rad/s)	-0.110270	-0.028498	0.135030
Initial Flywheel Angle (rad)	-0.375980	-0.810290	-1.134300
Pendulum Spring Constant (ft-lb/rad)	0.000031	0.000000	0.013874
Pendulum Damping Constant (ft-lb/rad/sec)	0.020442	0.003703	0.002133
Predicted Pendulum Length (in)	2.6185 (L) <sup>16</sup>	1.949900	2.005400
<b>Cost Function</b>	<b>0.40716</b>	<b>0.83715</b>	<b>2.48520</b>

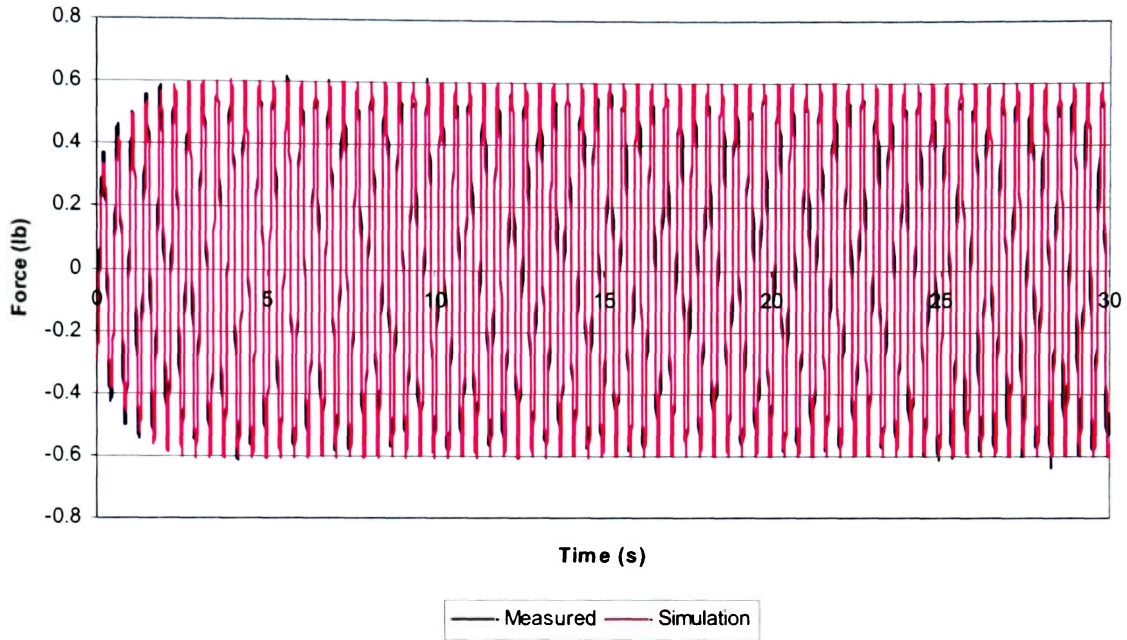
### 8.3. Tank Results

There were a total of 18 tank tests with each test converging successfully. Unlike the pendulum tests where each dataset looked roughly the same, the datasets for the tank tests varied greatly with fill level and frequency. The A series test datasets all had a very well defined beat characteristic that lasted for over 30 seconds. The C Series tests had a very weak beat characteristic that could not be calculated because it decayed after a few seconds. The results of the B series tests, as predicted, were in between the A and C series tests. Figure 8.5 illustrates a typical pendulum tank test result for a C series test. Steady-state peak force errors typically are less than 10%. Figure 8.6 shows a case with an A series test with a beat where the tank is very close to its natural frequency. Transient errors are typically less than 15%. The lengths of both the transient and steady-

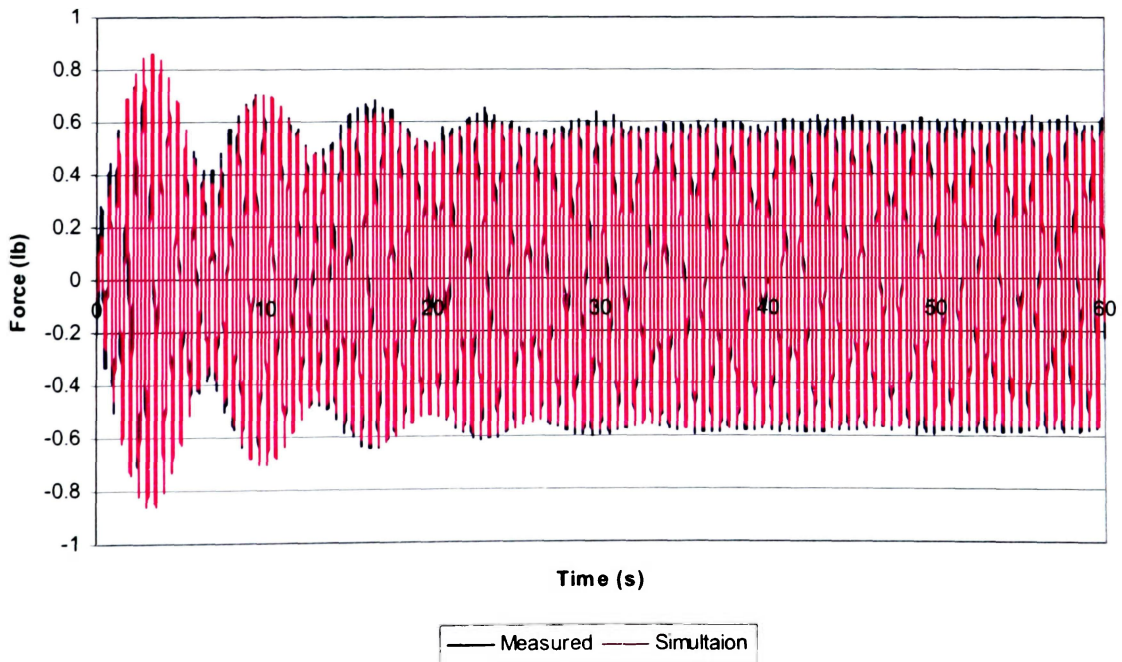
<sup>16</sup> (L) indicates that this value falls on one of the limits.



state region were also accurately simulated with each method as seen in Figures 8.5 and 8.6. The rest of the datasets are provided in Appendix H.



**Figure 8.5. Tank Test C3 (80% at 2.441 Hz)**



**Figure 8.6. Tank Test A3 (60% at 1.953 Hz)**

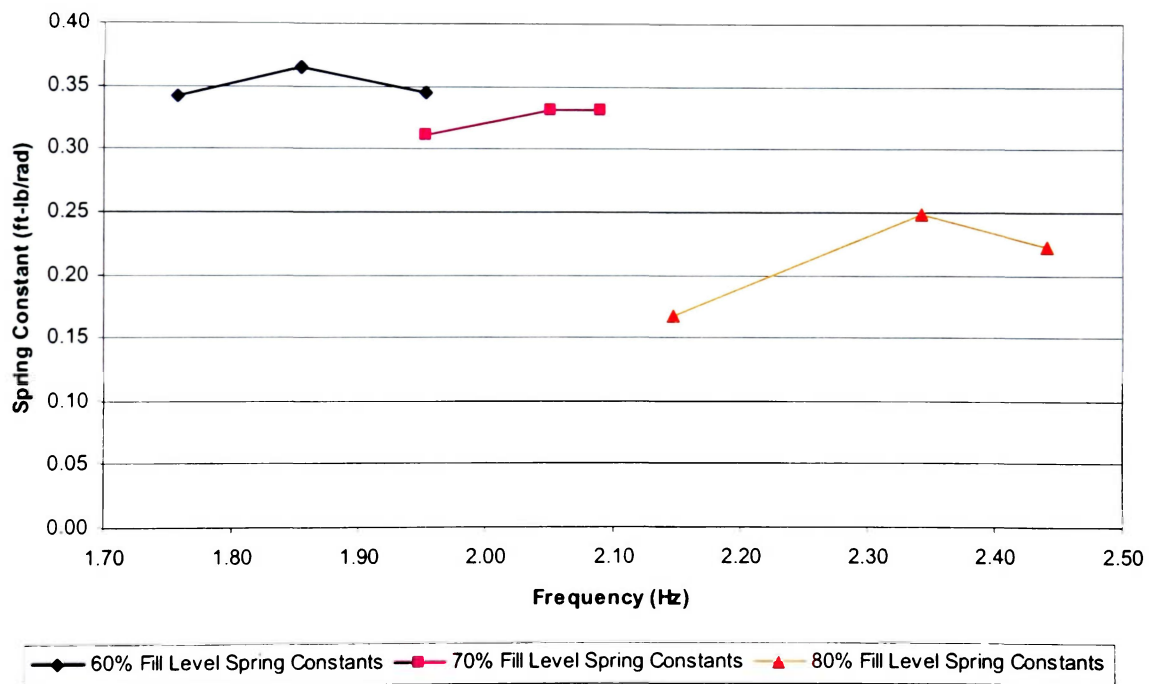
The table below represents the A series test results for each estimation method. Like the results for the pendulum, several things can be highlighted. The cost function still increases as the test frequency approaches the natural frequency. Also, the cost function is higher than the pendulum tests. This is most likely due to the longer transient region. Unlike the pendulum tests where the spring constant changed greatly when the simulation was allowed to converge, the values were relatively the same without much of a variation. An interesting result from the data is that the pendulum limit is reached on every test (A, B, and C series). Since these lengths are all “equal” relative to one another, comparisons of the spring and damping constants can be observed.

**Table 8.3  
60% Tank Results for Each Method**

<b>Code</b>			
Five Parameters	Fixed Mass (lb)	Pendulum Mass (lb)	
60% Fill Level Properties	3.2099	3.055	
Test ID	A1	A2	A3
Measured Test Frequency (Hz)	1.757	1.855	1.953
Angular Velocity Correction (rad/s)	0.2290898	-0.0466229	0.0603925
Flywheel Initial Angle (rad)	-0.2545408	-0.4927648	-0.6273952
Pendulum Spring Constant (ft-lb/rad)	0.3116654	0.3546299	0.3297325
Pendulum Damping Constant (ft-lb/rad/sec)	0.0072853	0.0016229	0.0012423
Predicted Pendulum Length (in)	2.5922730	2.6458800	2.6244016
Cost Function	5.53622	5.36823	9.89092
<b>Simulation (Parameter Estimation)</b>			
Test ID	A1	A2	A3
Measured Test Frequency (Hz)	1.757	1.855	1.953
Angular Velocity Correction (rad/s)	0.228970	-0.045928	0.060946
Flywheel Initial Angle (rad)	-0.253660	-0.466320	-0.603860
Pendulum Spring Constant (ft-lb/rad)	0.341980	0.364310	0.345410
Pendulum Damping Constant (ft-lb/rad/sec)	0.007548	0.001690	0.001264
Predicted Pendulum Length (in)	2.6667 (L)	2.6667 (L)	2.6667 (L)
Cost Function	5.5202	5.2405	9.4510

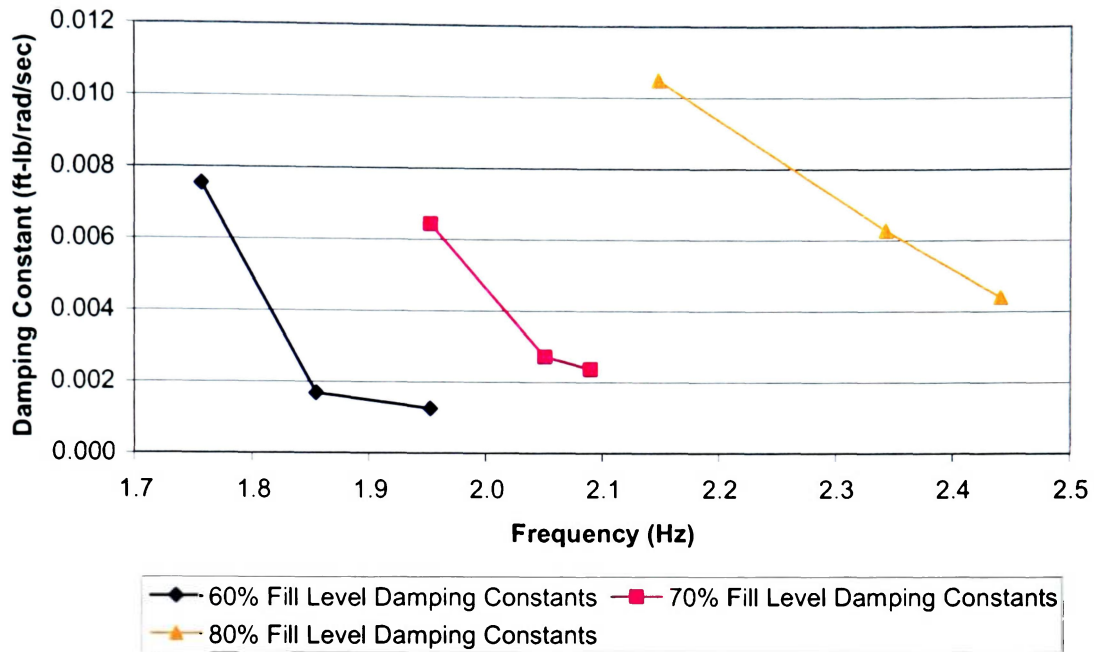
The calculated spring constants are shown in Figure 8.7. By observing the data, it can be seen that the spring constant depends both on fill level and frequency. As the fill level increases, the spring constant decreases. Also, as the frequency nears the natural frequency, the spring constant increases and decreases again. This trend is evident for each fill level. The calculated damping constants in Figure 8.8 follow a similar trend

with respect to each other. Unlike the spring constant, the damping constant is more dependent on frequency than on fill level. That is, for all of the tests, the damping drops as the tank nears its natural frequency. The spring/damping ratio was calculated as a final check to show the variation of the spring and damping constants with fill level and frequency. Figure 8.9 illustrates that the spring/damping ratio does appear to follow a near-linear trend. However, no clear conclusions can be made as this data is no more linear than the spring and damping plots. The rest of the datasets for the tank tests are provided in Appendix H.

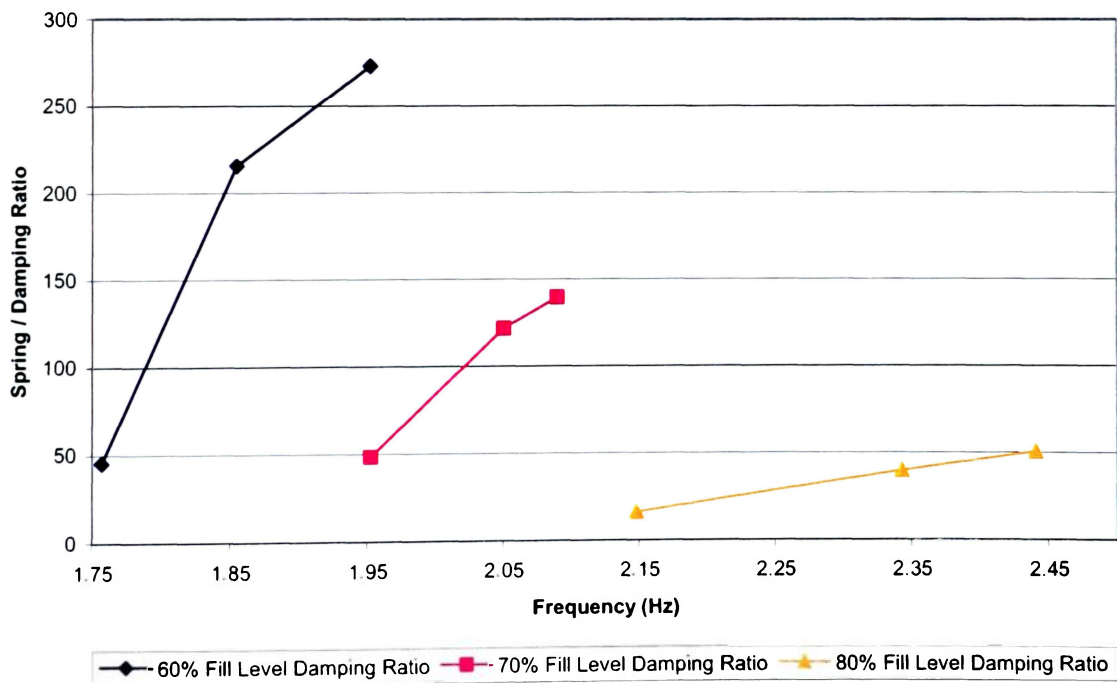


**Figure 8.7. Spring Constants at Various Fill Levels using Default Limits<sup>17</sup>**

<sup>17</sup> Default limits are provided in Table 8.1.



**Figure 8.8. Damping Constants at Various Fill Levels using Default Limits**



**Figure 8.9. Spring Damping Ratio for Various Fill Levels using Default Limits**

The beat frequency was also calculated for the A and B series tests on order to verify the theory. The results in Table 8.4 indicate that the theory is valid. Errors between the beat-calculated natural frequency are very close to the SLOSH predicted natural frequency. More importantly, they are in close proximity to each other. In other words, they are all slightly overestimating the natural frequency.

**Table 8.4**  
**Beat Frequency and Natural Frequency Calculation**

Test ID	A1	A2	A3	B1	B2	B3
Measured Frequency (Hz)	1.757	1.855	1.953	1.953	2.051	2.090
Angular Velocity Correction (Hz)	0.073	-0.014	0.019	0.033	-0.014	0.024
Approximate Beat Frequency (Hz)	0.326	0.283	0.151	0.373	0.292	0.221
Calculated Natural Frequency (Hz)	2.156	2.124	2.123	2.359	2.329	2.335
SLOSH Predicted Natural Frequency (Hz)	2.092	2.092	2.092	2.288	2.288	2.288
Percent Difference	3.06%	1.50%	1.49%	3.12%	1.79%	2.06%

This concludes the primary testing of the pendulum and tank. After observing these results, a number of questions can be asked. In an attempt to answer the more common questions, several case studies for the A series tests (Test A3 in particular) were performed and is discussed below.

## **9. CASE STUDIES FOR 60% TANK FILL LEVEL**

Test A3 was selected due to its distinguished beat and long transient region<sup>18</sup>. It is, in effect, the “worst” case scenario of all of the tests.

---

<sup>18</sup> Standard M-Code stopping criterion was used in all A series case studies (Approximately 25 iterations).

The following case studies were performed:

1. Test A3 30 second optimization with default limits.
2. Test A3 30 second optimization without pendulum length limits.
3. Test A3 30 second optimization with SLOSH pendulum length.
4. Test A3 30 second optimization with spring constant set to zero.

The following case study was performed using all A series data:

1. Test A1-A3 multiple dataset optimization.

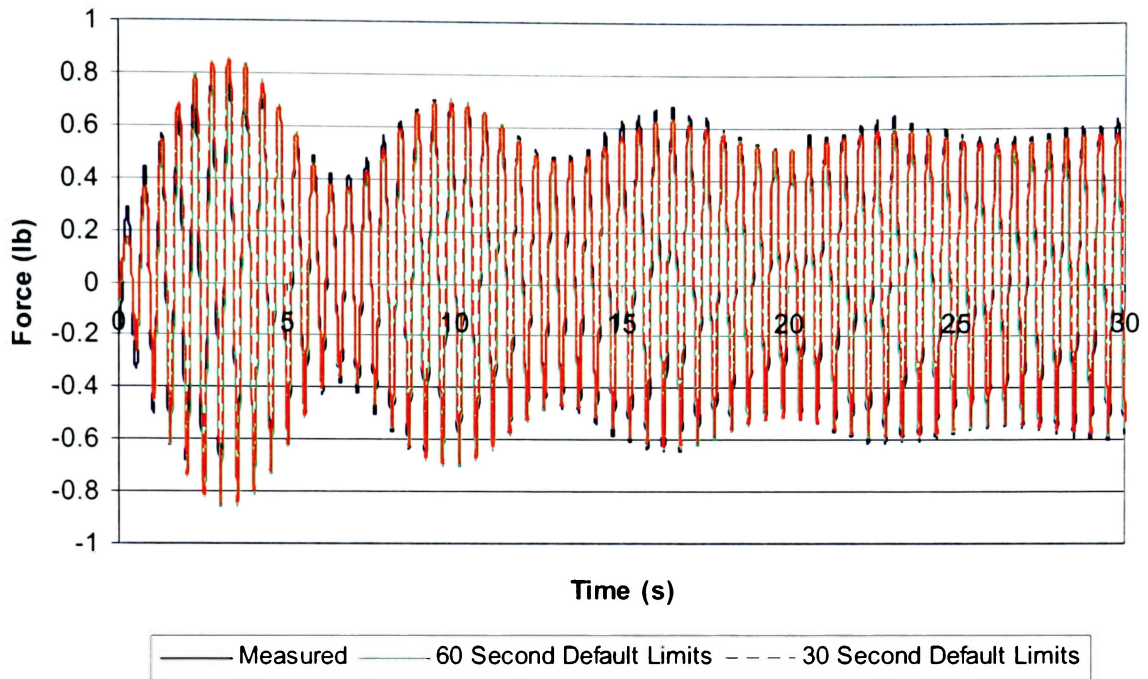
The following case study was performed on the tank at an A series fill level:

1. Frequency sweep for tank at an A series fill level.

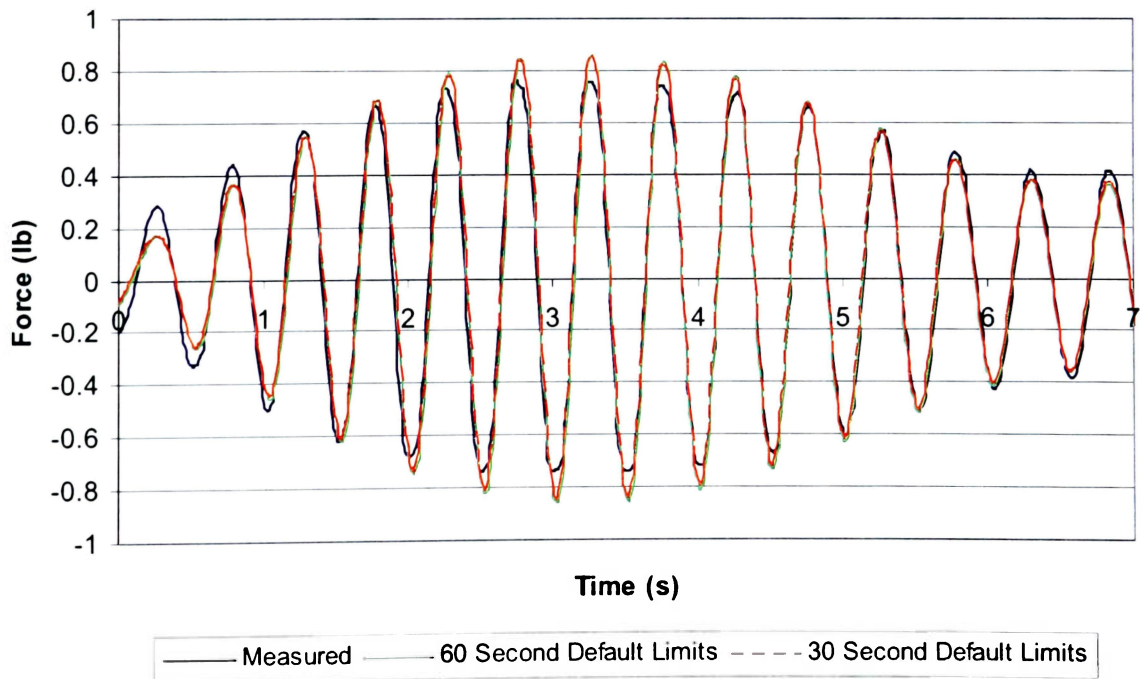
## **9.1. Test A3 Case Studies**

### **Case 1. A3 30 Second Optimization with Default Limits**

Unlike the majority of other datasets, the A series tank tests were optimized using 60 seconds of data instead of 30. This was done so that a portion of the steady-state data could be included in the optimization. However, the worst errors were encountered in the transient region in test A3. Would neglecting the steady-state region improve the results? The results for the 30 second optimization are shown in Figures 9.1 and 9.2. There is a small improvement, but it is less than a 2% difference in maximum error. However, this does prove that parameters can successfully be evaluated using a much shorter sample of dataset. The new parameters, displayed in Table 9.1, show very similar values to one another. The pendulum length still approaches the upper limit and the rest of the parameter values remain approximately the same.



**Figure 9.1. Test A3 Optimization Results for 30 Seconds (1.953 Hz)**



**Figure 9.2. Zoomed in View of Test A3 Optimization Results**

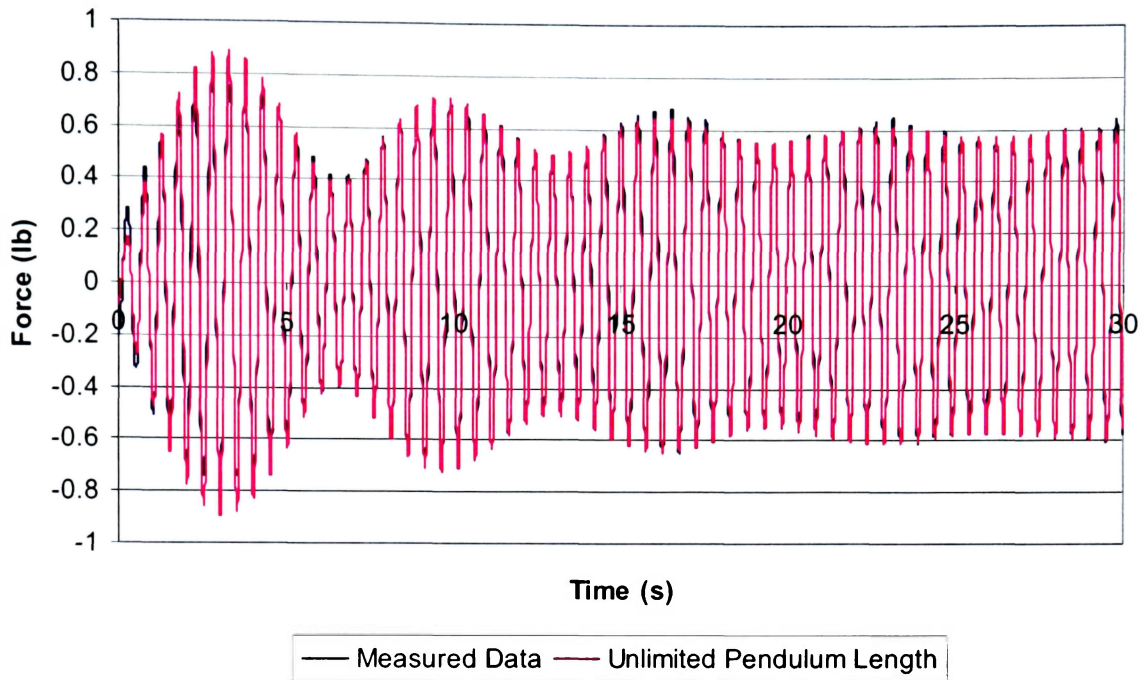
**Table 9.1**  
**Test A3 30 Second Optimization Results**

A3 Tank Series Test Case 1	Fixed Mass (lb)	Pendulum Mass (lb)
60% Fill Level Properties	3.2099	3.055
Test ID	A3: Original	A3: 30 Second
Measured Test Frequency (Hz)	1.953	1.953
Angular Velocity Correction (rad/s)	0.060946	0.0545930
Flywheel Initial Angle (rad)	-0.603860	-0.6925742
Pendulum Spring Constant (ft-lb/rad)	0.345410	0.3283041
Pendulum Damping Constant (ft-lb/rad/sec)	0.001264	0.0012845
Predicted Pendulum Length (in)	2.6667 (L)	2.6204830
<b>Cost Function</b>	<b>9.4510</b>	<b>4.82737</b>

**Case 2. Test A3 30 Second Optimization Without Pendulum Length Limits**

Since the first case study resulted in reasonable parameter identification using only half of the measured data, the rest of the case studies were conducted using 30 seconds of data instead of the 60 seconds used in the primary tests. The next obvious question concerns pendulum length. In every tank test, the pendulum length converged to the upper limit of +20% of the length predicted by the SLOSH code. The upper pendulum length limit for test A3 was increased so that the code would not converge to the upper limit. Ultimately, the pendulum length converged to 3.335 inches. This is over 50% greater than the predictions of the SLOSH code. The resulting dataset is shown in Figure 9.3 and the parameters shown in Table 9.2. It is interesting to note that, in order to compensate for the increased pendulum length, the spring constant almost doubles from 0.328 to 0.643 ft-lb/rad. The cost function, predictably, has dropped to 4.32. This is the lowest cost function obtained in the test A3 case studies.





**Figure 9.3. Test A3 Optimization with Unrestricted Pendulum Length**

**Table 9.2**

**Test A3 Unlimited Pendulum Length Results**

A3 Tank Series Test Case 2	Fixed Mass (lb)	Pendulum Mass (lb)
60% Fill Level Properties	3.2099	3.055
Test ID	A3: 30 Second	A3: Unlimited Pendulum Length
Measured Test Frequency (Hz)	1.953	1.953
Angular Velocity Correction (rad/s)	0.0545930	0.0551172
Flywheel Initial Angle (rad)	-0.6925742	-0.6954259
Pendulum Spring Constant (ft-lb/rad)	0.3283041	0.6434841
Pendulum Damping Constant (ft-lb/rad/sec)	0.0012845	0.0021559
Predicted Pendulum Length (in)	2.6204830	3.3359106
<b>Cost Function</b>	<b>4.82737</b>	<b>4.32796</b>

### Case 3. Test A3 30 Second Optimization with SLOSH Pendulum Length

As a continuation of case 2, the pendulum length was restricted to the length determined by the SLOSH code, or “correct” natural frequency length. Recall that natural frequency verification of the SLOSH code was verified using two separate methods (static test in Section 6.2 and beat frequency test in Section 8.3). The resulting dataset is shown in Figure 9.4 and the parameters are shown in Table 9.3. As expected with a fixed pendulum length the cost function increased by over 50%. Moreover, the spring constant decreased to compensate for the reduced pendulum length.

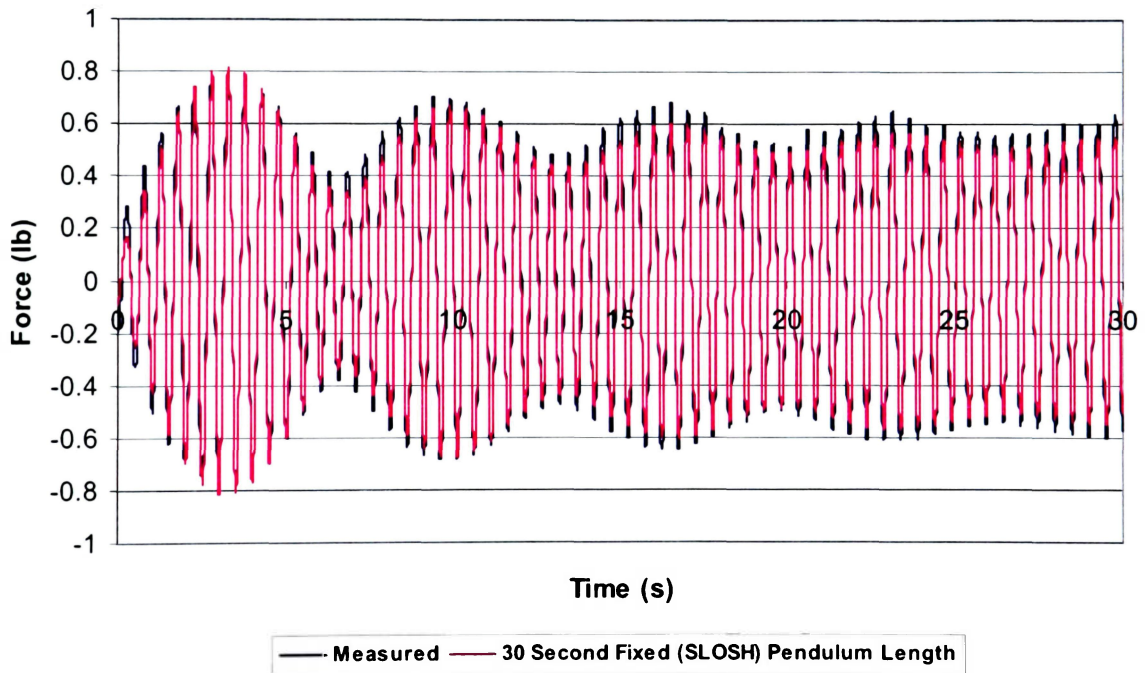


Figure 9.4. Test A3 Optimization with SLOSH Pendulum Length

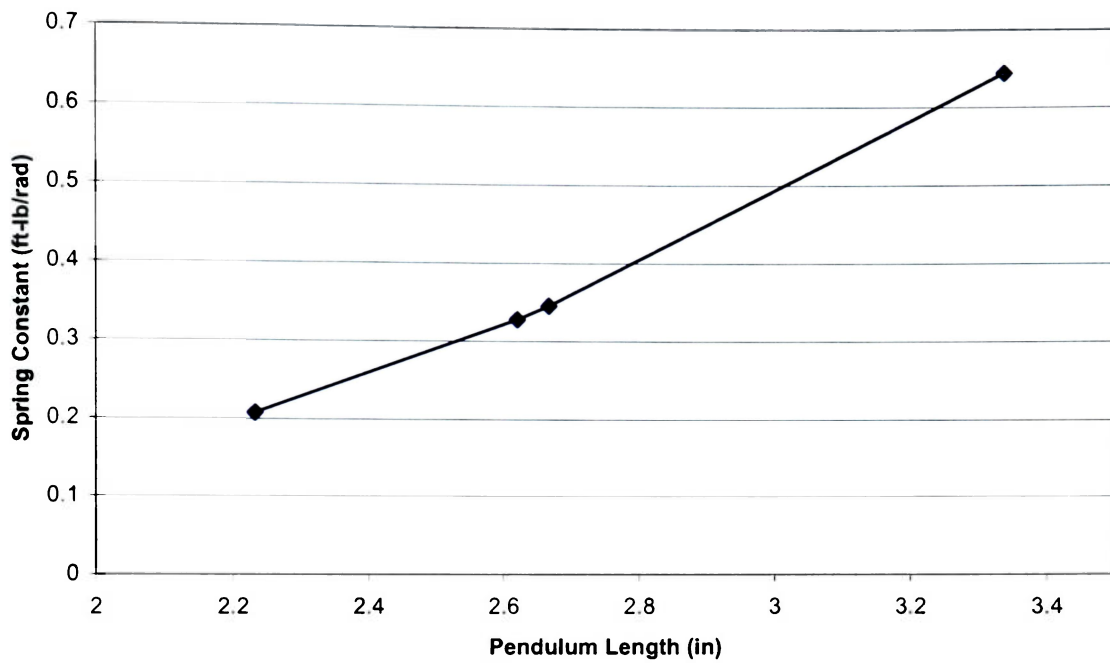
**Table 9.3**

**Test A3 SLOSH Pendulum Length Results**

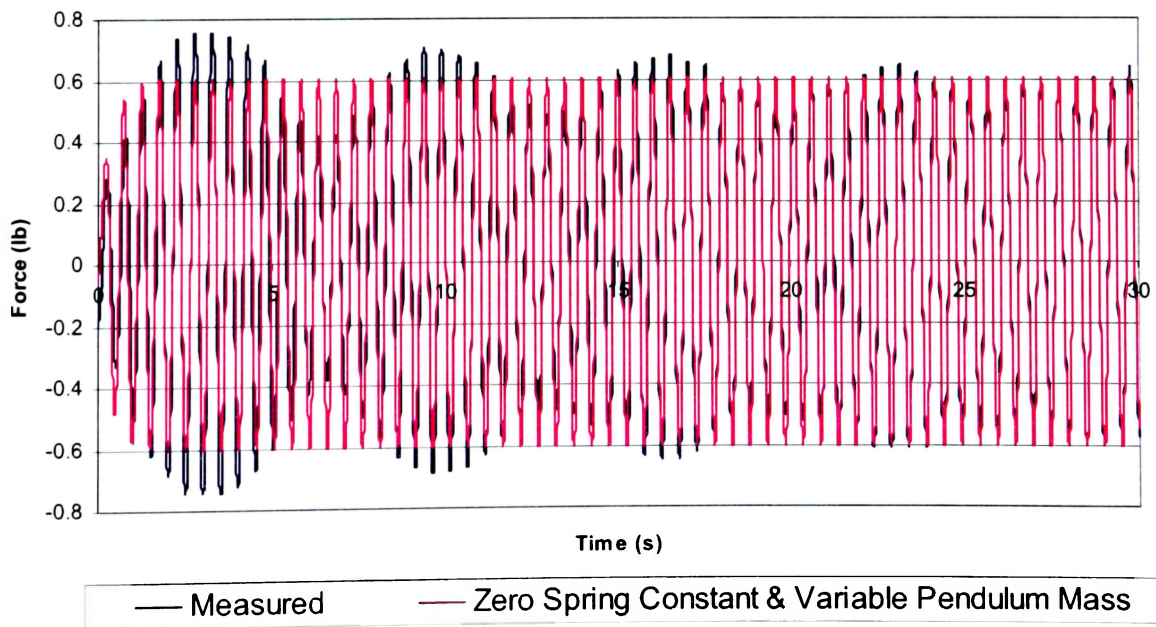
A3 Tank Series Test Case 3	Fixed Mass (lb)	Pendulum Mass (lb)
60% Fill Level Properties	3.2099	3.055
Test ID	A3: 30 Second	A3: SLOSH Pendulum Length
Measured Test Frequency (Hz)	1.953	1.953
Angular Velocity Correction (rad/s)	0.0545930	0.0540120
Flywheel Initial Angle (rad)	-0.6925742	-0.6942996
Pendulum Spring Constant (ft-lb/rad)	0.3283041	0.2076107
Pendulum Damping Constant (ft-lb/rad/sec)	0.0012845	0.0009218
Predicted Pendulum Length (in)	2.6204830	2.2327 (SLOSH)
<b>Cost Function</b>	<b>4.82737</b>	<b>7.51791</b>

**Case 4. Test A3 30 Second Optimization with Spring Constant set to Zero**

The final case study deals with the spring constant. For the last two cases where the pendulum length was changed, the spring constant increased or decreased accordingly. This relationship appears to be linear as shown in Figure 9.5. This last case sets the spring constant to zero with all of the other limits set at the default values. Also, the pendulum mass was varied to give the optimizer some degree of flexibility. The lower and upper mass limits were 4 and 15 lbs respectively. The results shown in Figure 9.6 indicate that, while the steady-state portion of the dataset is present, the natural frequency decay is not. This is illustrated by the lack of a beat in the simulation's dataset. This lack of a decaying natural frequency component associated with a spring constant causes the cost function and the pendulum mass to increase over 500% and 200% respectively. This illustrated that a spring constant at the pendulum hinge is required for accurate modeling of free surface fuel slosh.



**Figure 9.5. Test A3 Predicted Spring Constants and Pendulum Lengths**



**Figure 9.6. Test A3 Optimization with Spring Constant Equal to Zero**

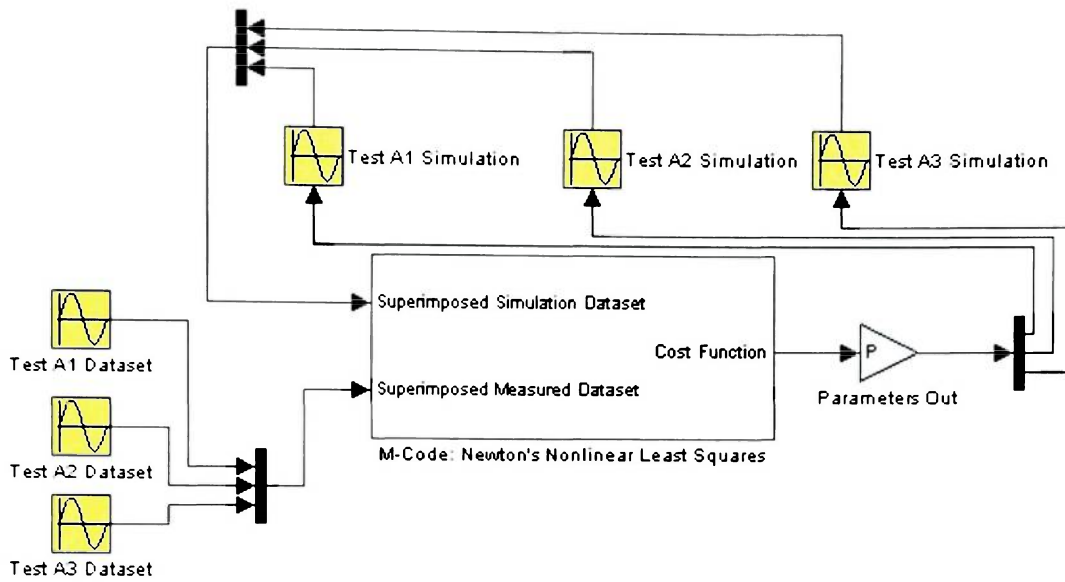
**Table 9.4****Test A3 with Zero Spring Constant and Variable Pendulum Mass Results**

A3 Tank Series Test Case 4	Fixed Mass (lb)	Pendulum Mass (lb)
60% Fill Level Properties	3.2099	3.055
Test ID	A3: 30 Second	A3: Zero Spring Constant
Measured Test Frequency (Hz)	1.953	1.953
Angular Velocity Correction (rad/s)	0.0545930	0.0748246
Flywheel Initial Angle (rad)	-0.6925742	-1.1343423
Pendulum Mass (lb)	3.055 (SLOSH)	9.1389753
Pendulum Damping Constant (ft-lb/rad/sec)	0.0012845	0.0501711
Predicted Pendulum Length (in)	2.6204830	1.9544683
<b>Cost Function</b>	<b>4.82737</b>	<b>29.30290</b>

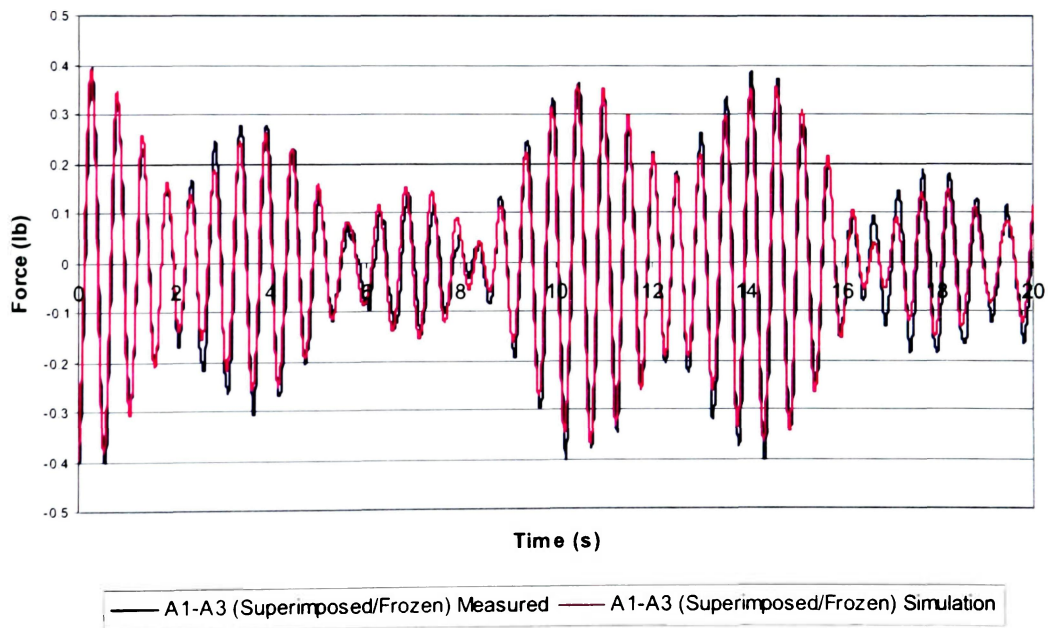
**9.2. A1-A3 Multiple Dataset Optimization**

Even though the tests optimized to a single frequency point toward a distinct change in the spring and damping constants, the idea of optimizing the data to all the A series data simultaneously seemed like a promising idea. Can a single spring constant and damping constant be applied so that it matches all of the data? The M-Code was modified to run multiple simulations simultaneously and to superimpose the simulation output to form a single dataset as illustrated in Figure 9.7<sup>19</sup>. The corresponding measured data was superimposed to create a single dataset for the optimization. But before this method was tested using the tank data, the method was first carried out using the frozen mass datasets A1-A3. The results from this test are shown in Figure 9.8 and in Table 9.5. This test, using the full sample of frozen mass data, performed well with a reasonable estimation of the frozen mass. Now that the method is proved, it can be applied to the tank test datasets A1-A3. The results for this test are shown in Figure 9.9 and in Table 9.6. After running the code with only 10 seconds of measured data, a reasonable cost function value was not reached. This illustrates that fixed values for spring and damping constants cannot be used for matching to multiple datasets taken at a constant frequency. The modified M-Code is provided in Appendix D.

<sup>19</sup> Default limits were used for both multiple dataset optimizations.



**Figure 9.7. Block Diagram of A1-A3 Multiple Dataset Optimization**

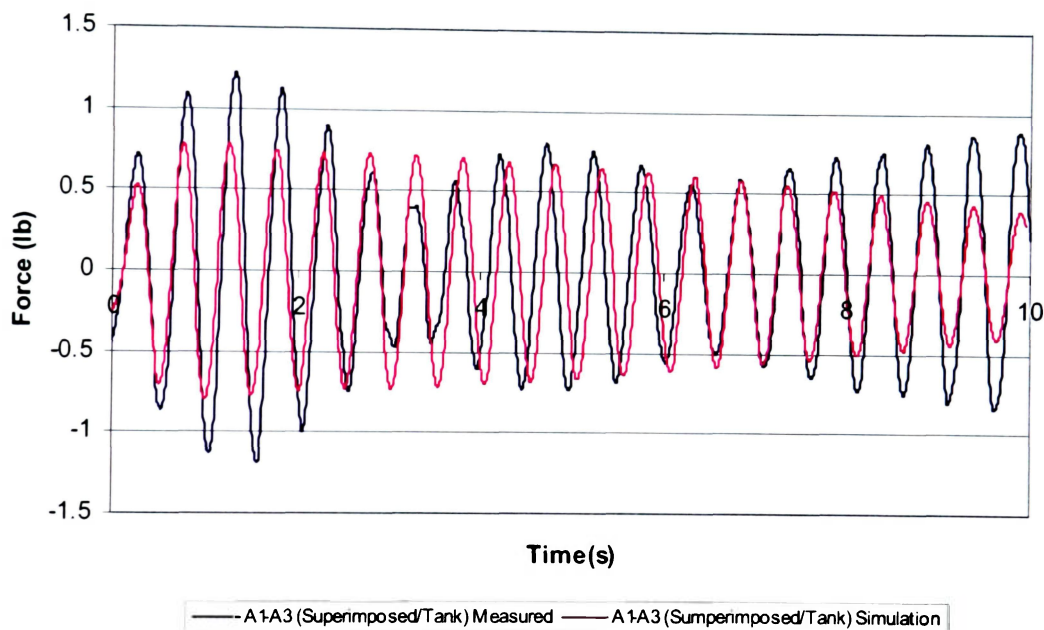


**Figure 9.8. A1-A3 Multiple Dataset (Frozen) Optimization**

**Table 9.5**

**A Series (Frozen) Multiple Dataset Optimization Results**

A Series (Frozen) Simultaneous Optimization	Fixed Mass (lb)
60% Fill Level Properties	6.2655
Test ID	A1-A3: 20 Seconds (Frozen)
Predicted Frozen Mass (lb)	5.9409
Mass Percent Difference from SLOSH	5.1808%
<b>Cost Function</b>	<b>4.8464</b>



**Figure 9.9. A1-A3 Multiple Dataset (Tank) Optimization**

**Table 9.6**

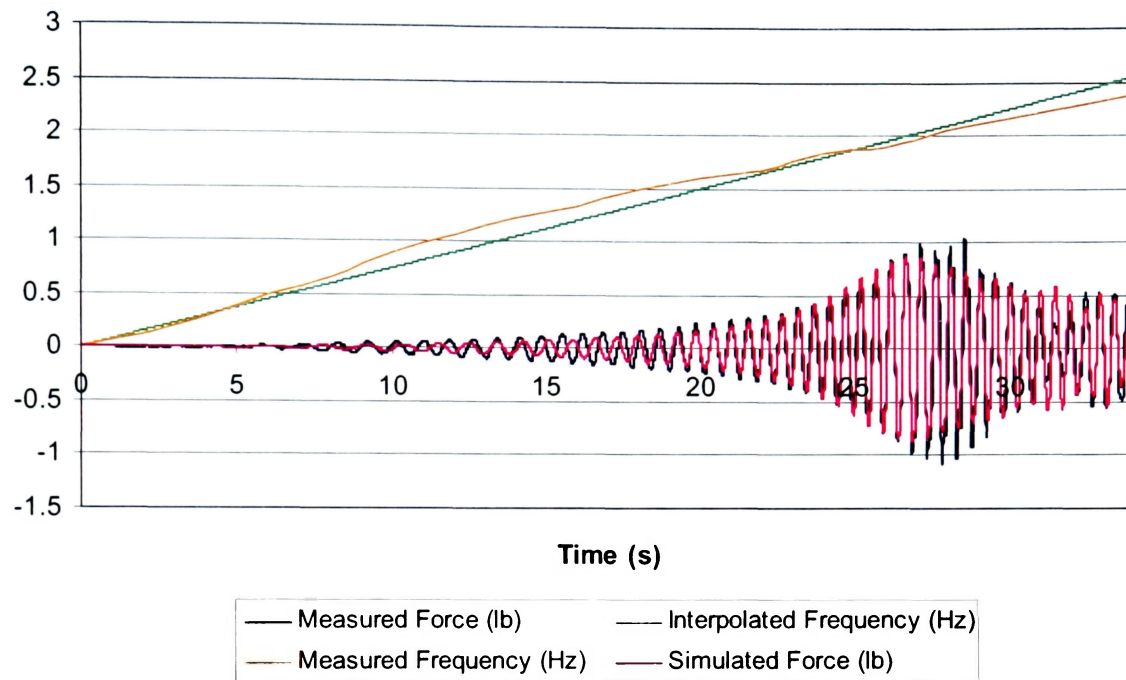
**A Series (Tank) Multiple Dataset Optimization Results**

A Series Frequency Sweep Optimization	Fixed Mass (lb)	Pendulum Mass (lb)
60% Fill Level Properties	3.2099	3.055
Test ID	A(All): Sweep	
Pendulum Spring Constant (ft-lb/rad)	0.0872433	
Pendulum Damping Constant (ft-lb/rad/sec)	0.0007045	
Predicted Pendulum Length (in)	1.6921373	
Final Angular Velocity Slope Correction (rad/s)	-0.0791584	
<b>Cost Function</b>	<b>46.3382</b>	

### 9.3. Frequency Sweep for Tank at an A Series Fill Level

The final case study deals with sweeping the frequency from zero to a value just above the natural frequency of the tank for a single test. All of the tests above were conducted using a constant frequency due to a lack of precise control of frequency variation over time provided by the DC motor control dial. LabVIEW is setup to record frequency over time and export this information similar to the force vs. time information. This frequency over time line can be interpolated and used in a lookup table in the simulation. Several methods were examined to interpolate the frequency data. Ultimately, it was found that setting up the frequency as a linear increase over time with a variable slope gave MATLAB the optimal control over the frequency sweep. The results for the frequency sweep test are provided in Figure 9.10 and in Table 9.7. As the table indicates, the cost function for this 34 second test is high though there is a visual match of the data. This “match” indicates that this type of test shows promise in future testing because datasets using a frequency sweep contain much more information about resonant modes than a constant frequency test. In the future, equipment enabling controlled frequency changes should be considered.





**Figure 9.10. A Series Frequency Sweep Data Comparison**

**Table 9.7**

**A Series Frequency Sweep Data Comparison**

A Series Frequency Sweep Optimization	Fixed Mass (lb)	Pendulum Mass (lb)
60% Fill Level Properties	3.2099	3.055
Test ID	A(All): Sweep	
Pendulum Spring Constant (ft-lb/rad)	0.0872433	
Pendulum Damping Constant (ft-lb/rad/sec)	0.0007045	
Predicted Pendulum Length (in)	1.6921373	
Final Angular Velocity Slope Correction (rad/s)	-0.0791584	
<b>Cost Function</b>	<b>46.3382</b>	

## **10. DISCUSSION**

Overall, 35 distinct datasets were optimized with each method to total over 70 optimizations. Six conference papers were published as a result of this research (Schlee et al. [13-18]). The parameter identification approach developed provides a viable method for determining parameters. The simulation behaves well at different conditions and is very robust. Settings are quick to change and it is easy to run different test cases once a method is established. The analyst has the freedom to substitute different mechanical slosh analogs in the SimMechanics model as well as have the option to add more slosh analogs if desired. Each method, M-Code and Parameter Estimator, provides its own strengths and weaknesses. The M-Code gives the analyst control over the optimization while the Parameter Estimator Toolbox provided multiple optimization options in a user friendly interface. A very large number of case studies can be performed and this research covers a small fraction of them. Parameter “test banks”, like the spring and damping plots in Section 8.3 can be developed and stored for future reference and to predict new datasets.

## **11. CONCLUSION**

The effects of fuel slosh aboard spinning spacecraft need to be accurately predicted to avoid mission failures. Using a combination of test derived fuel slosh parameters and computer simulations of the spacecraft dynamics, an improvement in the current ability to make predictions of NTC can be achieved. This parameter estimation approach was successfully applied to a simple and reliable model of a spacecraft fuel slosh system. Automating the parameter identification process will save time and thus allow earlier identification of potential vehicle performance problems. This, in turn, can reduce the cost and schedule penalty associated with needed design changes. Applications of an automated process to find the NTC will benefit all space exploration missions involving a spinning spacecraft. At present, all spinning spacecraft are used for unmanned missions. In the future, manned space exploration missions involving artificial gravity will greatly benefit from the automated parameter identification process.

Understanding and being able to confidently predict the stability of the spinning human habitat will be crucial for the success of all future manned missions.

## **12. FUTURE WORK**

In the future, the same experimental setup at Embry-Riddle can be used with tanks with PMD's to further evaluate the effectiveness of the parameter identification process. Also, the effects of different fluid viscosities, such as glycerin and saline solution, as well as the effects of lateral slosh can be evaluated. Ultimately, the proven process can be applied to the three-dimensional full sized spinning experimental setup, such as the SSTR, to quickly and accurately determine the slosh model parameters for a particular spacecraft mission.

## REFERENCES

1. Dodge, F.T., *Fuel Slosh in Asymmetrical Tank Software*.
2. Dodge, F.T., Unruh, J.F., Green, S.T., Cruse, M.W., *A Mechanical Model of Liquid Inertial Waves for Use with Spinning Craft*, Fluid Transients, FED-Vol. 198/PVP-Vol. 291, ASME 1994.
3. Gangadharan, S.N., Nikolaidis, E., Haftka, R.T., *Probabilistic System Identification of Flexible Joint Models*, AIAA Journal 1991.
4. Green, S., Burkey, R., Dodge, F., and Walter, D., *Nutation Time Constant Model Parameters for the Contour Spacecraft*, Final Report SwRI Project#18.04617 2002.
5. Greenspan, H.P., *The Theory of Rotating Fluids*, Cambridge University Press, Cambridge 1969.
6. Hubert, C., *Behavior of Spinning Space Vehicles with Onboard Liquids*, Hubert Astronautics, 2003.  
Hubert, C., *Introduction to the Dynamics and Control of Spinning Space Vehicles*, Hubert Astronautics, 2001.
7. MATLAB Software Version 7.0 SP2, The MathWorks Corporation.
8. Thomson, W.T., *Introduction to Space Dynamics*, John Wiley, New York 1961.
9. Weihs, D., and Dodge, F.T., *Liquid Motions in Nonaxisymmetric, Partially Filled Containers Rotating at Zero Gravity*, AIAA Journal of Spacecraft and Rockets, Vol. 28 1991.
10. Wertz, James R., editor, *Spacecraft Attitude Determination and Control*, copyright 1978, ISBN 90-277-0959-9
11. Wood, G.D., and Kennedy, D.C., *Simulating Mechanical Systems in Simulink with SimMechanics*, The Mathworks report 2003.
12. Cutnell, J.D., Johnson K.W., *Physics: Fourth Edition*, New York: John Wiley & Sons, Inc., 1998.
13. Schlee, K., Gangadharan, S.N., Ristow, J., Sudermann, J., Walker, C., and Hubert, C., *Modeling and Parameter Estimation of Spacecraft Fuel Slosh Mode*, In Proceedings, Winter Simulation Conference, Orlando, Florida, December 12-15, 2005

14. Schlee, K., Gangadharan, S.N., Ristow, J., Sudermann, J., Walker, C., and Hubert, C., *Advanced Method to Estimate Fuel Slosh Simulation Parameters*, In Proceedings, Paper # AIAA 2005-3596, AIAA/ASME/SAE/ASEE 41st Joint Propulsion Systems Conference, Tucson, Arizona, July 10-13, 2005.
15. Schlee, K., Sudermann, J., Walker, C., Gangadharan, S., and Ristow, J., *Modeling Resonance in Spacecraft Fuel Slosh Using Pendulum Analogs*, In Proceedings, 1<sup>st</sup> NASA/AIAA/AAS/NIA Space Exploration Conference, Orlando, Florida, January 2005.
16. Schlee, K., Gangadharan, S.N., Ristow, J., Sudermann, J., and Walker, C., *Educational Experiences of Embry-Riddle Students through NASA Research Collaboration*, Fourth International Latin American and Caribbean Conference for Engineering and Technology (LACCEI), In Proceedings, Paper #160, Mayaguez, Puerto Rico, June 21-23, 2006.
17. Schlee, K., Gangadharan, S.N., Ristow, J., Sudermann, J., Walker, C., and Hubert, C., *Modeling and Parameter Estimation of Spacecraft Fuel Slosh Using Pendulum Analogs*, AIAA/ASME/ASCE/AHS/ASC 47th Structures, Structural Dynamics and Materials (SDM) Conference, In Proceedings, Newport, Rhode Island, May 1-4, 2006.
18. Schlee, K., Gangadharan, S.N., Ristow, J., Sudermann, J., Walker, C., and Hubert, C., *Modeling and Parameter Estimation of Spacecraft Fuel Slosh*, 29th Annual AAS Guidance and Control Conference, In Proceedings, Paper # AAS-06-027, American Astronautical Society, Rocky Mountain Section, Breckenridge, Colorado, February 4-8, 2006.

---

## **APPENDICES**

**APPENDIX A**  
**PENDULUM/TANK ASSEMBLY CONSTRUCTION AND**  
**LOCOMOTIVE ASSEMBLY PROPERTIES**

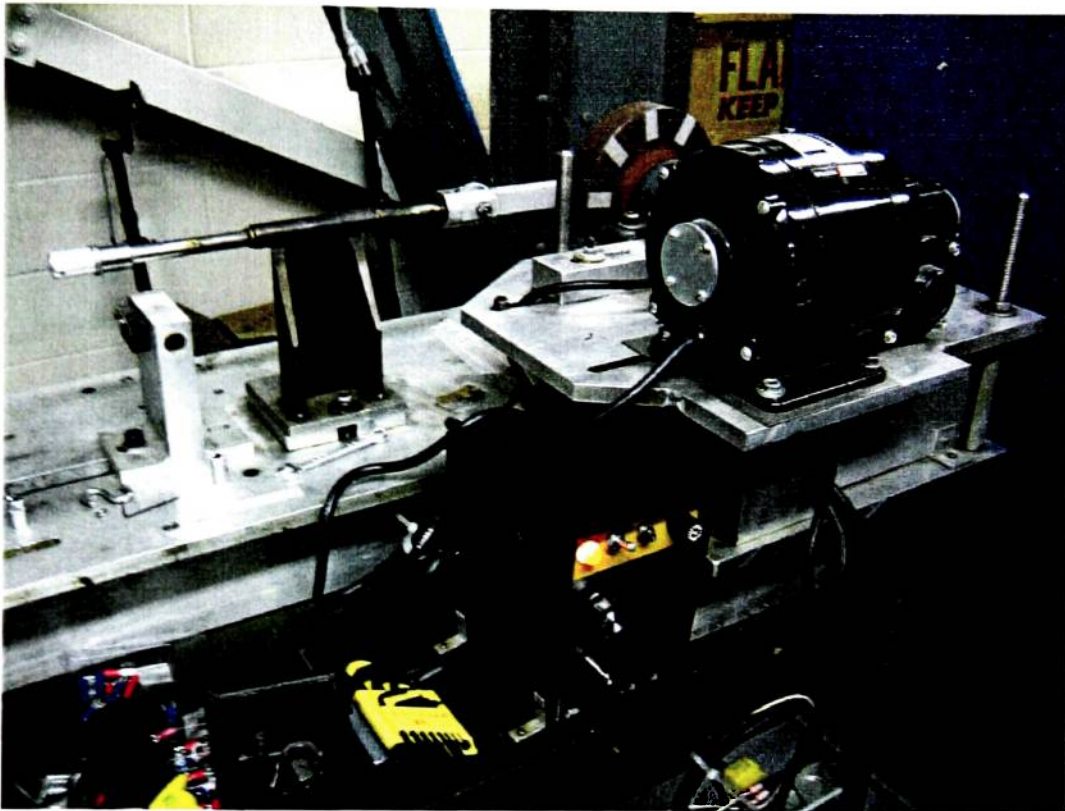
## A1. 1-DOF Pendulum Analog Experiment: Concept to Reality

Many methods were discussed to design the actuator system for the one degree-of-freedom pendulum experiment. The two final candidates were a “shaker” assembly and a locomotive assembly. Ultimately, the locomotive concept prevailed due to the availability of a locomotive assembly system at Embry-Riddle. The locomotive assembly is powered by a DC motor via a motor speed control dial as seen in Figure A1. This dial provides an accurate, steady, and repeatable frequency output from the DC motor. The entire DC motor/locomotive assembly is illustrated in Figure A2.



**Figure A1. DC Motor Speed Control Dial**





**Figure A2. DC Motor/Locomotive Assembly**

The SimMechanics simulation incorporates, as much as possible, the geometric properties of the locomotive assembly. These properties are listed in Table A1 and A2 respectively. It is important to accurately model the locomotive assembly because it provides a fundamental relationship to the operation of the real/virtual locomotive assemblies.

**Table A1**

**Locomotive Assembly Masses**

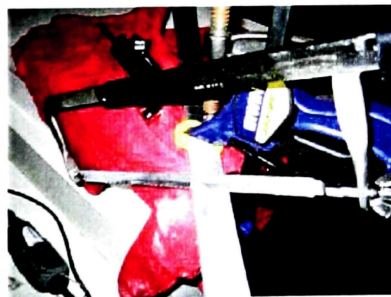
<b>Mass of steel constant (lb/ft<sup>3</sup>) →</b>	<b>490.05</b>	
<b>Locomotive Assembly Components</b>	<b>Volume (ft<sup>3</sup>)</b>	<b>Mass (lb)</b>
Mass of flywheel	1.87E-02	9.14E+00
Mass of flywheel linkage	1.54E-03	7.54E-01
Mass of "stinger"	3.93E-06	1.93E-03
Mass of locomotive rod	4.38E-04	2.14E-01

**Table A2**  
**Locomotive Assembly Lengths**

Locomotive Assembly Lengths:	Length (in)
Length of pendulum cable	54.00
Locomotive engine rod	13.00
Flywheel linkage	5.91
"Stinger" (wire)	7.00
Diameter of locomotive rod	0.50
Radius of flywheel	3.00
Width of flywheel	1.25
Width of flywheel linkage	0.55
Radius of flywheel linkage	0.72
Offset radius of flywheel linkage from flywheel center*	0.13
Distance from pendulum base to transducer	0.56
*Note: (2x = transverse motion dist.)	

### A3. Pendulum Frame Assembly Construction

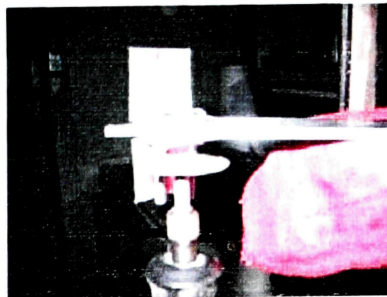
The pendulum frame is constructed out of 1 x 1/8 x 36 inch<sup>3</sup> aluminum beams. Corners are connected using 1 x 1 inch<sup>2</sup> angle aluminum bolted in place. Figure A3 illustrates the cutting of the aluminum beams and the placement of the corners of the pendulum frame.



(1) Cutting the Aluminum



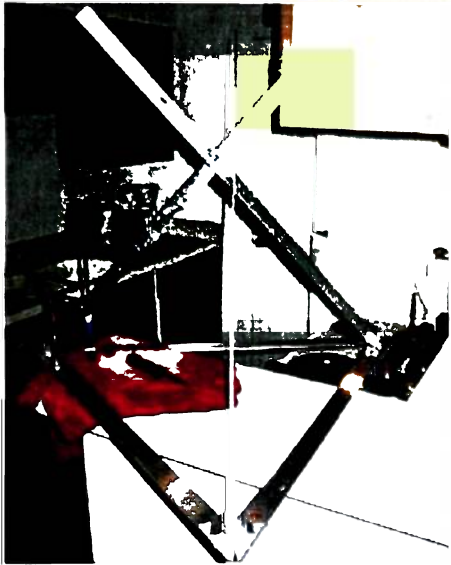
(2) Mounting/Drilling the Corners



(3) Trimming Bolts

### A3. Pendulum Frame Construction: Phase 1

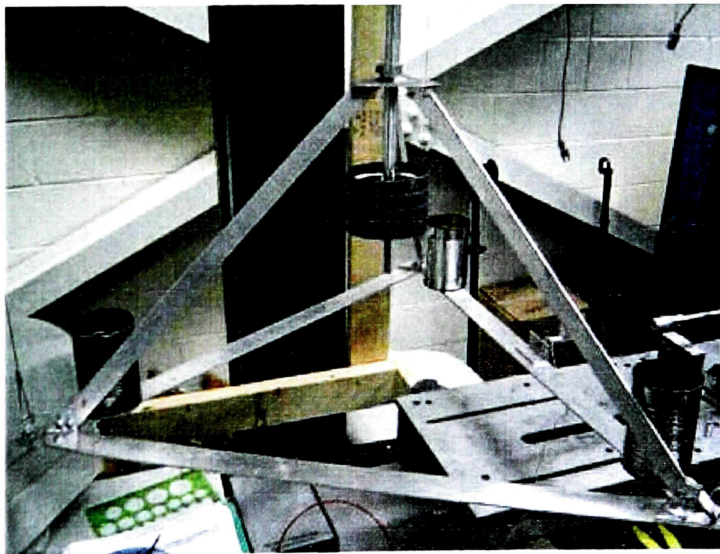
The frame resembles a triangular pyramid when assembled. The pendulum frame assembly, the installing of the pendulum, and the assembled configuration in Figure A4.



**(4) Setup of Pendulum Frame**



**(5) Pendulum Placement**



**(6) Final Pendulum Frame Assembly**

**Figure A4. Pendulum Frame Construction: Phase 2**

#### A4. Tank Assembly Construction

Unlike the pendulum frame assembly, which required a lengthy construction, the tank assembly was quick to assemble. The tank is an 8 inch acrylic sphere originally designed as a light casing. The tank assembly is constructed out of 1 inch angle aluminum that is mounted to the tank using epoxy. The construction process is shown below.



(1) Tank as Initially Received



(2) Partially Assembled Tank

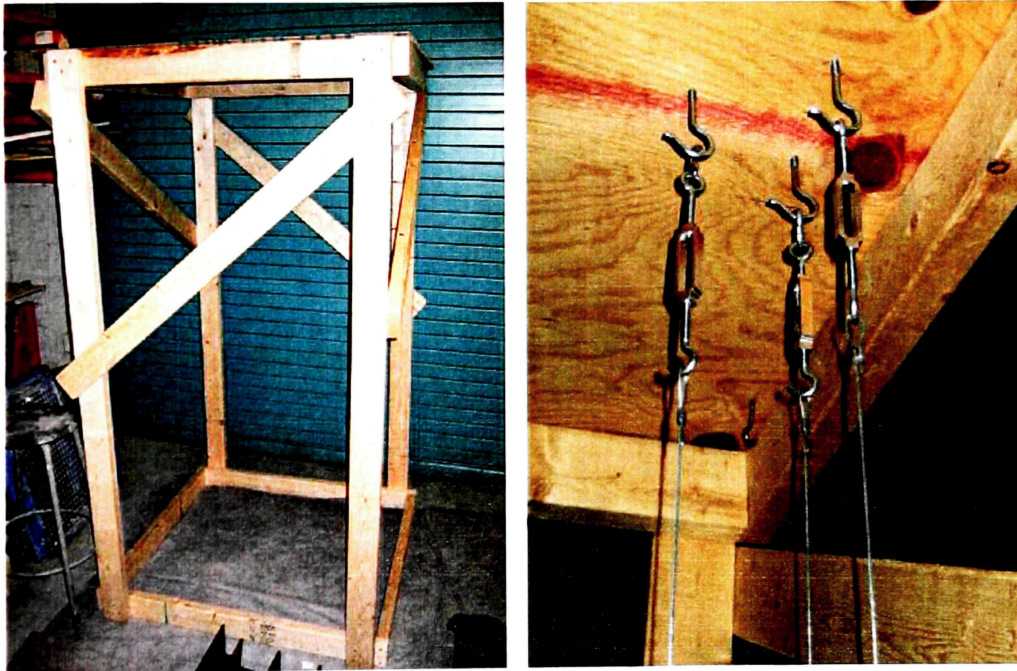


(3) Final Tank Assembly

Figure A5. Tank Assembly Construction

## **A5. Pendulum/Tank Assembly Support Frame Construction**

In order to assume that the motion of the pendulum/tank frame is transverse and not rotational, three cables were placed between the assemblies and the ceiling. The ceiling in the laboratory is too high for hanging the assemblies. As a result, a wooden pendulum/tank assembly support frame was designed and constructed. Hooks and turnbuckles were then placed on the frame for each assembly. Turnbuckles allowed for precise vertical placement and balancing of each assembly. Figure A6 illustrates pendulum/tank assembly support frame.



**Figure A6. Pendulum/Tank Support Frame and Turnbuckles**

**APPENDIX B**  
**SLOSH CODE OUTPUT TABLES**

**Table B1. SLOSH Code Output for an 8 Inch Diameter Sphere at Various Fill Levels**

Water Properties at 20 degrees C: Density = 998.2 kg/m <sup>3</sup> ; Kinematic Viscosity = 1.00e-6 m <sup>2</sup> /s							Frame Testing Region (due to mass constraints)				
Fill Level %	1	10	20	30	40	50	60	70	80	90	99
Liquid Mass (kg)	1.31E-03	1.23E-01	4.56E-01	9.47E-01	1.54E+00	2.19E+00	2.84E+00	3.44E+00	3.93E+00	4.26E+00	4.38E+00
Liquid Surface Height (m)	2.03E-03	2.03E-02	4.06E-02	6.10E-02	8.13E-02	1.02E-01	1.22E-01	1.42E-01	1.63E-01	1.83E-01	2.01E-01
<b>First Mode Parameters</b>											
Pend. Mass (kg)	1.29E-03	1.14E-01	3.90E-01	7.31E-01	1.05E+00	1.27E+00	1.34E+00	1.21E+00	8.98E-01	4.34E-01	2.62E-02
Pend. Length (m)	1.01E-01	9.47E-02	8.77E-02	8.05E-02	7.30E-02	6.51E-02	5.67E-02	4.74E-02	3.67E-02	2.35E-02	4.71E-03
Pend. Hinge z-location (m)	1.02E-01	1.02E-01	1.02E-01	1.02E-01	1.02E-01	1.02E-01	1.02E-01	1.04E-01	1.09E-01	1.15E-01	0.00E+00
Pend % Crit. Damping	3.00E+01	3.00E+00	1.50E+00	1.00E+00	7.50E-01	6.00E-01	7.03E-01	8.74E-01	1.22E+00	2.25E+00	2.07E+01
Ratio of Slosh Amplitude to Pendulum Amplitude	2.00E-01	6.28E-01	8.81E-01	1.07E+00	1.22E+00	1.34E+00	1.45E+00	1.54E+00	1.64E+00	1.78E+00	3.05E+00
<b>Second Mode Parameters</b>											
Pend. Mass (kg)	2.37E-08	1.85E-04	2.09E-03	7.61E-03	1.77E-02	3.19E-02	4.77E-02	6.27E-02	6.60E-02	4.54E-02	2.09E-03
Pend. Length (m)	1.46E-02	1.62E-02	1.77E-02	1.88E-02	1.94E-02	1.93E-02	1.85E-02	1.69E-02	1.44E-02	1.04E-02	2.89E-03
Pend. Hinge z-location (m)	9.84E-02	9.49E-02	9.49E-02	9.60E-02	9.74E-02	9.88E-02	1.00E-01	9.95E-02	9.46E-02	7.49E-02	2.03E-03
Pend. % Crit. Damping	3.00E+01	3.00E+00	1.50E+00	1.00E+00	7.50E-01	6.00E-01	7.03E-01	8.74E-01	1.22E+00	2.25E+00	2.07E+01
Ratio of Slosh Amplitude to Pendulum Amplitude	3.11E-03	7.18E-02	1.45E-01	2.05E-01	2.63E-01	3.28E-01	4.05E-01	5.06E-01	6.27E-01	7.77E-01	8.42E-01
<b>Fixed Mass Parameters</b>											
Mass (kg)	8.72E-06	8.35E-03	6.43E-02	2.09E-01	4.76E-01	8.90E-01	1.46E+00	2.16E+00	2.97E+00	3.78E+00	4.36E+00
Z-location (m)	1.02E-01	1.02E-01	1.02E-01	1.02E-01	1.02E-01	1.01E-01	1.01E-01	1.00E-01	9.95E-02	1.00E-01	1.02E-01
Mom. Inertia (kg*m <sup>2</sup> )	9.74E-10	8.95E-06	1.31E-04	6.00E-04	1.70E-03	3.68E-03	6.59E-03	1.03E-02	1.42E-02	1.70E-02	1.78E-02
1st Mode Slosh Frequency	1.57E+00	1.62E+00	1.68E+00	1.76E+00	1.85E+00	1.95E+00	2.09E+00	2.29E+00	2.60E+00	3.25E+00	7.26E+00
2nd Mode Slosh Frequency	4.12E+00	3.92E+00	3.74E+00	3.63E+00	3.58E+00	3.59E+00	3.67E+00	3.83E+00	4.15E+00	4.89E+00	9.27E+00
*Frequencies are cycles/sec.											
<b>English Units</b>	1	10	20	30	40	50	60	70	80	90	99
Total Sloshing Mass (kg)	1.29E-03	1.14E-01	3.92E-01	7.38E-01	1.07E+00	1.30E+00	1.39E+00	1.28E+00	9.64E-01	4.79E-01	2.83E-02
Liquid Mass (lb)	2.88E-03	2.71E-01	1.01E+00	2.09E+00	3.40E+00	4.84E+00	6.27E+00	7.58E+00	8.66E+00	9.40E+00	9.67E+00
Total Sloshing Mass (lb)	2.85E-03	2.52E-01	8.64E-01	1.63E+00	2.35E+00	2.87E+00	3.06E+00	2.82E+00	2.13E+00	1.06E+00	6.23E-02
Fixed Mass (lb)	1.92E-05	1.84E-02	1.42E-01	4.61E-01	1.05E+00	1.96E+00	3.21E+00	4.76E+00	6.54E+00	8.34E+00	9.60E+00
Pend. Length (in)	3.97E+00	3.73E+00	3.45E+00	3.17E+00	2.87E+00	2.57E+00	2.23E+00	1.87E+00	1.45E+00	9.26E-01	1.86E-01

**Table B2**

**SLOSH Code Predicted Natural Frequencies for an 8 Inch Diameter Sphere**

Fill Level %	Length (m)	Length (in)	Frequency Hz	Period (T) Sec.	Frequency (cycles/min)
1%	1.009E-01	3.97	1.5685	0.6375	94.1107
10%	9.474E-02	3.73	1.6187	0.6178	97.1221
20%	8.770E-02	3.45	1.6824	0.5944	100.9450
30%	8.046E-02	3.17	1.7565	0.5693	105.3889
40%	7.296E-02	2.87	1.8446	0.5421	110.6732
50%	6.514E-02	2.56	1.9521	0.5123	117.1280
60%	5.671E-02	2.23	2.0922	0.4780	125.5321
70%	4.742E-02	1.87	2.2880	0.4371	137.2790
80%	3.672E-02	1.45	2.6001	0.3846	156.0032
90%	2.352E-02	0.93	3.2487	0.3078	194.9244
99%	4.711E-03	0.19	7.2590	0.1378	435.5402

The value of acceleration due to gravity  $g = 9.8 \text{ m/s}^2$



**APPENDIX C**  
**BALLAST AND LIQUID MEASUREMENT TABLES**

**Table C1**

Ballast Tables for 8" Diameter Sphere Experimental Testing (English Units)											
Mass Information (lb)						SLOSH Code Output		60%	70%	80%	90%
Frame (No Pendulum)	3.18					Total Sloshing Mass (kg)		1.3857	1.2767	0.9637	0.4793
Pendulum Container	0.35					Liquid Mass (lb)		6.2655	7.5794	8.6619	9.3960
Bead Container	0.32					Total Sloshing Mass (lb)		3.0550	2.8146	2.1246	1.0568
Frame Mass Distribution						Fixed Mass (lb)		3.2099	4.7641	6.5366	8.3400
Container (1,3)	37.32%					Pend. Length (in)		2.2327	1.8669	1.4457	0.9260
Container (1,2)	30.82%										
Container (2,3)	31.86%										
Frozen Mass Testing (lb)		60%	70%	80%	90%	Liquid Mass Testing (lb)		60%	70%	80%	90%
Total Liquid Mass	6.27	7.58	8.66	9.40	Total Liquid Mass		6.27	7.58	8.66	9.40	
Mass to be added to frame	3.09	4.40	5.48	6.22	Mass to be added to frame		0.03	1.58	3.36	5.16	
Mass in Container (1,3)	1.15	1.64	2.05	2.32	Mass to be added to Pendulum		2.71	2.46	1.77	0.71	
Mass in Container (1,2)	0.95	1.36	1.69	1.92	Mass in Container (1,3)		0.01	0.59	1.25	1.93	
Mass in Container (2,3)	0.98	1.40	1.75	1.98	Mass in Container (1,2)		0.01	0.49	1.03	1.59	
						Mass in Container (2,3)		0.01	0.50	1.07	1.64
Scale Readings for Frozen Masses*						Scale Readings for Liquid Masses*					
Mass for Container (1,3)	1.47	1.96	2.37	2.64	Mass for Container (1,3)		0.33	0.91	1.57	2.25	
Mass for Container (1,2)	1.27	1.68	2.01	2.24	Mass for Container (1,2)		0.33	0.81	1.35	1.91	
Mass for Container (2,3)	1.30	1.72	2.07	2.30	Mass for Container (2,3)		0.33	0.82	1.39	1.96	
*This takes into account the mass of the bead container						Mass for Pendulum		3.03	2.78	2.09	1.03
						*This takes into account the mass of the bead container					

**Table C2**

Liquid Mass Tables of 8" Diameter Sphere Experimental Testing				
Mass Information (lb)				
Eight Inch Sphere Assembly*	0.820			
Clear Container	0.192			
Brown Container	0.170			
*Mass will not be subtracted from total liquid mass				
SLOSH Code Output	60%	70%	80%	90%
Total Liquid Mass (lb)	6.265	7.579	8.662	9.396
Pend. Length (in)	2.233	1.867	1.446	0.926
Frequency (Hz)	2.092	2.288	2.600	3.249
Period (s)	0.478	0.437	0.385	0.308
	60%	70%	80%	90%
Scale Readings for Liquid Masses*	6.4352	7.5794	8.6619	9.3960
*This takes into account the mass of the brown container				
	60%	70%	80%	90%
Transducer Mounting Location (in)	2.90	3.18	3.47	3.77

**APPENDIX D**  
**M-CODE INCOPORATING THE “lsqnonlin” ALGORITHM**

## D1. M-Code (Standard)

The code provided was used for all but the multiple dataset optimization. The comments provide a step-by-step breakdown of the code's operation.

### D1.1 Main Program: ERAU\_NonLinSQ.m

```
% Emory-Riddle Aeronautical University Fuel Slosh Project: Non Linear
Least Squares Parameter Estimator - ERAU_NonLinSQ.m
% Keith Schlee Spring 2006
% Files required (4):
% 1) parametervariables.m
% 2) parametermatrix.m
% 3) xls(A1-C5)PC.m (Table of experimental data [time, force])
% 4) erau_massless_nlls.mdl (SimMechanics model of experiment)
tic
clc
clear
format long
global TANK m av delay angle l k b
%_initialize all parameter variables (parametervariables.m)
parametervariables

%Call up experimental data and setup force and time columns
load('A1PC.mat')
ex_len = length(Time);
V = Force;
t = Time;

TANK = [V,t];

%Input initial parameter variables here...
disp('Initial Parameter Guesses [Angular Velocity, Initial Flywheel
Angle k b]')
Parameters = [av k b l]
%If more parameters...
%Parameters = [av k b l m delay]

%Give parameter lower and upper bounds (remember to have your initial
guess
%be within these bounds.
%Example lb = [-0.05(av) 0(k) 0(b) -2.6667(l)]
lb = [-0.5 0 0 -2.6667];
ub = [0.5 1 1 -1.5];

%If more than less parameters...
%lb=[-0.5 0];
%ub=[0.5 1];
```

```

%Setup and run the lsqnonlin algorithm. This calls up the
parametermatrix.m file
options =
optimset('LargeScale','on','Display','iter','MaxFunEvals',1000,'MaxIter',
',30','TolX',0.000001,'TolFun',0.000001);

[sd,resnorm,residual,exitflag,output]=lsqnonlin(@parametermatrix,Parameters,lb,ub,options);

%Show final residual value and results
disp('Final Optimization')
resnorm;
sd

%Setup plot
Values = load('out.mat');
Valueplot=Values.ans;
Var2=Valueplot(2,1:1:3401);

PlotOn=1;
if PlotOn == 1
    hold on
    plot(V,'b')
    plot(Var2,'r')
    legend('Experiment','Simulation')
    title('Experiment vs. Simulation')
    xlabel('Data Points')
    ylabel('Force (lb)')
    hold off
end
toc

```

## D1.2. Function: parametermatrix.m

```
% Embry-Riddle Aeronautical University Fuel Slosh Project: Non Linear
% Least Squares Parameter Estimator - parametermatrix.m
% Keith Schlee Spring 2006
% Find the difference between experiment and the simulation (current
% iteration) data
function R = parametermatrix(Parameters)
global TANK m av delay angle k b l pm

%Experimental simulation output (force and time)
V=TANK(:,1);
t=TANK(:,2);

%Setup parameteroutput here in order of appearance
av=Parameters(1);
k=Parameters(2);
b=Parameters(3);
l=Parameters(4);

% If more than four parameters...
% m=Parameters(5);
% delay=Parameters(6);

% Run SimMechanics simulation and load output values...
sim('erau_massless_nlls.mdl');
Values = load('out.mat');

% Setup Experiment length.
% Important: The simulation output table must have the same number of
% points as the measured data table.

% sim_len = Length of the simulation
sim_len = 3401;

% Load Excel of experimental data...
load('A3PC.mat')

% ex_len = Length of the experiment
ex_len = 3401;

% Assign simulation force output to a table in the MATLAB workspace...
Var2=Values.ans(2,1:1:3401)';

%Set stopping criterion for Newton's method
R=V-Var2;

% The residual (R) is defined as the sum of the individual differences.
```

### D1.3. Function: `parametervariables.m`

```
% Embry-Riddle Aeronautical University Fuel Slosh Project: Non Linear
% Least
% Squares Parameter Estimator - parametervariables.m
% Keith Schlee Spring 2006
```

```
global TANK m av delay angle k b l
```

```
%Assign other parameter initial guesses...
```

```
%Angular acceleration (rad/s)
av=-0.0791090;
```

```
%Spring and Damping Constants
k=0.08788;
b=0.0007102;
```

```
%Pendulum Length
l=-1.69;
```

```
%Examples of other parameters to estimate...
```

```
%Tank "Frozen" Mass (lb)
%m = 9.5;
```

```
%Locomotive arm travel length (in)
%r=0.11;
```

```
%Transport Delay (not in this SimMechanics Model...)
%delay=0.0000000001;
```

```
%Flywheel Initial Angle (x pi)
%angle=-0.01;
```



## D2. M-Code (Multiple Dataset)

The following is a modified version of the M-Code. For more detailed comments on the code's basic operation, please refer to the previous section.

### D2.1. Main Program: ERAU\_NonLinSQ.m

```
% Embry-Riddle Aeronautical University Fuel Slosh Project: Non Linear
% Least
% Squares Parameter Estimator - ERAU_NonLinSQ.m
% Keith Schlee Spring 2006
% Files required (+):
%   parametervariables.m
%   parametermatrix.m
%   A(1-3)FrozenPCxls.m (Excel tables of experimental data)
%   erau_massless_nlls.mdl (SimMechanics model of experiment)
tic
clc
clear
format long
global TANK k b l Var2

% Initialize all parameter variables
parametervariables

% Call up experimental datasets and superimpose them to form one force
%vector
load('A1FrozenPCxls.mat')
load('A2FrozenPCxls.mat')
load('A3FrozenPCxls.mat')
ex_len = length(TimeA3);
V = ForceA1+ForceA2+ForceA3;
t = TimeA3;

TANK = [V,t];

% Input initial parameter variables here...
disp('Initial Parameter Guesses [k b l av1 av2 av3 angle1 angle2
angle3]')
Parameters = [m]
lb = [4];
ub = [8];

% Setup and run the lsqnonlin algorithm
options =
optimset('LargeScale','on','Display','iter','MaxFunEvals',1000,'MaxIter',
',5','TolX',0.000001,'TolFun',0.000001);

[sd,resnorm,residual,exitflag,output]=lsqnonlin(@parametermatrix,Parameters,lb,ub,options);
```

```

% Show final residual value and results
disp('Final Optimization')
resnorm;
sd

% Setup plot
PlotOn=1;
if PlotOn == 1
    hold on
    plot(V,'b')
    plot(Var2,'r')
    legend('Experiment','Simulation')
    title('Experiment vs. Simulation')
    xlabel('Data Points')
    ylabel('Force (lb)')
    hold off
end

delete('A1out.mat');
delete('A2out.mat');
delete('A3out.mat');
toc

```

## D2.2. Function: parametermatrix.m

```

% Embry-Riddle Aeronautical University Fuel Slosh Project: Non Linear
% Least
% Squares Parameter Estimator - parametermatrix.m
% Keith Schlee Spring 2006
% Find the difference between experiment and the simulation (current
% iteration) data

function R = parametermatrix(Parameters)

global TANK m k b l Var2
% Experimental simulation output (force and time)
V=TANK(:,1);
t=TANK(:,2);

% Setup parameters
m=Parameters(1);

% If more than one parameter...
% av=Parameters(2);

%Run SimMechanics simulation and load output values...
sim('erau_fixedmass_only_60_A1');
ValuesA1 = load('A1out.mat');

```

```

sim('erau_fixedmass_only_60_A2');
ValuesA2 = load('A2out.mat');

sim('erau_fixedmass_only_60_A3');
ValuesA3 = load('A3out.mat');

% Set simulation length.
% Important:
% Simulation length (data points) must equal = Experimental Length

%sim_len = Length of the simulation
sim_len = 2001;
%Load Excel of all simulation out data...
load('A1FrozenPCxls.mat')
load('A2FrozenPCxls.mat')
load('A3FrozenPCxls.mat')

% ex_len = Length of the experiment
ex_len = 2001;

% Superimpose simulation data for comparison to measured (experimental)
data
VarA1=ValuesA1.ans(2,1:1:2001)';
VarA2=ValuesA2.ans(2,1:1:2001)';
VarA3=ValuesA3.ans(2,1:1:2001)';

Var2=VarA1+VarA2+VarA3;

%Set stopping criterion for Newton's Method
R=V-Var2;
% The residual is defined as the sum of the individual differences.

```

### **D2.3. Function: parametervariables.m**

```

% Embry-Riddle Aeronautical University Fuel Slosh Project: Non Linear
Least
% Squares Parameter Estimator - parametervariables.m
% Keith Schlee Spring 2006

global TANK m k b l Var2

%Tank Mass (lb)
%True A series mass = 6.2655 lb
m = 4.5;

%Pendulum Properties
k=0.5469;
b=0.02182;
l=-2.587;

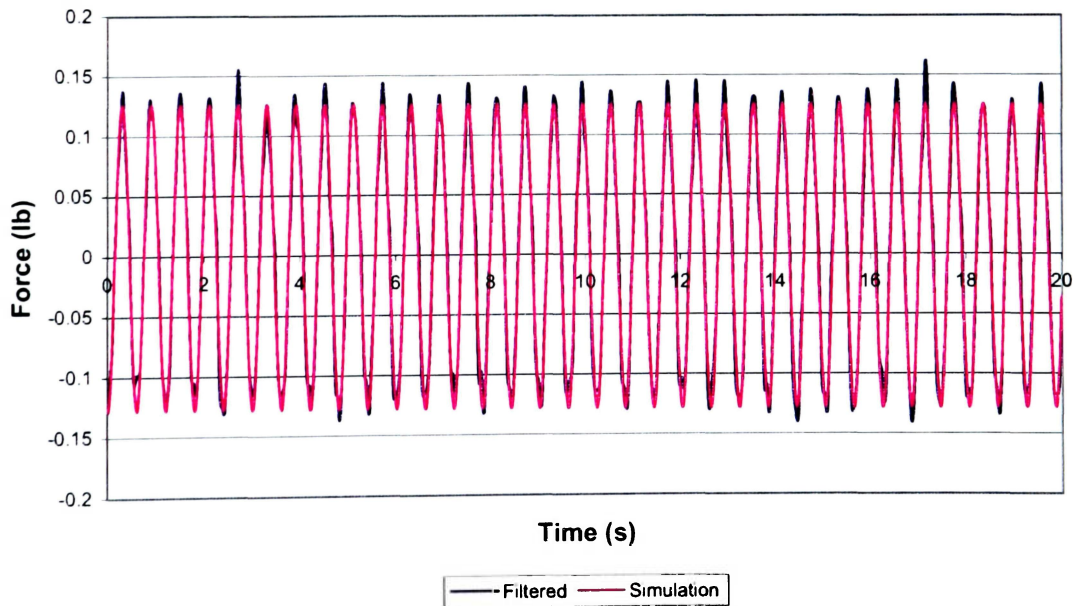
```

**APPENDIX E**  
**“FROZEN” TANK TEST RESULTS**

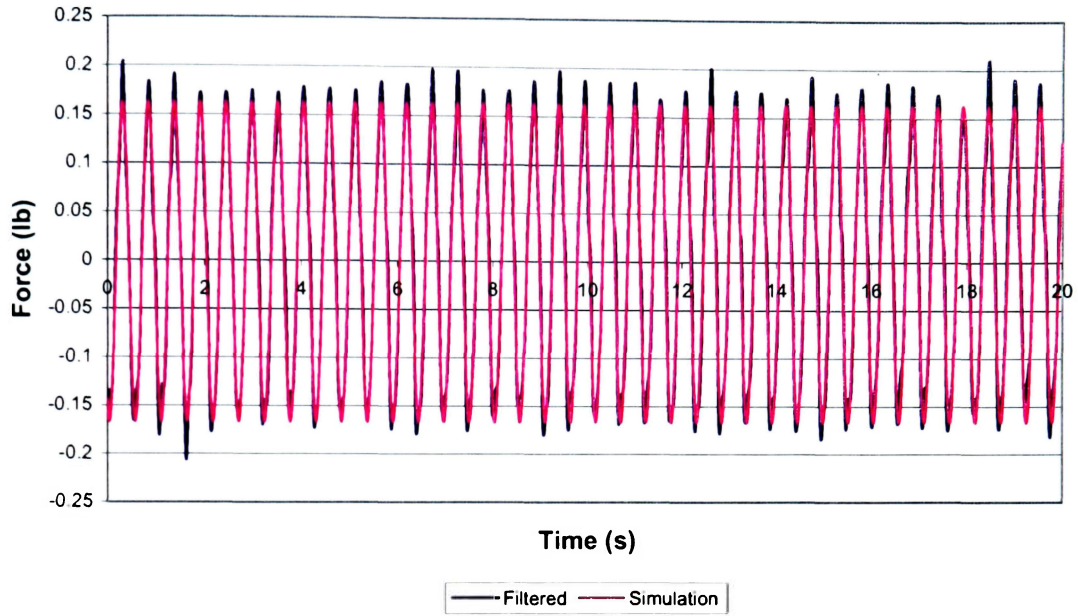
**Table D1**

**“Frozen” Tank Parameter Estimation Results**

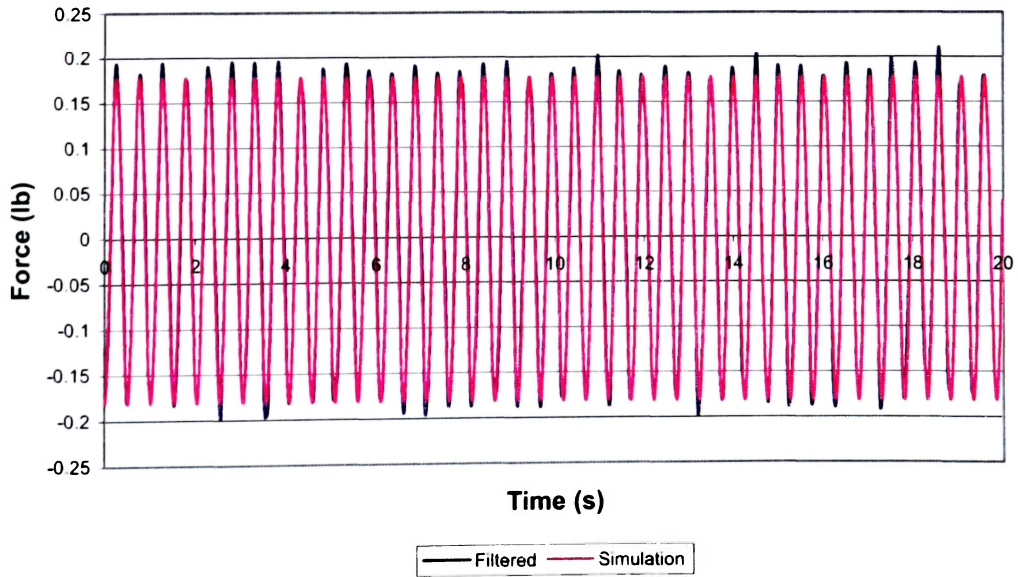
<b>“Frozen” Tank Simulation (M-Code)</b>					
Measured 60% Mass (lb)	6.2655				
Pendulum Container Mass (lb)	0.8187				
Test ID	A1	A2	A3	A4	A5
Measured Test Frequency (Hz)	1.660	1.855	1.953	2.070	2.441
Predicted Mass (lb)	6.9243	7.0600	7.0000	7.2369	7.3042
Flywheel Initial Angle (rad)	-0.1040	-0.5249	-0.0820	-0.0328	0.0382
Angular Velocity Correction (rad/s)	0.0059	0.1164	0.0744	0.1442	0.0757
Mass % Difference	2.26%	0.34%	1.19%	2.16%	3.11%
<b>“Frozen” Tank Simulation (Parameter Estimator)</b>					
Measured Test Frequency (Hz)	1.660	1.855	1.953	2.070	2.441
Predicted Mass (lb)	6.9240	7.0680	7.1118	7.1481	7.2788
Flywheel Initial Angle (rad)	-0.1041	-0.5575	-0.2097	-0.2025	0.0249
Angular Velocity Correction (rad/s)	0.0059	0.1190	0.0835	0.1572	0.0766
Mass % Difference from Measured	2.26%	0.23%	0.39%	0.90%	2.75%
<b>Mass % Difference from M-Code</b>	<b>0.004%</b>	<b>0.113%</b>	<b>1.572%</b>	<b>1.242%</b>	<b>0.349%</b>



**Figure E1. “Frozen” Tank Test A1 (60% at 1.660Hz)**



**Figure E2. “Frozen” Tank Test A2 (60% at 1.855Hz)**



**Figure E3. “Frozen” Tank Test A3 (60% at 1.953Hz)**

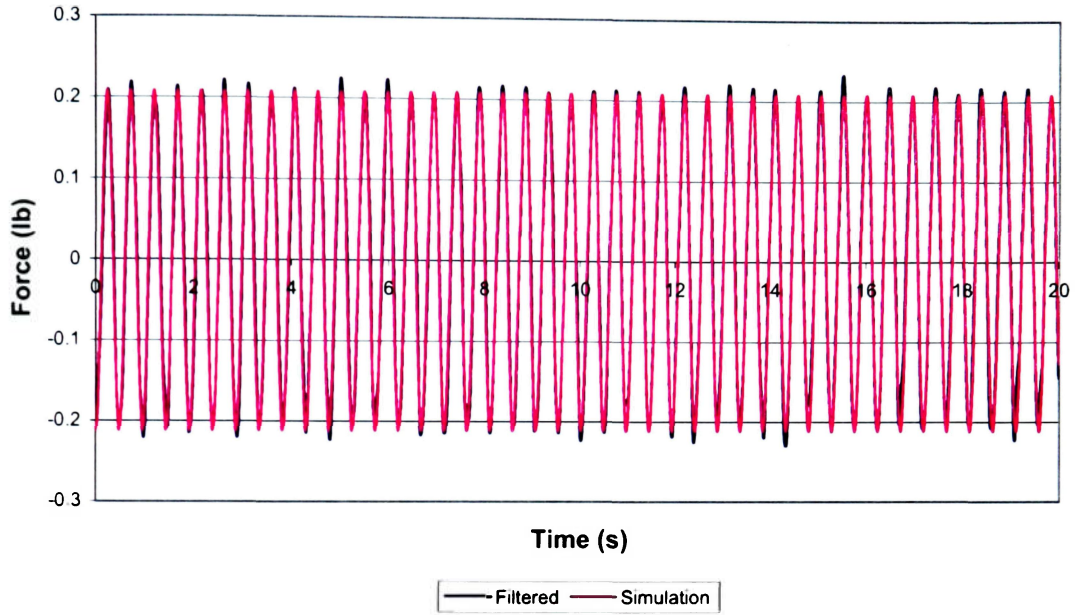


Figure E4. “Frozen” Tank Test A4 (60% at 2.070Hz)

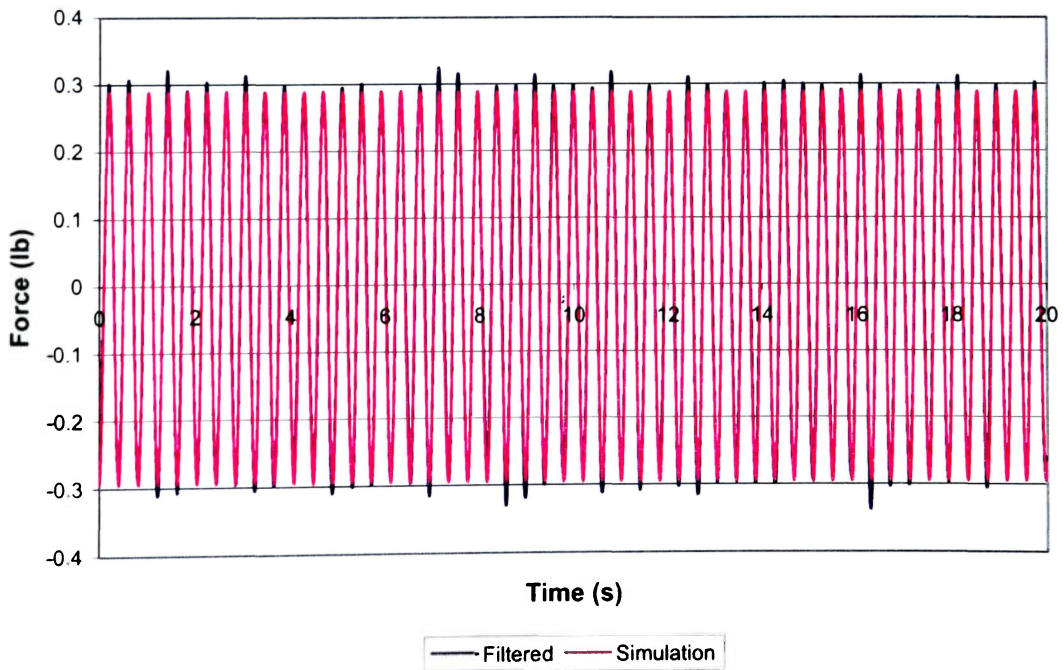


Figure E5. “Frozen” Tank Test A5 (60% at 2.441Hz)

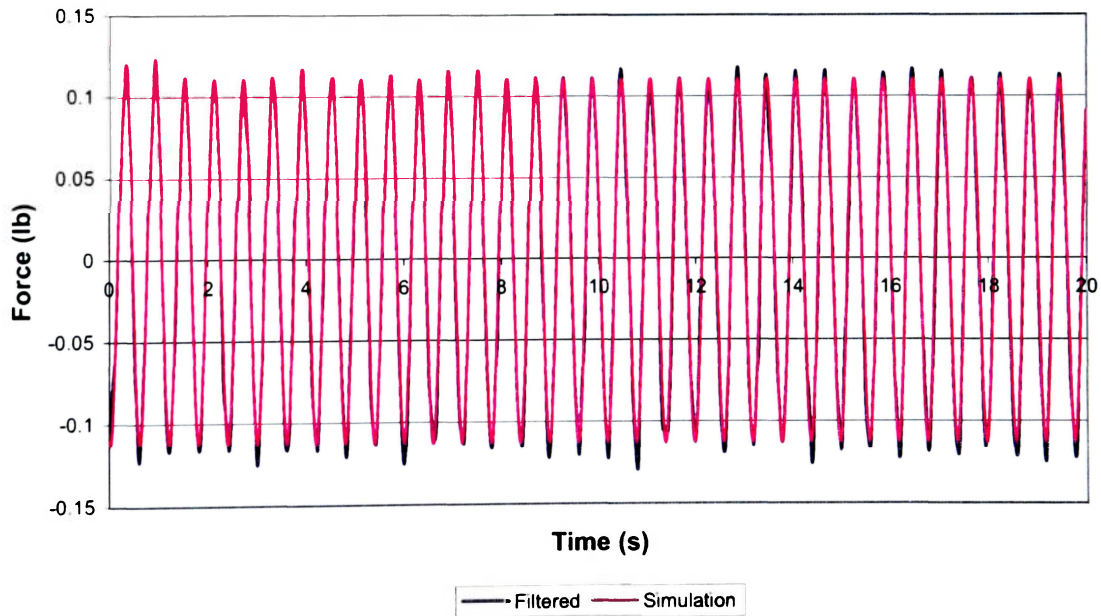
**APPENDIX F**  
**“FROZEN” PENDULUM FRAME RESULTS**



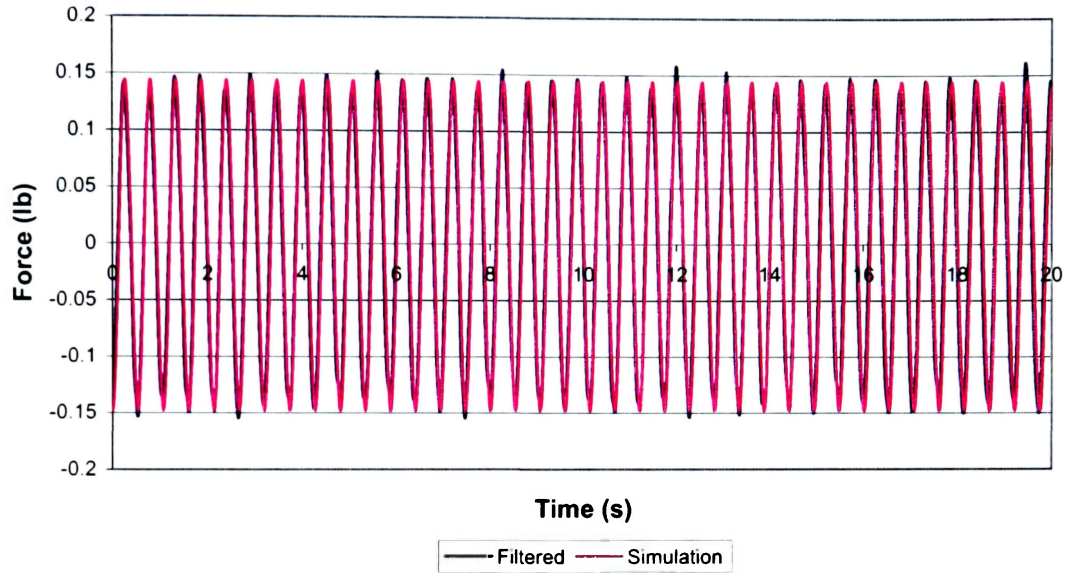
**Table F1**

**“Frozen” Pendulum Frame at 60% Fill Level Parameter Estimation Results**

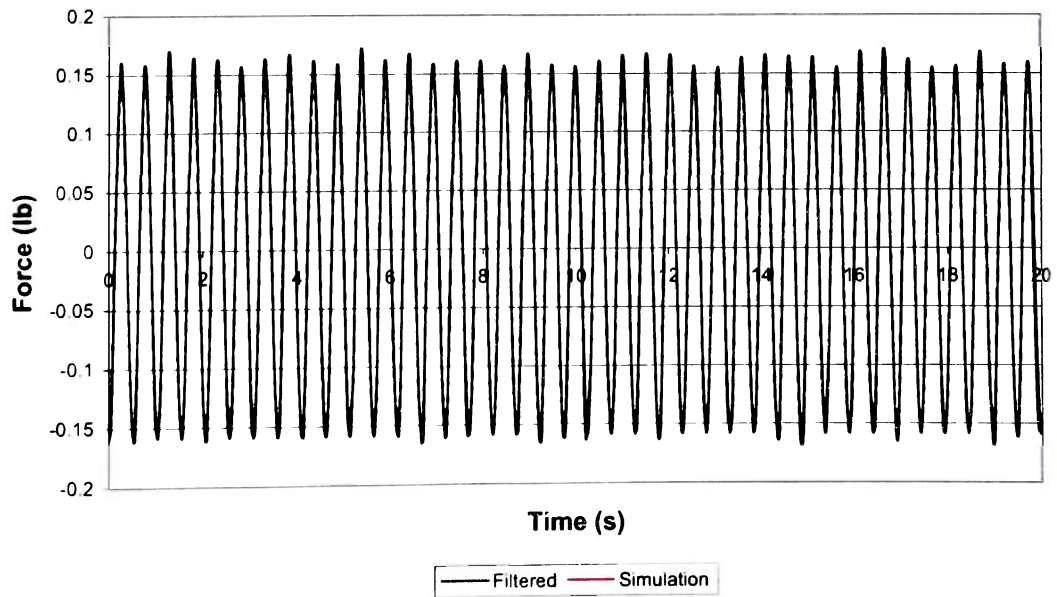
<b>“Frozen” Pendulum Frame Simulation (M-Code)</b>					
Measured 60% Mass (lb)	6.2655				
Test ID	A1	A2	A3	A4	A5
Measured Test Frequency (Hz)	1.66	1.855	1.953	2.343	2.637
Predicted Mass (lb)	6.0302	6.1236	6.1937	6.0173	5.9599
Flywheel Initial Angle (rad)	-0.2373	-0.0775	-0.1191	-0.2034	-0.5209
Angular Velocity Correction (rad/s)	0.0752	0.1159	-0.0004	0.4369	-0.0794
Mass % Difference	3.76%	2.26%	1.15%	3.96%	4.88%
<b>“Frozen” Pendulum Frame Simulation (Parameter Estimator)</b>					
Measured Test Frequency (Hz)	1.66	1.855	1.953	2.343	2.637
Predicted Mass (lb)	6.0307	6.1241	6.1939	6.0176	5.9605
Flywheel Initial Angle (rad)	-0.2855	-0.0759	-0.1177	-0.2082	-0.5205
Angular Velocity Correction (rad/s)	0.0817	0.1192	0.0038	0.4392	-0.0714
Mass % Difference from Measured	3.75%	2.26%	1.14%	3.96%	4.87%
<b>Mass % Difference from M-Code</b>	<b>0.008%</b>	<b>0.008%</b>	<b>0.003%</b>	<b>0.005%</b>	<b>0.010%</b>



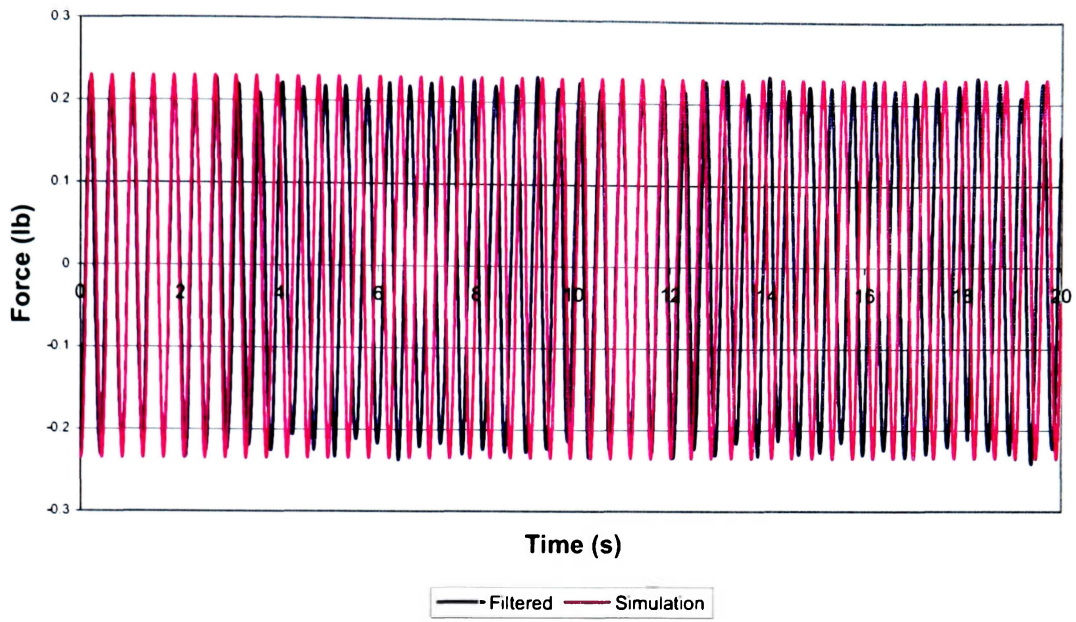
**Figure F1. “Frozen” Pendulum Frame Test A1 (60% at 1.660Hz)**



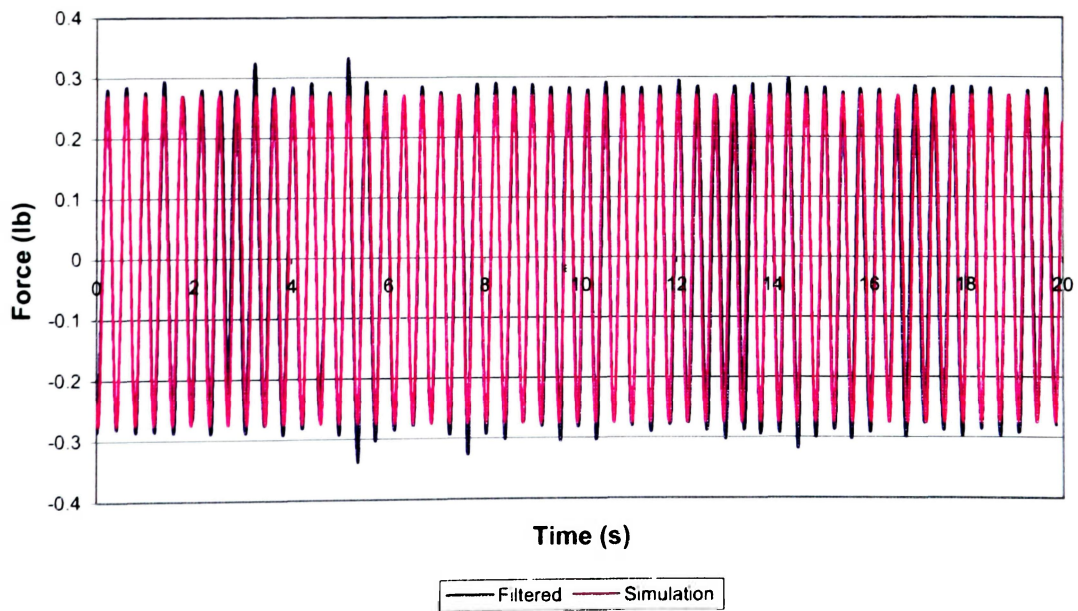
**Figure F2. “Frozen” Pendulum Frame Test A2 (60% at 1.855Hz)**



**Figure F3. “Frozen” Pendulum Frame Test A3 (60% at 1.953Hz)**



**Figure F4. “Frozen” Pendulum Frame Test A4 (60% at 2.343Hz)**

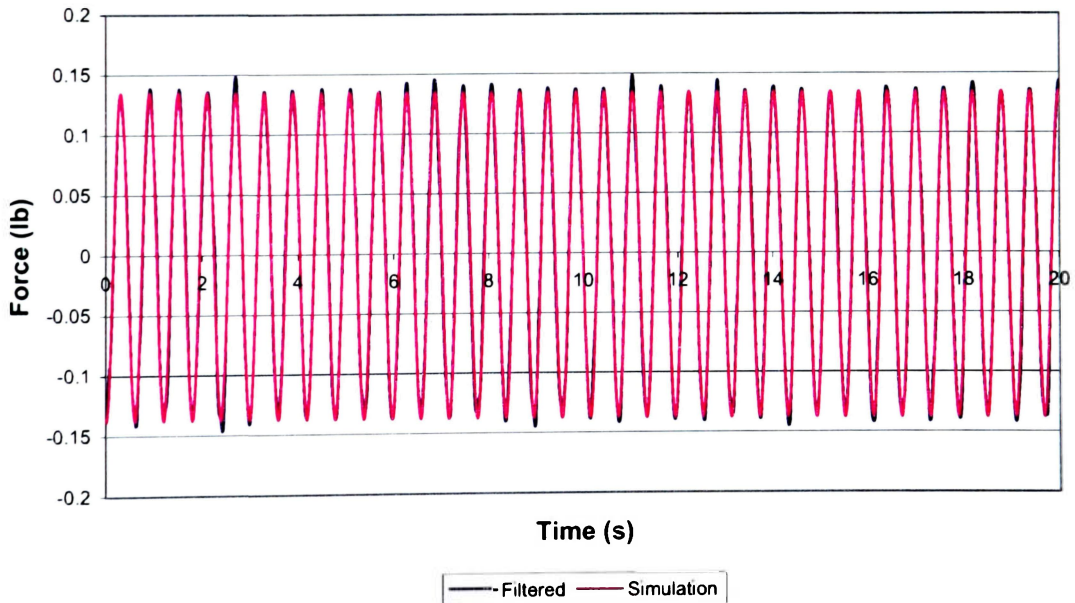


**Figure F5. “Frozen” Pendulum Frame Test A5 (60% at 2.637Hz)**

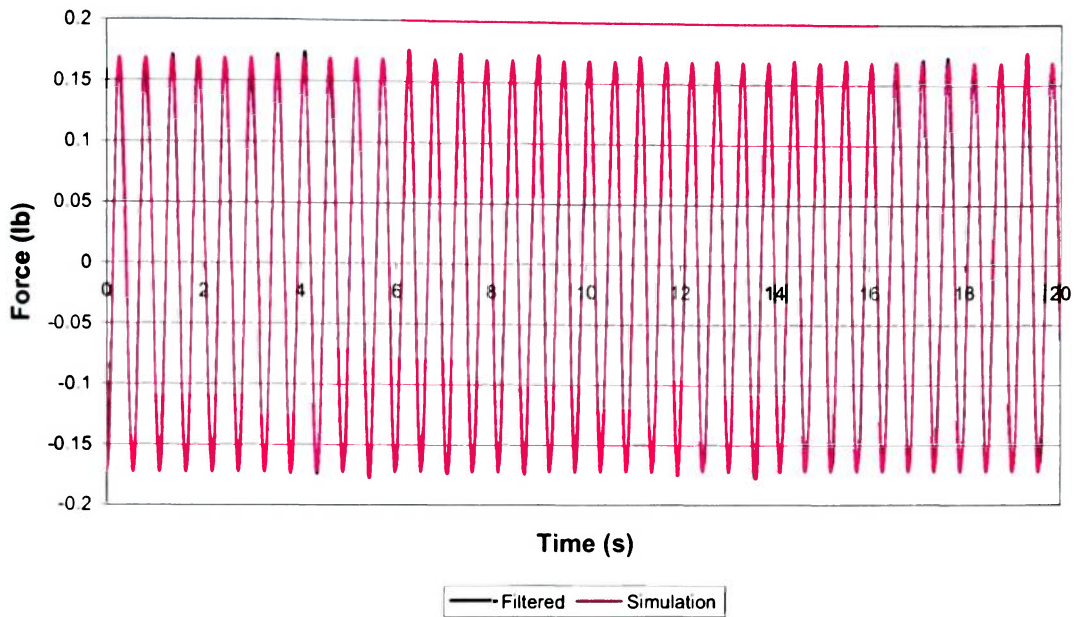
**Table F2**

**“Frozen” Pendulum Frame at 70% Fill Level Parameter Estimation Results**

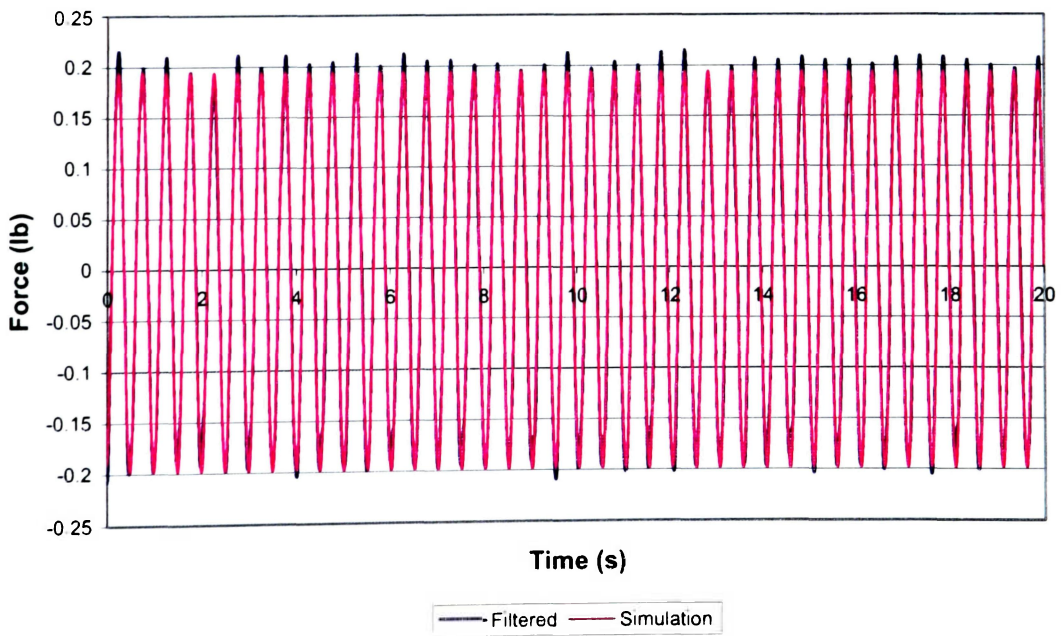
<b>*Frozen* Pendulum Frame Simulation (M-Code)</b>					
Measured 70% Mass (lb)	7.5794				
Test ID	B1	B2	B3	B4	B5
Measured Test Frequency (Hz)	1.66	1.855	1.953	2.24	2.44
Predicted Mass (lb)	7.2861	7.3778	7.4880	7.6190	7.7067
Flywheel Initial Angle (rad)	-0.1657	-0.0073	0.2818	-0.1454	-0.0778
Angular Velocity Correction (rad/s)	0.1072	-0.0916	0.2028	-0.0179	-0.0141
Mass % Difference	3.87%	2.66%	1.21%	0.52%	1.68%
<b>*Frozen* Pendulum Frame Simulation (Parameter Estimator)</b>					
Measured Test Frequency (Hz)	1.66	1.855	1.953	2.24	2.44
Predicted Mass (lb)	7.2870	7.3778	7.4881	7.6190	7.7058
Flywheel Initial Angle (rad)	-0.1702	-0.0073	0.2818	-0.1454	-0.0781
Angular Velocity Correction (rad/s)	0.1077	-0.0916	0.2029	-0.0179	-0.0140
Mass % Difference from Measured	3.86%	2.66%	1.20%	0.52%	1.67%
<b>Mass % Difference from M-Code</b>	<b>0.012%</b>	<b>0.000%</b>	<b>0.001%</b>	<b>0.000%</b>	<b>0.012%</b>



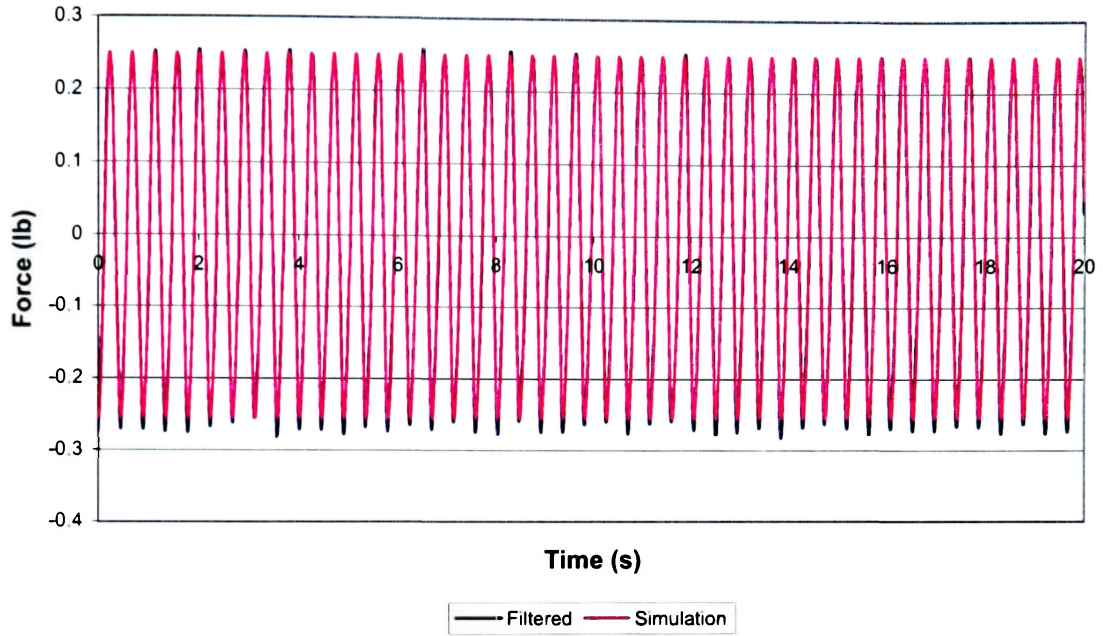
**Figure F6. “Frozen” Pendulum Frame Test B1 (70% at 1.660Hz)**



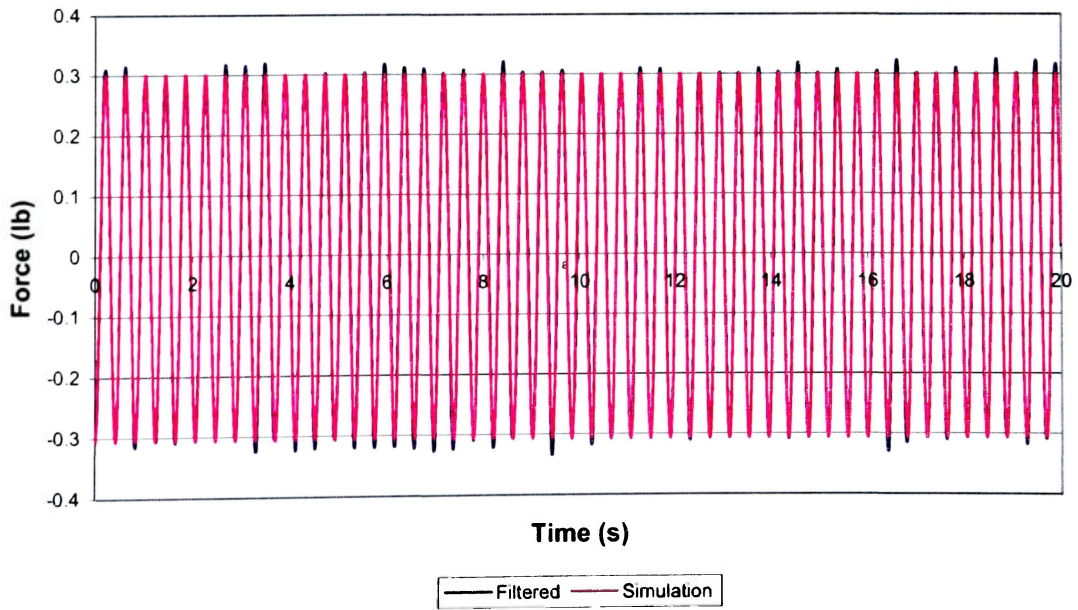
**Figure F7. “Frozen” Pendulum Frame Test B2 (70% at 1.855Hz)**



**Figure F8. “Frozen” Pendulum Frame Test B3 (70% at 1.953Hz)**



**Figure F9. “Frozen” Pendulum Frame Test B4 (70% at 2.240Hz)**

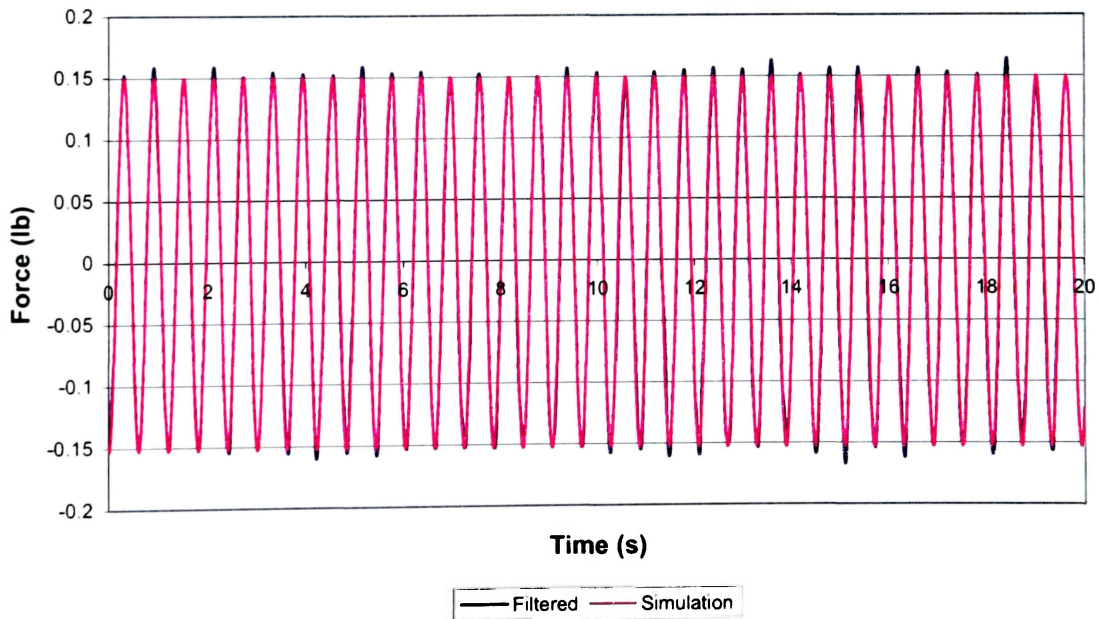


**Figure F10. “Frozen” Pendulum Frame Test B5 (70% at 2.440Hz)**

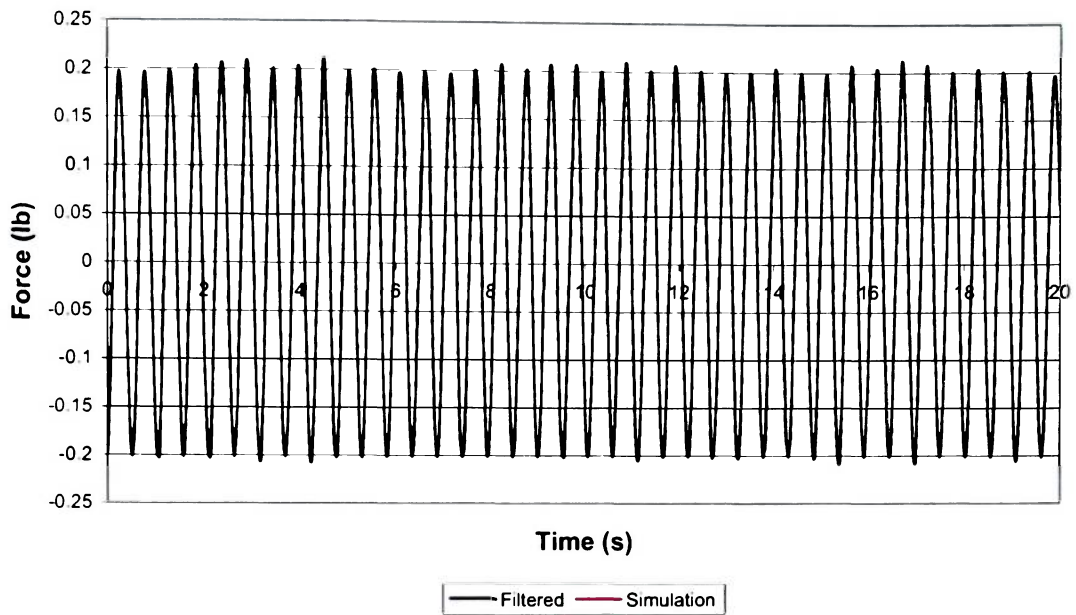
**Table F3**

**“Frozen” Pendulum Frame at 80% Fill Level Simulation Results**

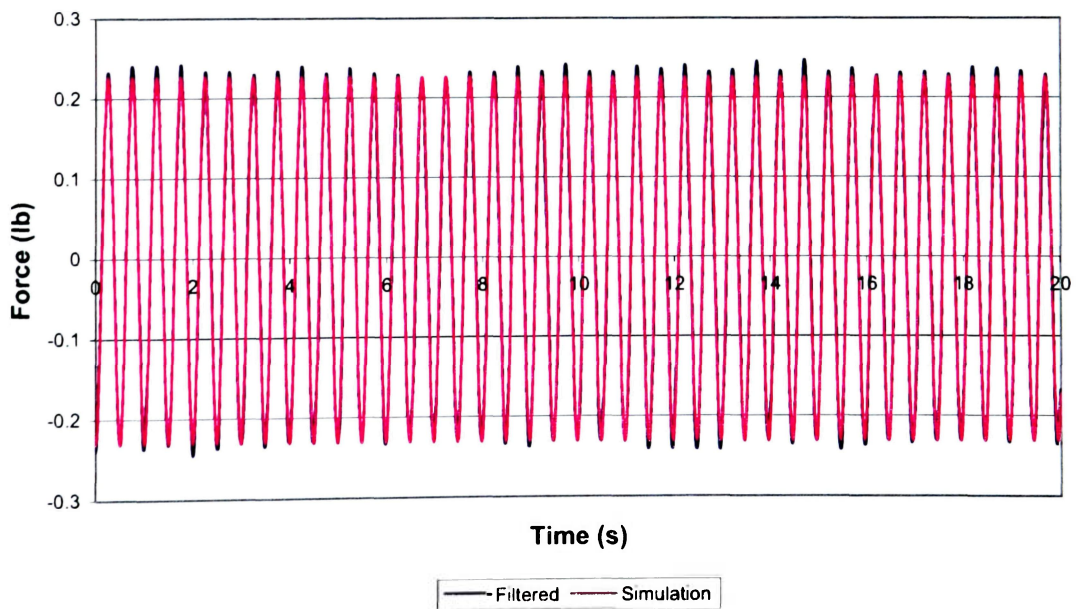
<b>“Frozen” Pendulum Frame Simulation (M-Code)</b>					
Measured 80% Mass (lb)	8.6619				
Test ID	C1	C2	C3	C4	C5
Measured Test Frequency (Hz)	1.66	1.855	2.03	2.246	2.441
Predicted Mass (lb)	8.3062	8.4404	8.5596	8.6884	8.7499
Flywheel Initial Angle (rad)	-0.1090	0.1494	-0.0487	-0.1775	0.1248
Angular Velocity Correction (rad/s)	-0.0253	0.1813	-0.1501	-0.0532	0.1782
Mass % Difference	4.11%	2.56%	1.18%	0.31%	1.02%
<b>“Frozen” Pendulum Frame Simulation (Parameter Estimator)</b>					
Measured Test Frequency (Hz)	1.66	1.855	2.03	2.246	2.441
Predicted Mass (lb)	8.2842	8.4404	8.5596	8.6685	8.7500
Flywheel Initial Angle (rad)	-0.1216	0.1494	-0.0487	-0.1969	0.1248
Angular Velocity Correction (rad/s)	-0.0243	0.1813	-0.1501	-0.0517	0.1782
Mass % Difference from Measured	4.36%	2.56%	1.18%	0.08%	1.02%
Mass % Difference from M-Code	0.266%	0.000%	0.000%	0.230%	0.001%



**Figure F11. “Frozen” Pendulum Frame Test C1 (80% at 1.660Hz)**

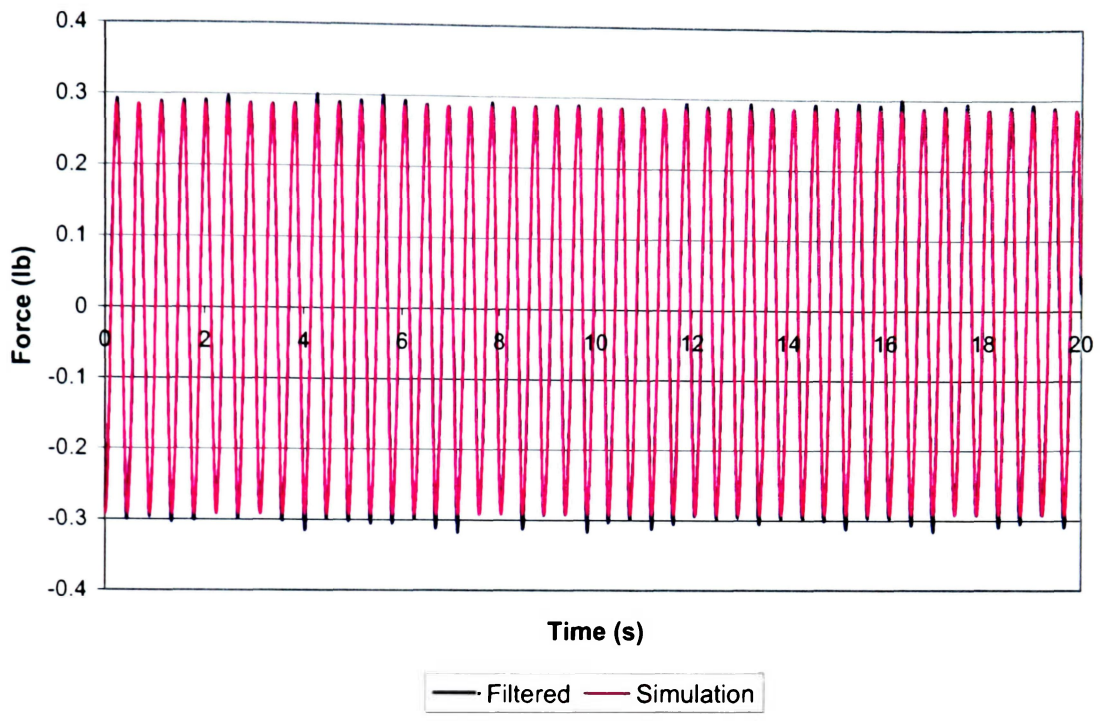


**Figure F12. “Frozen” Pendulum Frame Test C2 (80% at 1.855Hz)**

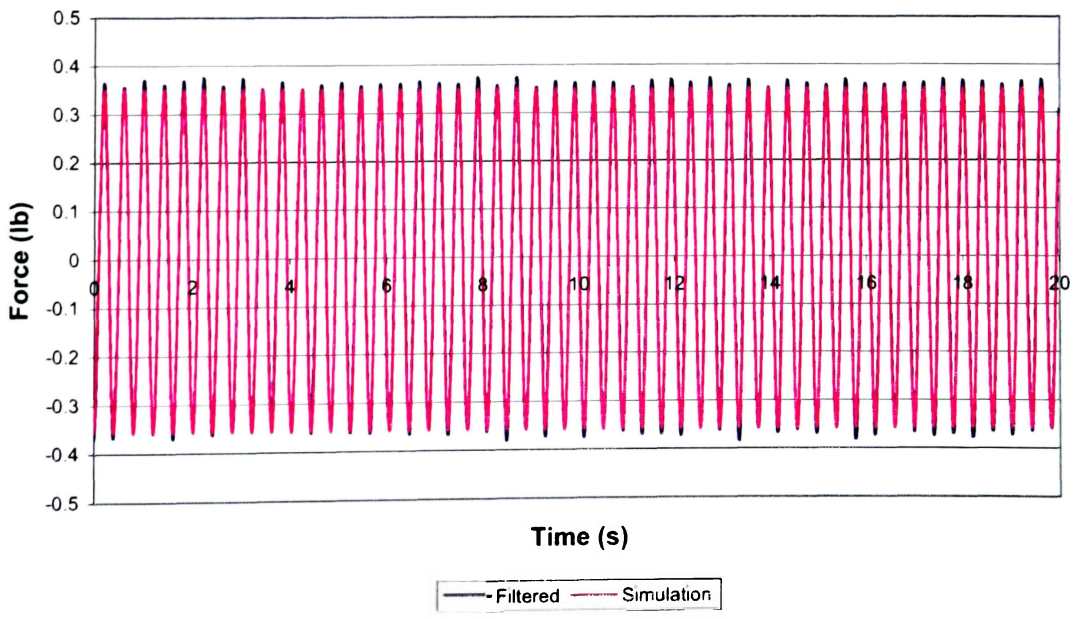


**Figure F13. “Frozen” Pendulum Frame Test C3 (80% at 2.030Hz)**





**Figure F14. “Frozen” Pendulum Frame Test C4 (80% at 2.246Hz)**



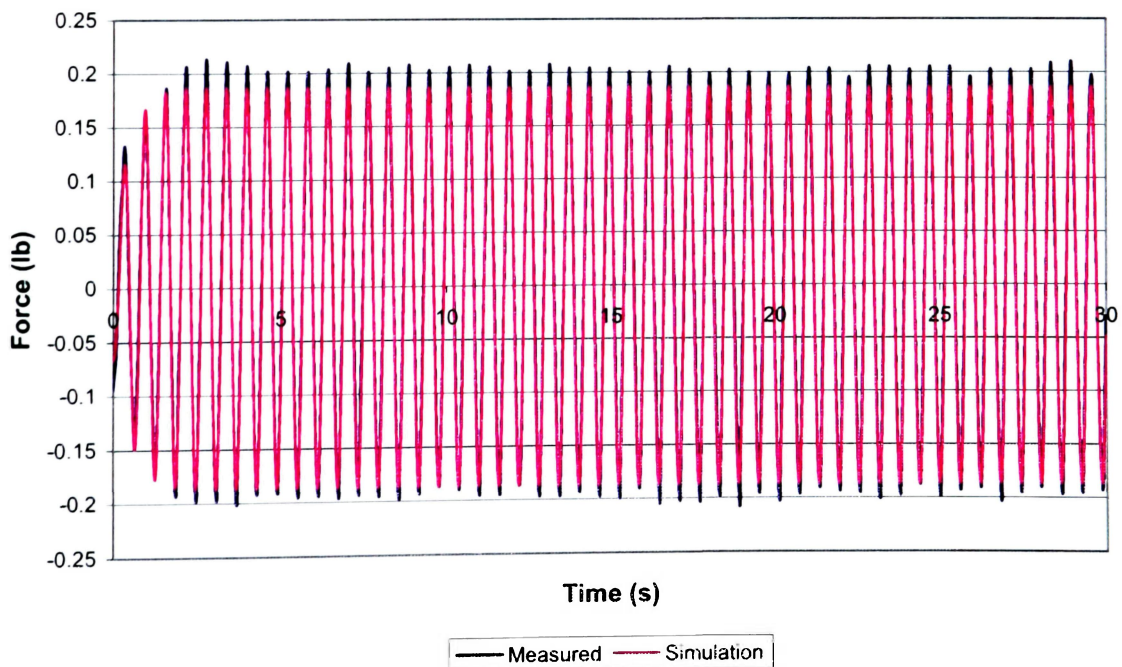
**Figure F15. “Frozen” Pendulum Frame Test C5 (80% at 2.441Hz)**

**APPENDIX G**  
**PENDULUM FRAME TEST RESULTS**

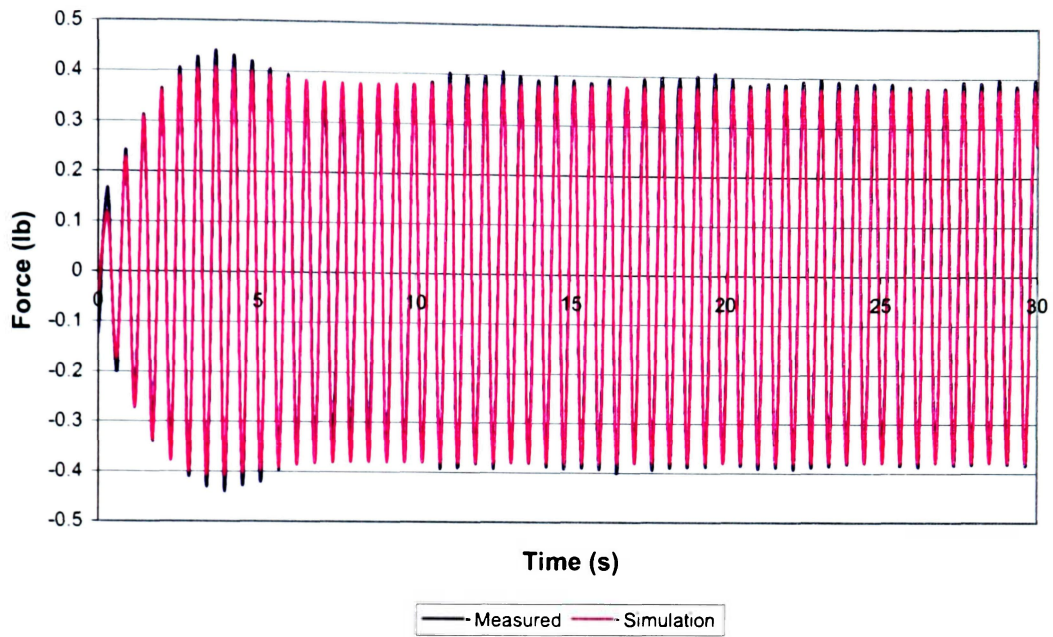
**Table G1**

**Pendulum Frame at 60% Fill Level Parameter Estimation Results**

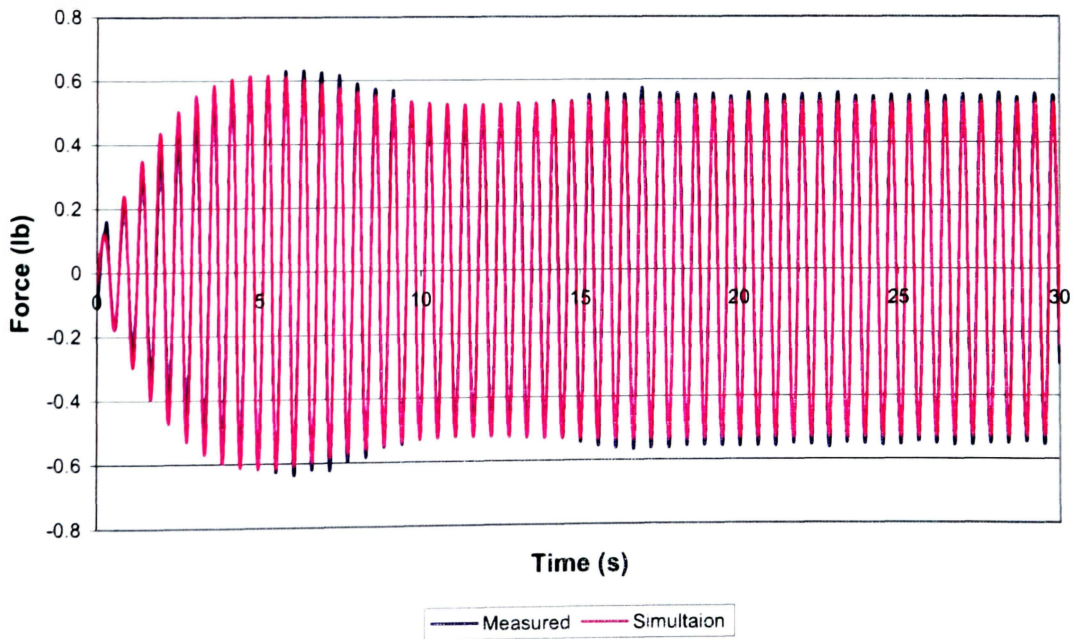
<b>M-Code: 5 Parameters</b>			
60% Fill Level Properties	Fixed Mass (lb)	Pendulum Mass (lb)	
Test ID	A1	A2	A3
Measured Test Frequency (Hz)	1.660	1.757	1.770
Angular Velocity Correction (rad/s)	-0.1124420	-0.0274759	0.1357546
Initial Flywheel Angle (rad)	-0.2676705	-0.8283001	-1.1392384
Pendulum Spring Constant (ft-lb/rad)	0.0443370	0.0454400	0.0302538
Pendulum Damping Constant (ft-lb/rad/sec)	0.0213000	0.0053249	0.0024797
Predicted Pendulum Length (in)	2.6167000	2.2831900	2.1315700
<b>Cost Function</b>	<b>0.41629</b>	<b>0.89570</b>	<b>2.52411</b>
<b>Simulation (Parameter Estimation)</b>			
Test ID	A1	A2	A3
Measured Test Frequency (Hz)	1.660	1.757	1.770
Angular Velocity Correction (rad/s)	-0.110270	-0.028498	0.135030
Initial Flywheel Angle (rad)	-0.375980	-0.810290	-1.134300
Pendulum Spring Constant (ft-lb/rad)	0.000031	0.000000	0.013874
Pendulum Damping Constant (ft-lb/rad/sec)	0.020442	0.003703	0.002133
Predicted Pendulum Length (in)	2.6185 (L)	1.949900	2.005400
<b>Cost Function</b>	<b>0.40716</b>	<b>0.83715</b>	<b>2.48520</b>



**Figure G1. Pendulum Frame Test A1 (60% at 1.660Hz)**



**Figure G2. Pendulum Frame Test A2 (60% at 1.757Hz)**

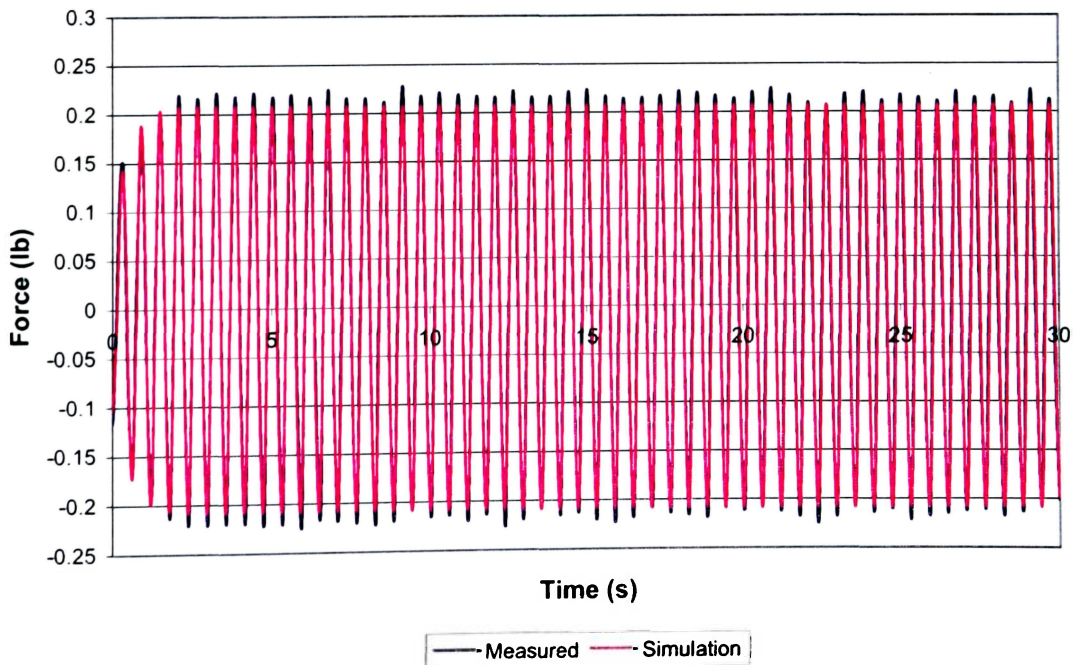


**Figure G3. Pendulum Frame Test A3 (60% at 1.770Hz)**

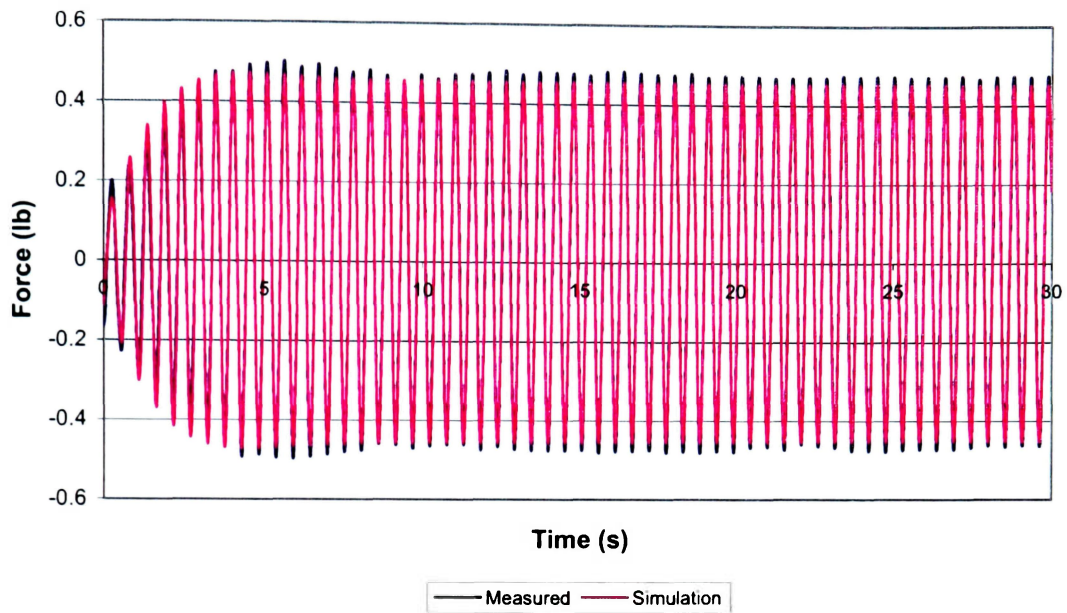
**Table G2**

**Pendulum Frame at 70% Fill Level Parameter Estimation Results**

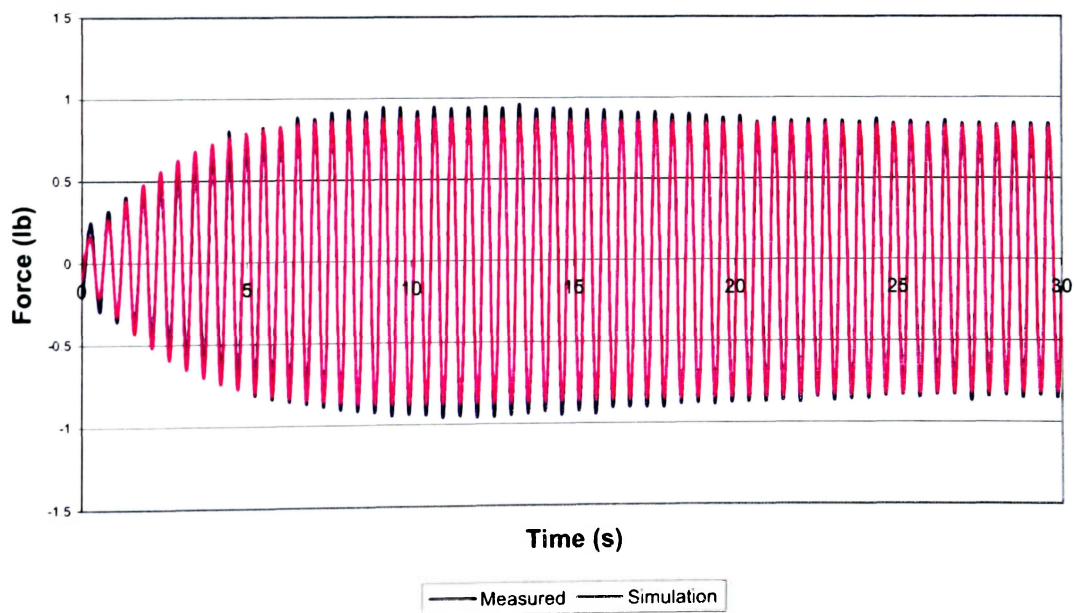
<b>70% Fill Level Properties</b>			
M-Code: 5 Parameters	Fixed Mass (lb)	Pendulum Mass (lb)	
70% Fill Level Properties	4.7641	2.8146	
Test ID	B1	B2	B3
Measured Test Frequency (Hz)	1.660	1.855	1.953
Angular Velocity Correction (rad/s)	0.2502437	0.0181199	-0.2687322
Initial Flywheel Angle (rad)	-0.2523610	-0.5001407	-0.7264287
Pendulum Spring Constant (ft-lb/rad)	0.0134840	0.0676120	0.0568440
Pendulum Damping Constant (ft-lb/rad/sec)	0.0146440	0.0046780	0.0019453
Predicted Pendulum Length (in)	2.1267100	2.1384440	2.0278480
<b>Cost Function</b>	<b>0.40960</b>	<b>0.79830</b>	<b>3.32559</b>
<b>Simulation (Parameter Estimator)</b>			
Test ID	B1	B2	B3
Measured Test Frequency (Hz)	1.660	1.855	1.953
Angular Velocity Correction (rad/s)	0.256420	0.019672	-0.268730
Initial Flywheel Angle (rad)	-0.290630	-0.687770	-0.726430
Pendulum Spring Constant (ft-lb/rad)	0.000000	0.039017	0.056846
Pendulum Damping Constant (ft-lb/rad/sec)	0.015558	0.004770	0.001946
Predicted Pendulum Length (in)	2.2404 (L)	2.060700	2.027900
<b>Cost Function</b>	<b>0.39810</b>	<b>0.67735</b>	<b>3.32560</b>



**Figure G4. Pendulum Frame Test B1 (70% at 1.660Hz)**



**Figure G5. Pendulum Frame Test B2 (70% at 1.855Hz)**

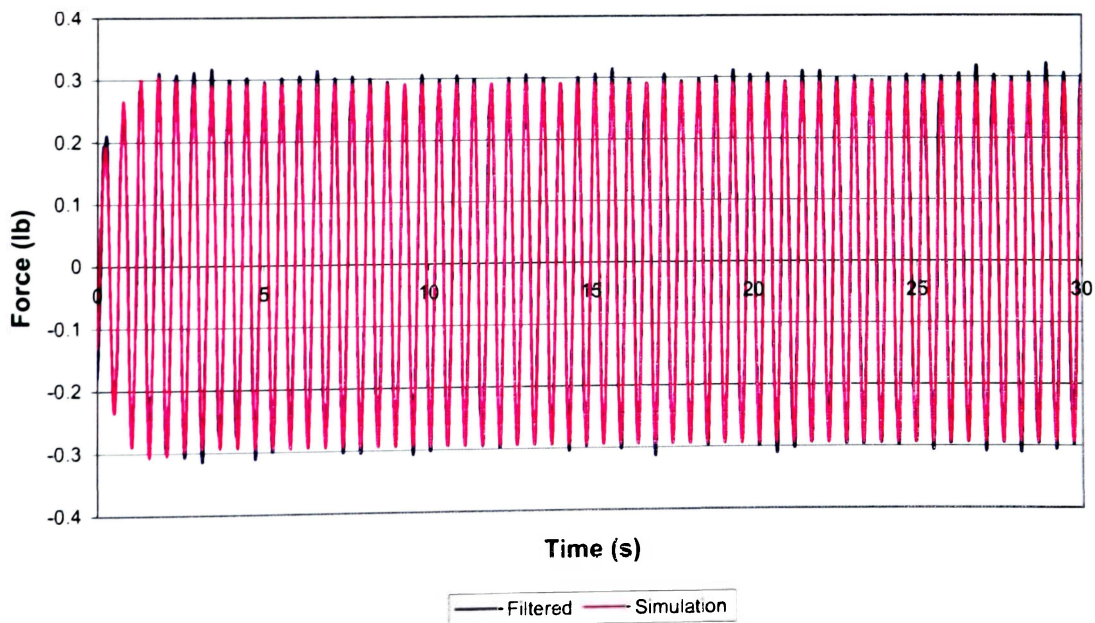


**Figure G6. Pendulum Frame Test B3 (70% at 1.953Hz)**

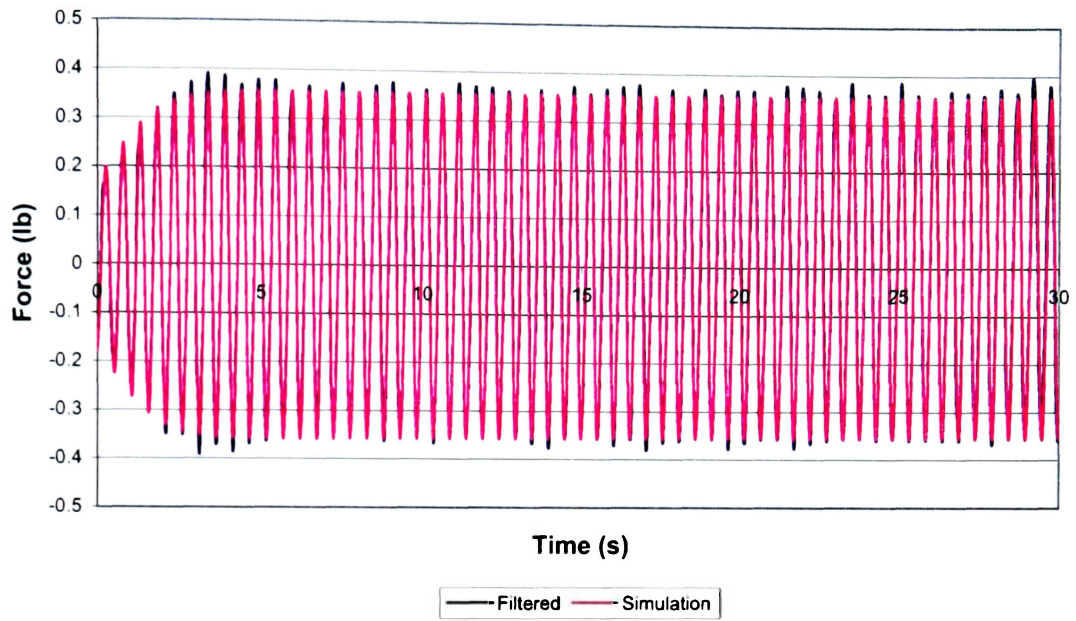
**Table G3**

**Pendulum Frame at 60% Fill Level Parameter Estimation Results**

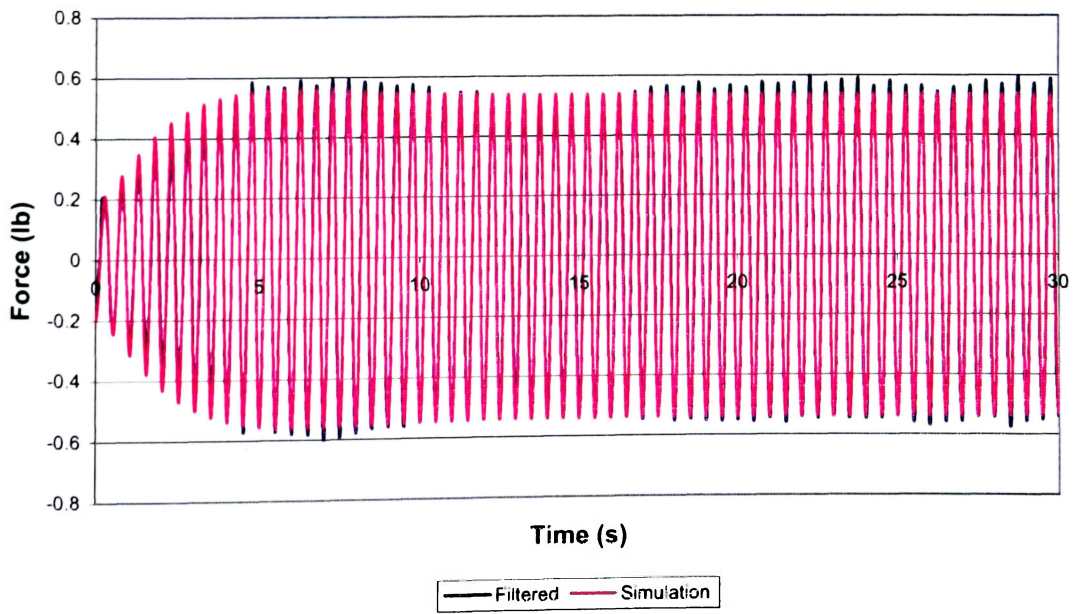
<b>Pendulum Simulation (M-Code)</b>			
M-Code: 5 Parameters	Fixed Mass (lb)	Pendulum Mass (lb)	
80% Fill Level Properties	6.5366	2.1246	
Test ID	C1	C2	C3
Measured Test Frequency (Hz)	1.855	1.953	2.050
Angular Velocity Correction (rad/s)	0.1585749	-0.1145348	-0.2952056
Initial Flywheel Angle (rad)	-0.6353138	-0.2996149	-0.0057741
Pendulum Spring Constant (ft-lb/rad)	0.0737703	0.0205405	0.0411740
Pendulum Damping Constant (ft-lb/rad/sec)	0.0039869	0.0030600	0.0016003
Predicted Pendulum Length (in)	1.731987 (L)	1.5410104	1.6057106
<b>Cost Function</b>	<b>0.8355100</b>	<b>1.8818200</b>	<b>3.63988</b>
<b>Pendulum Simulation (Parameter Estimator)</b>			
Test ID	C1	C2	C3
Measured Test Frequency (Hz)	1.855	1.953	2.050
Angular Velocity Correction (rad/s)	0.157230	-0.112720	-0.297750
Initial Flywheel Angle (rad)	-0.627160	-0.388630	0.043937
Pendulum Spring Constant (ft-lb/rad)	0.024690	0.022491	0.027992
Pendulum Damping Constant (ft-lb/rad/sec)	0.001561	0.003648	0.001026
Predicted Pendulum Length (in)	1.162400	1.695700	1.351500
<b>Cost Function</b>	<b>0.76381</b>	<b>1.86700</b>	<b>3.42940</b>



**Figure G7. Pendulum Frame Test C1 (80% at 1.855Hz)**



**Figure G8. Pendulum Frame Test C2 (80% at 1.953Hz)**



**Figure G9. Pendulum Frame Test C3 (80% at 2.050Hz)**

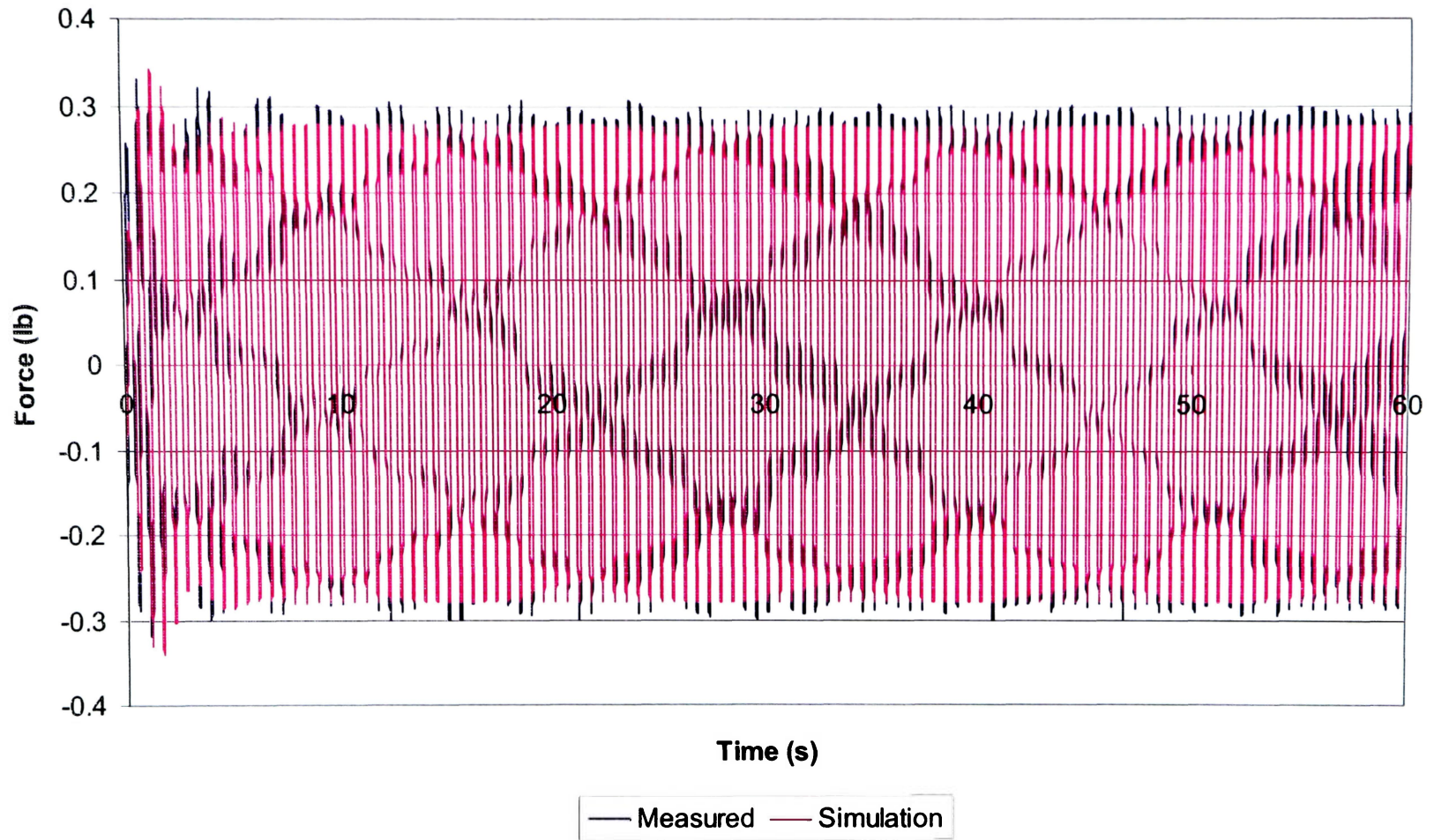


**APPENDIX H**  
**TANK TEST RESULTS**

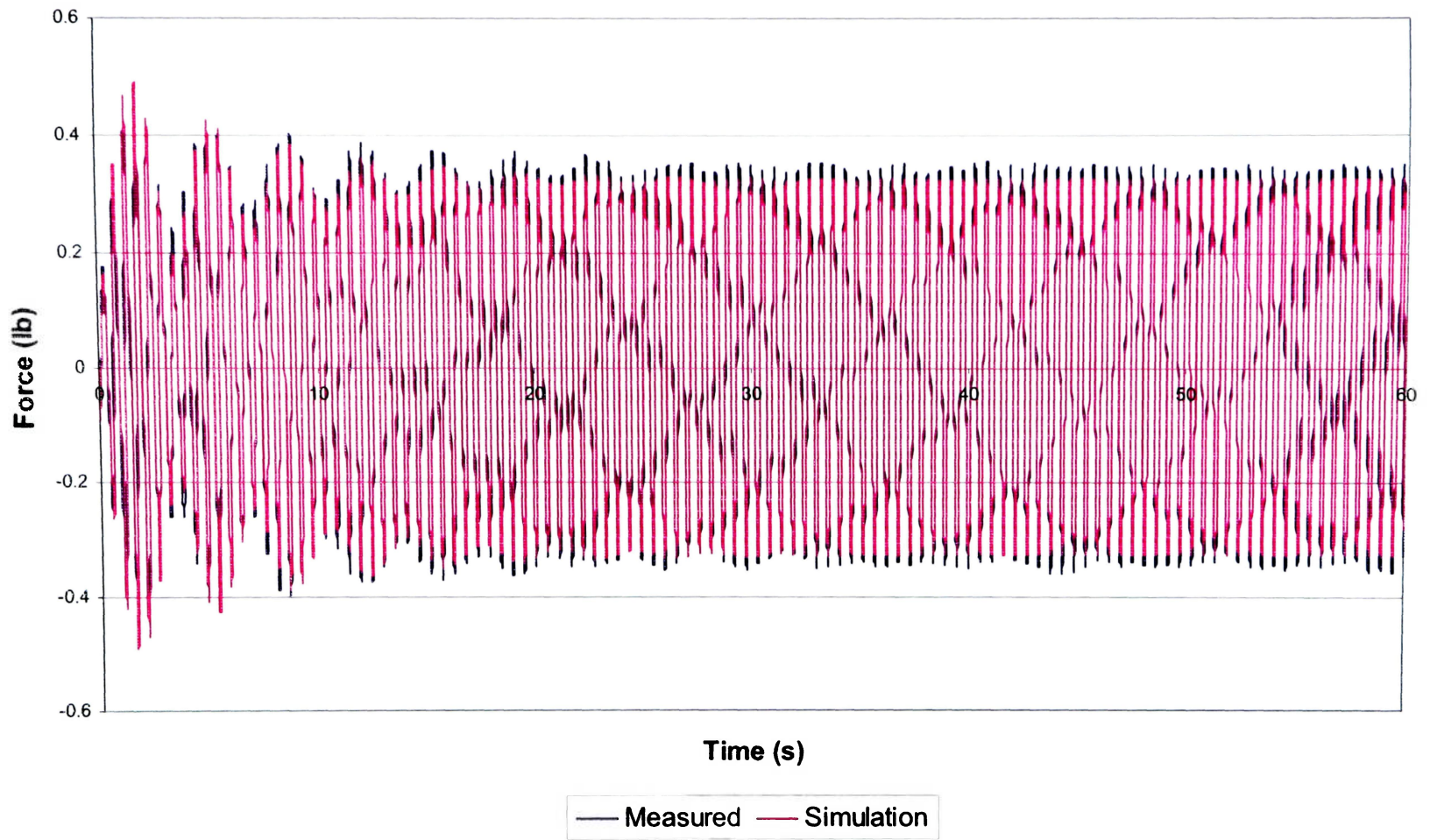
**Table H1**

**Tank at 60% Fill Level Parameter Estimation Results**

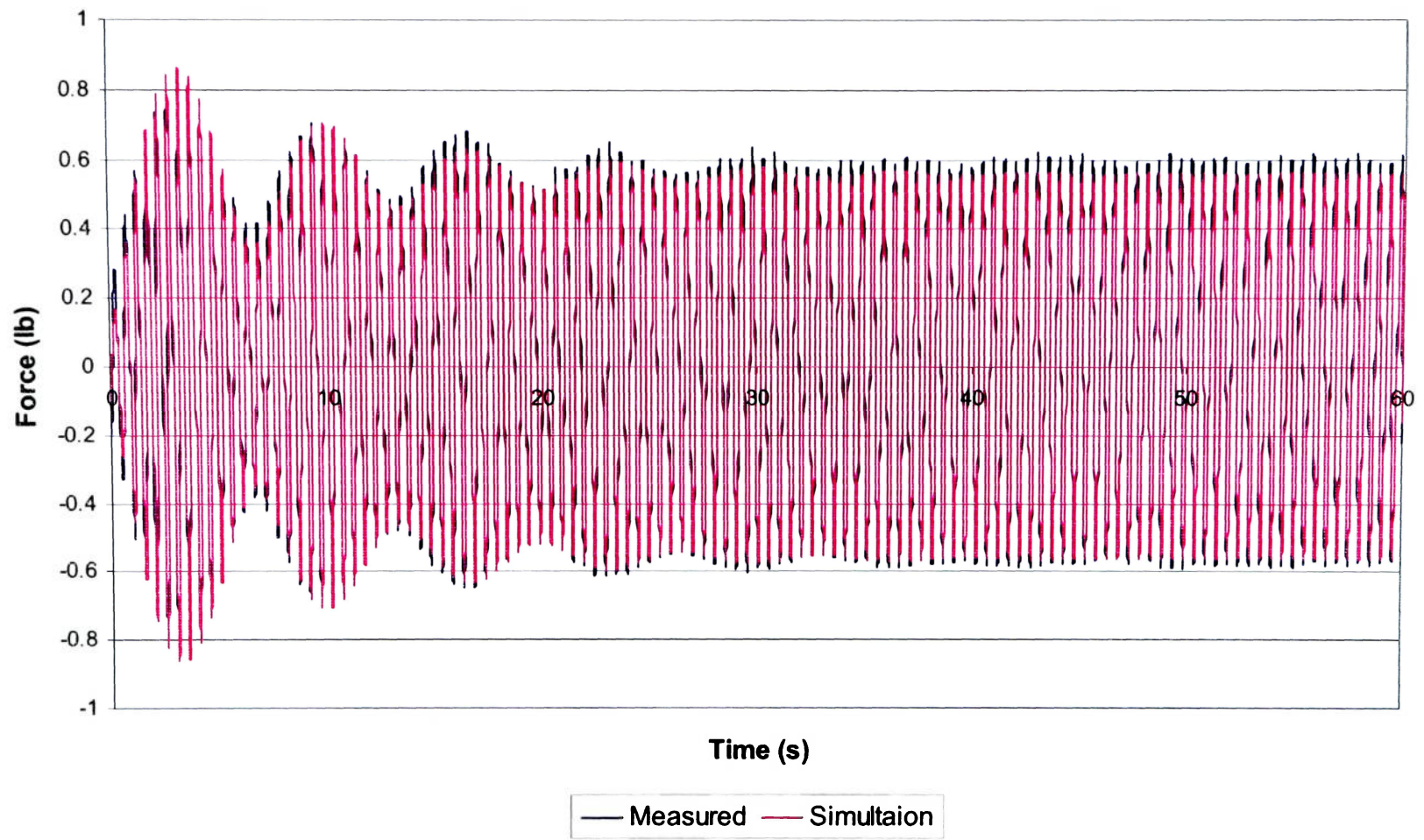
Simulation			
M-Code: 5 Parameters	Fixed Mass (lb)	Pendulum Mass (lb)	
60% Fill Level Properties	3.2099	3.055	
Test ID	A1	A2	A3
Measured Test Frequency (Hz)	1.757	1.855	1.953
Angular Velocity Correction (rad/s)	0.2290898	-0.0466229	0.0603925
Flywheel Initial Angle (rad)	-0.2545408	-0.4927648	-0.6273952
Pendulum Spring Constant (ft-lb/rad)	0.3116654	0.3546299	0.3297325
Pendulum Damping Constant (ft-lb/rad/sec)	0.0072853	0.0016229	0.0012423
Predicted Pendulum Length (in)	2.5922730	2.6458800	2.6244016
<b>Cost Function</b>	<b>5.53622</b>	<b>5.36823</b>	<b>9.89092</b>
Initial Parameter Values			
Test ID	A1	A2	A3
Measured Test Frequency (Hz)	1.757	1.855	1.953
Angular Velocity Correction (rad/s)	0.228970	-0.045928	0.060946
Flywheel Initial Angle (rad)	-0.253660	-0.466320	-0.603860
Pendulum Spring Constant (ft-lb/rad)	0.341980	0.364310	0.345410
Pendulum Damping Constant (ft-lb/rad/sec)	0.007548	0.001690	0.001264
Predicted Pendulum Length (in)	2.6667 (L)	2.6667 (L)	2.6667 (L)
<b>Cost Function</b>	<b>5.5202</b>	<b>5.2405</b>	<b>9.4510</b>



**Figure H1. Tank Test A1 (60% at 1.757Hz)**



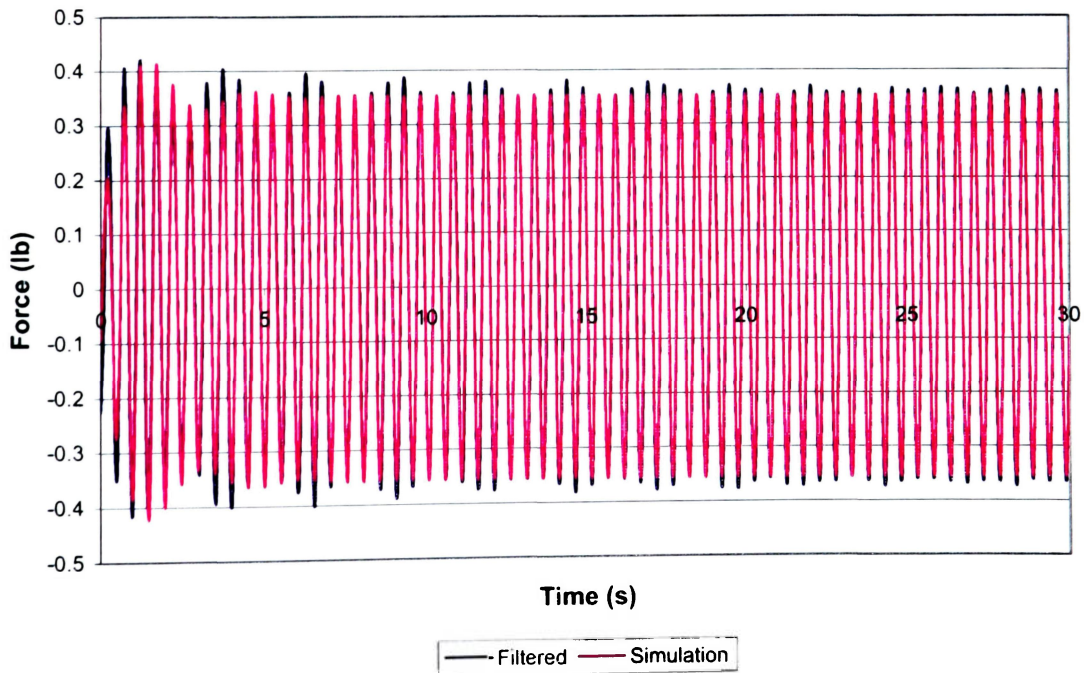
**Figure H2. Tank Test A2 (60% at 1.855Hz)**



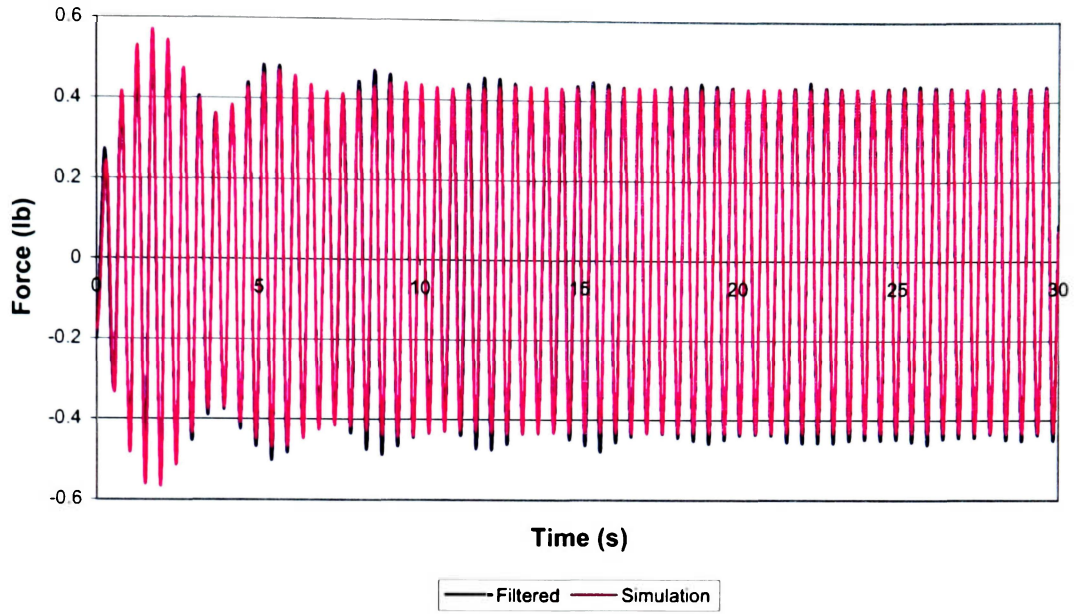
**Figure H3. Tank Test A3 (60% at 1.953Hz)**

**Table H2**  
**Tank at 70% Fill Level Parameter Estimation Results**

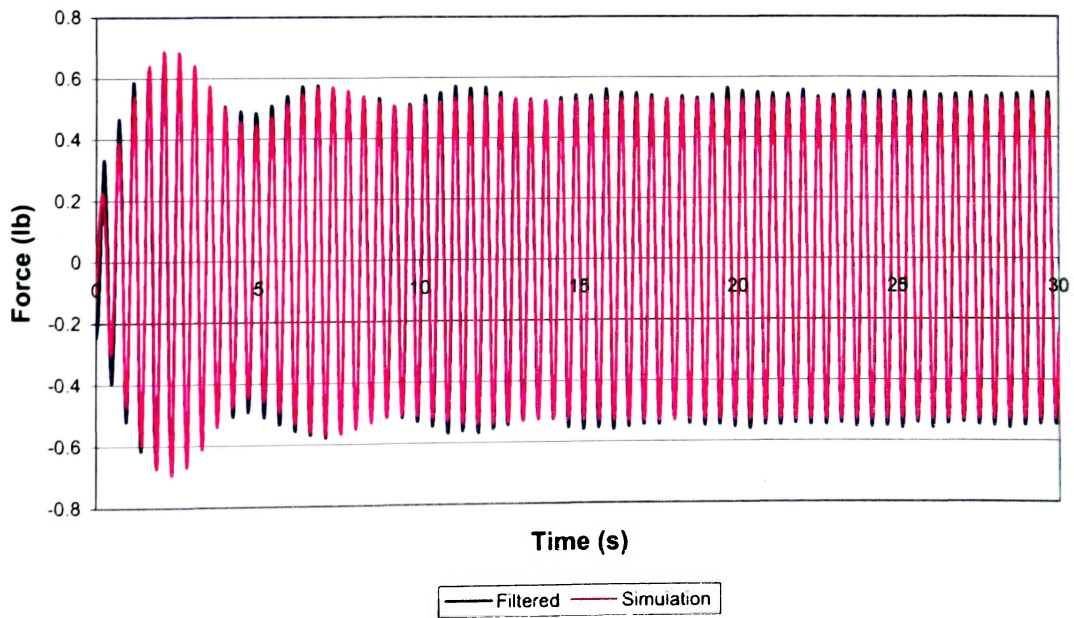
<b>3b)</b>			
M-Code: 5 Parameters	Fixed Mass (lb)	Pendulum Mass (lb)	
70% Fill Level Properties	4.7641	2.8146	
Test ID	B1	B2	B3
Measured Test Frequency (Hz)	1.953	2.051	2.090
Angular Velocity Correction (rad/s)	0.1029418	-0.0466891	0.0744836
Flywheel Initial Angle (rad)	-0.9427968	0.0348379	-0.9324601
Pendulum Spring Constant (ft-lb/rad)	0.2672687	0.3068688	0.3062238
Pendulum Damping Constant (ft-lb/rad/sec)	0.0046195	0.0026536	0.0021636
Predicted Pendulum Length (in)	2.0830903	2.1710780	2.1665813
<b>Cost Function</b>	<b>2.01168</b>	<b>2.38040</b>	<b>5.06085</b>
<b>Simulation (Parameter Estimator)</b>			
Test ID	B1	B2	B3
Measured Test Frequency (Hz)	1.953	2.051	2.090
Angular Velocity Correction (rad/s)	0.104691	-0.046604	0.073951
Flywheel Initial Angle (rad)	-0.950776	0.039813	-0.949830
Pendulum Spring Constant (ft-lb/rad)	0.311504	0.331410	0.330720
Pendulum Damping Constant (ft-lb/rad/sec)	0.006439	0.002723	0.002371
Predicted Pendulum Length (in)	2.2404 (L)	2.2404 (L)	2.2404 (L)
<b>Cost Function</b>	<b>1.9341</b>	<b>2.3122</b>	<b>4.7543</b>



**Figure H4. Tank Test B1 (70% at 1.953Hz)**



**Figure H5. Tank Test B2 (70% at 2.051Hz)**

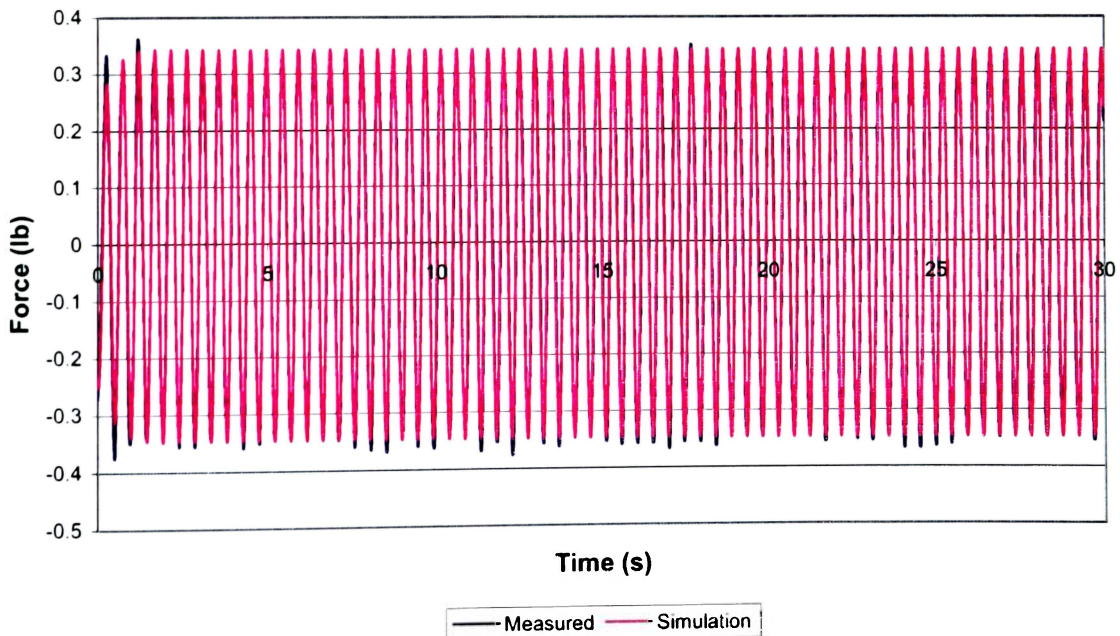


**Figure H6. Tank Test B3 (70% at 2.090Hz)**

**Table H3**

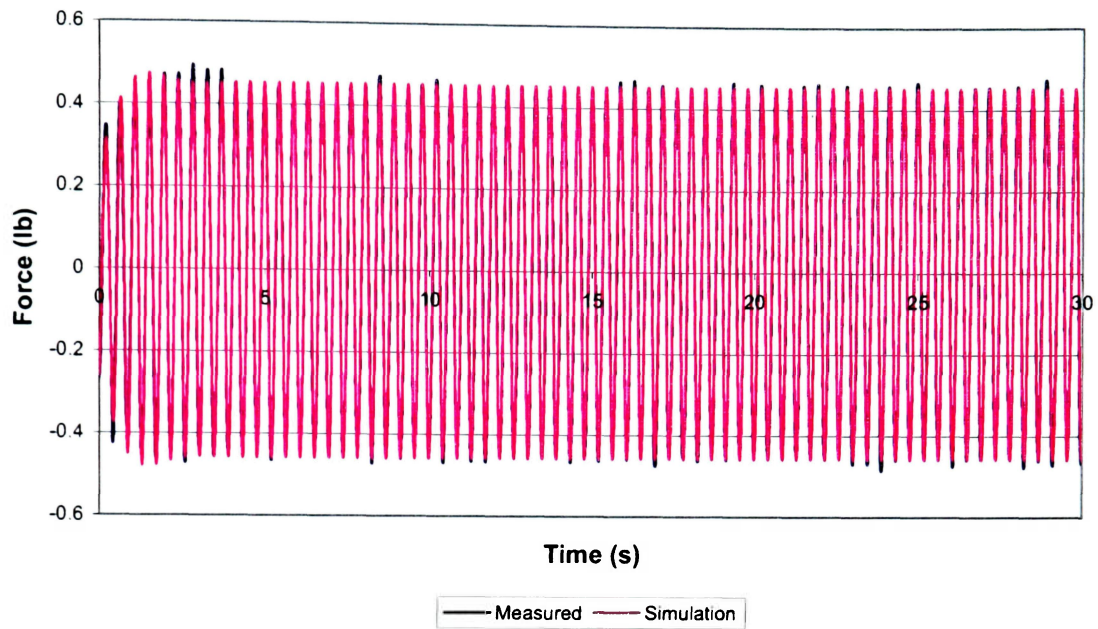
**Tank at 80% Fill Level Parameter Estimation Results**

Simulation (Parameter Estimator)			
M-Code: 5 Parameters	Fixed Mass (lb)	Pendulum Mass (lb)	
80% Fill Level Properties	6.5366	2.1246	
Test ID	C1	C2	C3
Measured Test Frequency (Hz)	2.148	2.343	2.441
Angular Velocity Correction (rad/s)	-0.1517624	-0.2729089	-0.2299123
Flywheel Initial Angle (rad)	0.1993426	-0.4447964	-0.2861995
Pendulum Spring Constant (ft-lb/rad)	0.1471721	0.2561186	0.2204100
Pendulum Damping Constant (ft-lb/rad/sec)	0.0096583	0.0055077	0.0043716
Predicted Pendulum Length (in)	1.6769303	1.7095140	1.7294317
<b>Cost Function</b>	<b>1.27448</b>	<b>1.51998</b>	<b>10.62430</b>
Simulation (Parameter Estimator)			
Test ID	C1	C2	C3
Measured Test Frequency (Hz)	2.148	2.343	2.441
Angular Velocity Correction (rad/s)	-0.151930	-0.278280	-0.230020
Flywheel Initial Angle (rad)	0.212970	-0.478500	-0.284690
Pendulum Spring Constant (ft-lb/rad)	0.167660	0.248660	0.222170
Pendulum Damping Constant (ft-lb/rad/sec)	0.010487	0.006281	0.004403
Predicted Pendulum Length (in)	1.7352 (L)	1.7352 (L)	1.7352 (L)
<b>Cost Function</b>	<b>1.2729</b>	<b>1.5014</b>	<b>10.6230</b>

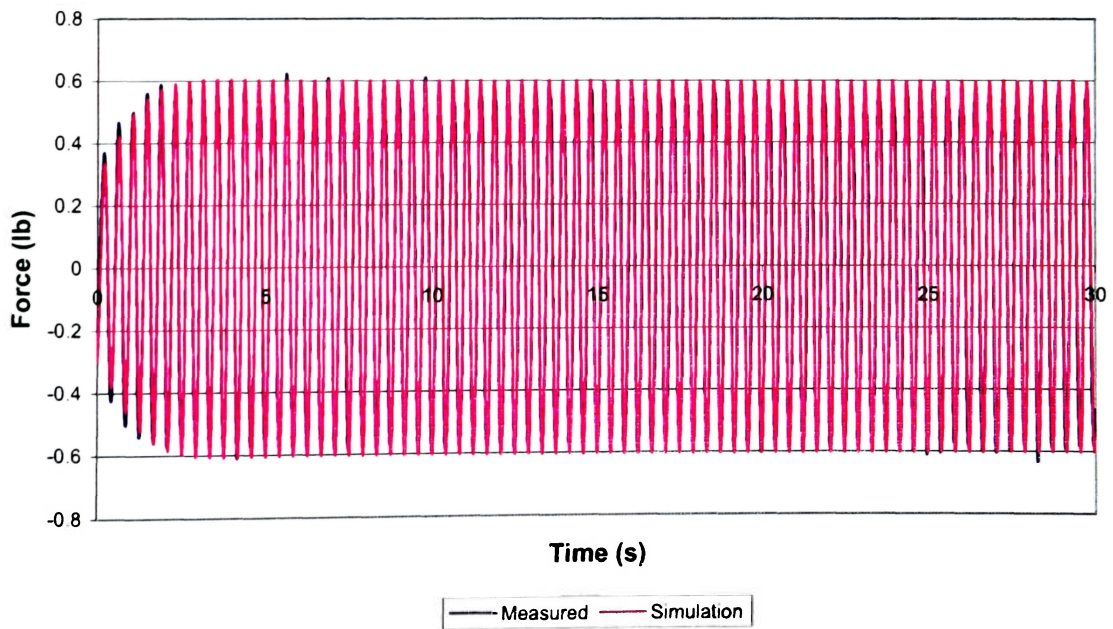


**Figure H7. Tank Test C1 (80% at 2.148Hz)**





**Figure H8. Tank Test C2 (80% at 2.343Hz)**



**Figure H9. Tank Test C3 (80% at 2.441Hz)**